



Room 14-0551
77 Massachusetts Avenue
Cambridge, MA 02139
Ph: 617.253.5668 Fax: 617.253.1690
Email: docs@mit.edu
<http://libraries.mit.edu/docs>

DISCLAIMER OF QUALITY

Due to the condition of the original material, there are unavoidable flaws in this reproduction. We have made every effort possible to provide you with the best copy available. If you are dissatisfied with this product and find it unusable, please contact Document Services as soon as possible.

Thank you.

Some pages in the original document contain color pictures or graphics that will not scan or reproduce well.

**Proteomic Analysis of the Function of DMPK,
the Myotonic Dystrophy Protein Kinase**

by

Brenda Sierra Luciano

B. S. Biochemistry
Western Washington University, 1993

Submitted to the Department of Biology in Partial
Fulfillment of the Requirements for the Degree of

Doctor of Philosophy
at the
Massachusetts Institute of Technology

September, 2001

copyright 2001 Massachusetts Institute of Technology. All rights reserved

Signature of Author: _____

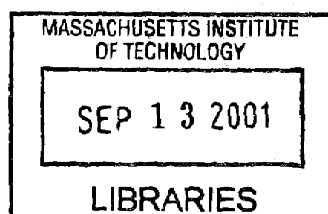
Department of Biology
September 1, 2001

Certified by: _____

David Evan Housman
Ludwig Professor of Biology
Thesis Supervisor

Accepted by: _____

Alan Grossman
Professor of Biology
Chairperson, Graduate Committee



ARCHIVES

Proteomic Analysis of the Function of DMPK, the Myotonic Dystrophy Protein Kinase

by

Brenda Sierra Luciano

Submitted to the Department of Biology
on September 1, 2001 in Partial Fulfillment of the
Requirements for the Degree of Doctor of Philosophy in
Biology

ABSTRACT

Myotonic Dystrophy type 1 (DM1), the most common form of adult-onset skeletal muscle dystrophy, is caused by expansion of a CTG repeat sequence embedded in the 3'UTR of a gene which encodes a serine threonine kinase, DMPK. The precise mechanism by which CTG repeat expansion causes the complex pathology of DM1 is under active investigation. Repeat expansion leads to a failure of transport of DMPK mRNA from nucleus to cytoplasm indicating that reduction in DMPK expression levels is at least one major consequence of repeat expansion. Mouse models suggest that haploinsufficiency of DMPK accounts for at least a portion of the symptoms of DM1. *DMPK*^{-/-} mice exhibit a progressive muscle myopathy similar to that seen in DM1, and both *DMPK*^{-/-} and *DMPK*^{+/-} mice reiterate cardiac conduction abnormalities characteristic of DM1 patients. However, the *in vivo* role of DMPK, the identity and nature of its substrate(s) and the biological pathway(s) within which it functions remain to be elucidated.

To determine the *in vivo* function of DMPK I have taken a proteomics-based approach that utilizes 2-dimensional SDS-PAGE and mass spectrometry to compare directly heart proteins of wild-type and *DMPK*^{-/-} mice in order to identify proteins that are altered in the absence of DMPK. I have identified several proteins with altered mobility on 2D SDS-PAGE gels in mutant versus wild-type cells in heart and peripheral muscle of *DMPK*^{-/-} animals. Two of these were analyzed by mass spectrometry and identified as fatty acid binding proteins (FABPs). The altered mobility of these proteins suggests that they have different properties in the absence of DMPK. Further investigation of these FABPs could potentially shed light into the *in vivo* role of DMPK and into the biological pathway(s) in which DMPK functions.

Thesis Supervisor: David Evan Housman
Ludwig Professor of Biology

Dedication

This thesis is dedicated in part to Dr. Fred G. Knapman, a great scientist, wonderful professor, and good friend. When I was eight years old he introduced me to his granddaughter, a very fine person and my oldest friend, and when I was in college, he helped me to stay dedicated to my goal of becoming a scientist. I will always remember him with great fondness.



Fred G. Knapman

1910-2001

Acknowledgements:

First I would like to thank David Housman, my advisor, who has been very supportive throughout my graduate school experience. David has always been ready to listen and help me see a positive side to every experiment. I am grateful for the opportunity to receive my training and grow as a scientist in the Housman lab.

I would like to thank the members of my thesis committee, past and present, for their great advice and help over the years. I would first like to thank Richard Hynes and Jackie Lees who have been on my committee since my prelim. I really appreciate their time and support, their scientific guidance, and their career advice. I would like to thank Frank Solomon, who has been a great help to me and a good listener. And I would also like to thank Frank Gertler and Michael Volkert for joining my committee and being there for my defense. I thank everyone very much for their help and advice.

The members of the Housman lab have been very helpful and supportive to me and it has been a real pleasure working with such a great group of people. I would like to thank all members of the Housman lab, past and present. In particular, I would like to thank Brigid Davis and Sita Reddy for their help and insight on the myotonic dystrophy project. I would like to also particularly thank Julia Alberta, Mary Badura, Julian Borrow, Alain Charest, Jessica Greenwood, Hiroaki Kawasaki, Dianne Keen, and Michele Maxwell. These people have all been incredibly generous with their help, advice, and time. Almost every technique I learned in the lab, I learned from them.

I also thank Bing Wang and Ivan Correia, who taught me many of the proteomic techniques I learned, and showed me how to learn the rest for myself. Also I am sincerely grateful for having Raluca Verona and Ken Moberg as colleagues. They were good classmates and friends, and always ready with scientific advice, a cheery word, or sushi when necessary.

I am grateful to my parents for believing in me, and for their multidimensional support during my time in graduate school. It has meant a lot knowing they were behind me completely. I would like to thank my sister Laura for moving here, babysitting her niece and nephew, for coming through in sushi emergencies, for being my friend, and for computers and various other gadgets in times of need. And I thank my sister Loo and her husband Joe for keeping me in touch with the world outside and helping me remember that life is supposed to be fun.

Last but not least I thank my family. I thank my husband Peter for taking care of our children by himself almost every weekend for the past six years, for being my best friend, for believing in and supporting me, and for not complaining much even when he'd had enough. And I thank my daughter Sierra and my son Joe for being so patient while I finished up, for brightening my life, and for helping me get my priorities straight.

TABLE OF CONTENTS

Abstract	2
Dedication	3
Acknowledgements	4
Table of Contents	6
List of Figures	8
List of Tables.....	9
Chapter 1: Introduction to myotonic dystrophy	10
Clinical Aspects of myotonic dystrophy	11
Congenital myotonic dystrophies.....	16
The myotonic dystrophies.....	16
Myotonic dystrophy and the trinucleotide repeat diseases.....	17
The <i>DMPK</i> gene and the triplet repeat expansion	21
CTG triplet repeat instability.....	22
Disease mechanisms	23
Haploinsufficiency of <i>DMPK</i>	23
Gain of function <i>DMPK</i> mRNA	25
The effect of the expansion on neighboring genes	27
Mouse models of myotonic dystrophy	28
<i>DMPK</i> ^{-/-} mice.....	29
<i>DMPK</i> overexpression mice.....	31
CTG repeat expansion mice.....	31
Interpretation of mouse models.....	35
<i>DMPK</i> protein.....	37
Structural domains	38
Alternative splice forms.....	39
Substrate specificity	43
Summary.....	44
References.....	46
Chapter 2: Proteomic Analysis of the Function of <i>DMPK</i>	53
Abstract.....	54
Proteomics	55
Separation techniques	55
Visualization methods.....	56
Protein digestion and mass spectrometry.....	60
MALDI-TOF mass spectrometry.....	61
Electrospray ionization mass spectrometry (ESI-MS).....	64
Tandem mass spectrometry (MS/MS)	64
Protein bioinformatics	67
Genomics, proteomics, and human disease	68
A proteomic approach to investigate the role of <i>DMPK</i>	68
Results	72
Initial comparison of gels reveals the location of <i>DMPK</i>	72
High resolution analysis of the wild-type and <i>DMPK</i> ^{-/-} -proteomes.....	75
Comparison of proteins from wild-type and <i>DMPK</i> ^{-/-} -2-DE gels	79
MALDI-TOF analysis of two selected proteins	96
LC-MS/MS analysis of two selected proteins	101

LC-MS/MS analysis of H-FABP from DMPK ^{-/-} -gels.....	108
Fatty acid binding proteins in skeletal muscle and brain.....	117
Further analysis	128
Phosphorylation state of Sample B and 3.....	128
Summary	129
Materials and Methods	132
Sample Preparation	132
2-dimensional gel electrophoresis.....	134
Silver staining.....	134
Sample preparation for MALDI-TOF MS.....	135
MALDI-TOF MS	136
Analysis of MALDI-TOF MS spectra	137
MS-MS peptide sequencing	137
References.....	139
Acknowledgements	142
Chapter 3: Discussion.....	143
Part 1: Fatty acid binding proteins and their potential role in DM1.....	144
Proteins that are altered by DMPK loss: the fatty acid binding proteins	146
Fatty Acid Metabolism.....	146
Fatty acid binding proteins (FABPs).....	147
FABP mobility forms	148
H-FABP.....	149
A-FABP.....	151
The alteration of H-FABP and A-FABP in the absence of DMPK.....	152
DM1 and insulin resistance	154
Conclusions.....	155
Future experiments.....	157
Part 2: Proteomic analysis in models of human disease.....	159
Future directions and technological advances.....	161
Further application of proteomics to the study of DMPK ^{-/-} mice	162
Fractionating to enrich for phosphoproteins	163
Gel imaging software	166
Visualization Methods.....	167
Summary.....	168
References.....	169
Appendix A: Generation of DMPK^{-/-}:MyoD^{-/-} mice and analysis of their phenotype.....	174
Appendix B: Protocols	198
Biographical Sketch.....	215

List of Figures

1-1: The cardiac conduction defect in DM1	13-14
1-2: DMPK splice forms	40-41
2-1: Two-dimensional gel electrophoresis (2-DE)	57-58
2-2: MALDI-TOF mass spectrometry.....	62-63
2-3: ESI mass spectrometry.....	65-66
2-4: Experimental Overview	70-71
2-5: 2-DE comparison of wild-type and <i>DMPK</i> ^{-/-} mouse heart proteins.....	73-74
2-6: Reduced pH gradient gels for systematic analysis of the proteome	77-78
2-7: Types of mobility shifts found in gel comparison.....	81-82
2-8: 2-DE gel comparison of whole cell lysate from heart	83-84
2-9: 2-DE gel comparison of wild-type and <i>DMPK</i> ^{-/-} skeletal muscle proteins.....	85-86
2-10: Comparison of fractionated protein samples: extract 1	88-89
2-11: Repeat of the mobility shift seen in figure 2-10	90-91
2-12: Comparison of fractionated protein samples: extract 2	92-93
2-13: Comparison of fractionated protein samples: extract 2, pH 4-7	94-95
2-14: Comparison of fractionated protein samples: extract 2, pH 4.5-5.5	97-98
2-15: Comparison of fractionated protein samples: extract 2, 8 month old mice	99-100
2-16: MALDI-TOF identification of Sample A, A-FABP	102-103
2-17: MALDI-TOF identification of Sample A, coverage map.....	104-105
2-18: MALDI-TOF identification of Sample B, ambiguous results.....	106-107
2-19: LC-MS/MS analysis of Sample A, A-FABP	109-110
2-20: LC-MS/MS analysis of Sample A, coverage map	111-112
2-21: LC-MS/MS analysis of Sample B, H-FABP.....	113-114
2-22: LC-MS/MS analysis of Sample B, coverage map	115-116
2-23: Comparison of fractionate protein samples: extract 2, skeletal muscle.....	118-119
2-24: Color overlay of figure 2-23.....	120-121
2-25: Comparison of fractionate protein samples: extract 2, skeletal muscle 2.....	122-123
2-26: Comparison of fractionate protein samples: extract 2, brain.....	124-125
2-27: Color overlay of figure 2-26.....	126-127
3-1: Scheme to enrich for phosphoproteins.....	164-165
A-1: The role of MyoD in skeletal muscle regeneration.....	179-180
A-2: Comparison of mouse weight over time, male.....	185-186
A-3: Comparison of mouse weight over time, female.....	185,187
A-4: Fiber type comparison of <i>DMPK</i> ^{-/-} and <i>DMPK</i> ^{-/-} : <i>MyoD</i> ^{-/-} -skeletal muscle..	189-190

List of Tables

Table 1-1: Systemic involvement in myotonic dystrophy	15
Table 1-2: Features of triplet repeat diseases	20
Table 1-3: The cardiac conduction defect in the DM1 mouse model	30
Table 1-4: Comparison of human DM1 and mouse models	34
Table 3-1: FABP isoforms.....	148
Table 3-2: FABP mobility forms	149
Table A-1: Genotype proportion in neonatal death in <i>MyoD</i> $-/-$ background	183

Chapter 1: Introduction to Myotonic Dystrophy

Myotonic dystrophy, or *dystrophia myotonica* type one (DM1), is the most common inherited adult-onset muscle disorder (Harper, 1989). DM1 affects approximately one person in 8000 in North American and European populations. It is autosomal dominant and is a complex and variable disease involving a variety of muscle and non-muscle systems. The mutation associated with DM1 is an expanded CTG repeat that occurs within the 3'UTR of the *DMPK* gene, which encodes a serine/threonine protein kinase. The precise mechanism by which the mutation causes the complex pathology of DM1 is unclear, although it has three major effects in the cell: 1) it reduces the amount of DMPK protein by half, 2) it produces a mutant mRNA with dominant negative properties, and 3) it reduces the expression of neighboring genes. Each effect of the mutation likely contributes to the etiology of DM1.

The myotonic dystrophy protein kinase (DMPK) is a serine/threonine protein kinase with unknown cellular function. The reduced dosage of DMPK in DM1 patients likely contributes to the cardiac and muscle pathology characteristic of this disease, suggesting that DMPK has a critical role in maintaining the proper function in these tissues. There is currently no *in vivo* data to tell us the precise function of DMPK in the cell. Chapters 1-3 illustrate a proteomics-based, *in vivo* analysis of the function of DMPK.

Clinical Aspects of Myotonic Dystrophy

Myotonic dystrophy can be difficult to diagnose because of the variability of the type and severity of symptoms. The hallmark of the disease is myotonia, hyperexcitability of the muscle cell membrane that results in the inability to relax a muscle immediately after voluntary contraction. It is usually a clinical demonstration of myotonia coupled with observed muscle weakness that allows diagnosis of DM1 (Meola, 2000). However, genetic testing is becoming more common as several phenotypically similar myotonic myopathies have recently been characterized (described below).

Skeletal muscle of DM1 patients becomes progressively weaker over time. Histological analysis of skeletal muscle reveals typical features of muscle degeneration and regeneration such as type I (slow) fiber atrophy, abundant central nuclei, sarcoplasmic masses, ringed fibers, and fibrosis (Ueda, 1999, Reddy, 1996). Furthermore, ultrastructural analysis of muscle sections reveals extensive disorganization of fiber structure including distorted A and Z lines, abnormally large and dysmorphic mitochondria, and disruption of the sarcoplasmic reticulum. The muscles most frequently affected are the facial and jaw muscles, sternomastoids, distal limb muscles, the external ocular muscles, and the small muscles of the hands and feet. In addition to skeletal muscle effects in DM1, degeneration of smooth muscle also occurs and this accounts for

most of the gastrointestinal symptoms seen in patients. Loss of esophageal motility is common, as is anal sphincter malfunction (Harper, 1989).

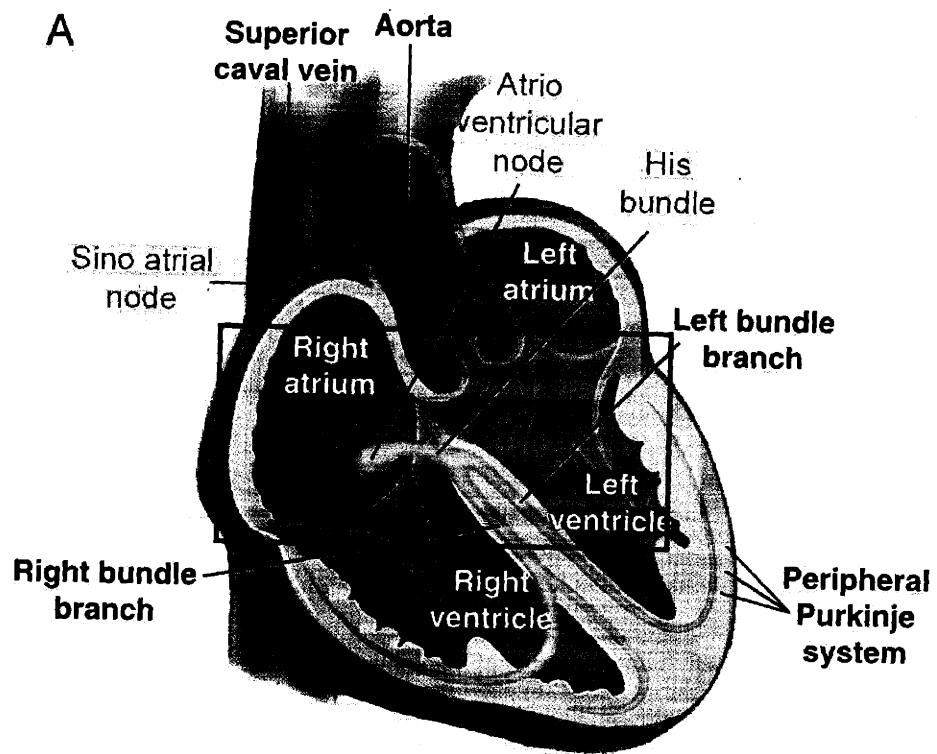
Heart tissues of deceased DM1 patients show heterogeneous replacement of myocardium and conductive system by fatty infiltration and fibrosis (Nguyen H.H., 1988). Indeed, the majority of adults affected with the disease develop cardiac conduction defects, mitral valve prolapse, or congestive heart failure, and higher-grade atrioventricular (AV) block is a significant cause of death (Berul, 1999). The conduction defect can be demonstrated by an electrocardiogram (EKG) reading. As the heart beats, the conduction signal, communicated by the polarization of the membranes of conductive fibers, travels from the sinoatrial node to the atrioventricular node. The EKG trace of myotonic dystrophy patients shows a significant elongation of the PR interval when compared to normal individuals (Fragola, 1994) (Figure 1) and this effect is also seen in *DMPK* *-/-* mice (Berul, 2000). A significant percentage of this delay has been traced in *DMPK* *-/-* mice to a holdup at the Bundle of His (Saba, 1999), a region of concentration of conductive fibers intermediate between the SA and AV nodes.

In contrast to the muscle weakness and cardiac conduction defects, other symptoms of myotonic dystrophy can be extremely variable; for example, only an estimated 1.6 % of DM1 patients are clinically diabetic, whereas 63% are insulin resistant. Table 1 shows a compilation of symptoms.

Figure 1. The cardiac conduction phenotype associated with myotonic dystrophy

Panel A is an illustrated overview of the human heart outlining the physiology of the conduction system. The sinoatrial (SA) node is the cardiac pacemaker. It initiates an electrical impulse that spreads to the atrioventricular (AV) junction, causing the contractions that allow the heart to beat.

Panel B is a representation of the EKG trace as the conduction signal travels from the SA node to the AV node.



Adapted from Harvey & Rosenthal *Heart Development* 1999 Academic Press

B

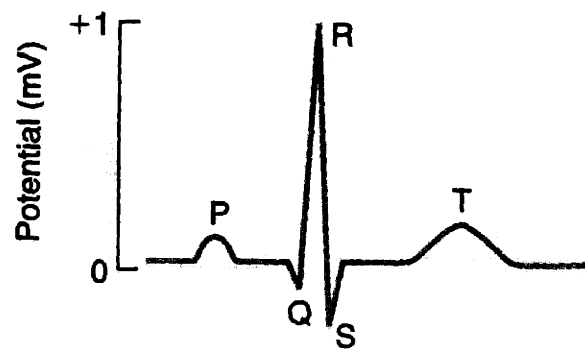


Table 1: Systemic involvement in Myotonic Dystrophy

<p><u>Skeletal muscle</u>: most common are facial weakness, ptosis, myotonia, weakness in jaw muscles, sternomastoids, distal limb muscles</p> <p><u>Smooth muscle</u>: weakness in esophagus, colon, uterus</p> <p><u>Cardiac</u>: conduction defect (expanded P-R interval), mitral valve prolapse, cardiomyopathy, atrial and ventricular tachyarrhythmia</p> <p><u>Ocular</u>: cataract, retinal degeneration, ptosis, extraocular weakness</p> <p><u>Endocrine</u>: testicular atrophy, insulin resistance, abnormal growth hormone release, parathyroid adenoma</p> <p><u>Peripheral nerve</u>: variable, minor sensory loss</p> <p><u>Lungs</u>: aspiration pneumonia from esophageal and diaphragmatic involvement, hypoventilation</p> <p><u>Brain</u>: severe involvement in myotonia congenita, mild mental deterioration frequent in adults, hypersomnia</p> <p><u>Skin</u>: premature balding, calcifying epithelioma</p> <p><u>Immune</u>: reduced serum concentration of immunoglobulins</p> <p><u>Renal</u>: abnormal handling of calcium</p>

DM1 differs from the other muscular dystrophies in that it is the distal muscles (those furthest from the torso), rather than the proximal or limb girdle muscles (pelvic and scapular) that are most seriously affected (Harper, 1989). Facial muscle weakness is very common, ptosis (drooping eyelids) being the most visible. Myotonia is absent in the other dystrophies, as is central nervous system involvement, although CNS impairment in myotonic dystrophy is variable and only especially prominent in congenital cases (see below). The cardiac conduction defect is unique to DM1, and the general cardiomyopathy seen in Duchenne's muscular dystrophy occurs infrequently in myotonic dystrophy. Smooth muscle symptoms and the widespread involvement of non-muscle systems are usually absent in other dystrophies as well.

Congenital Myotonic dystrophy

Myotonic dystrophy can also occur as a congenital disease. The congenital variant differs from the adult disease in that the symptoms are present at birth, muscles are hypotonic as opposed to hypertonic, myotonia is absent, and it is usually maternally inherited. Those patients that survive the potentially lethal effects of respiratory difficulties and feeding difficulties caused by muscle weakness exhibit severe mental retardation, delayed muscle development, and many of the other symptoms of adult DM. The basis for the congenital variant of myotonic dystrophy is not clearly understood, nor is the fact that it almost exclusively results from maternal transmission.

The Myotonic Dystrophies

Clinical diagnosis of DM1 is further complicated by the discovery in recent years of several DM1-like disorders that are phenotypically very similar to myotonic dystrophy but do not carry the CTG expansion in the *DMPK* gene. These were named PROMM (proximal myotonic myopathy) (Ricker, 1995), PDM (proximal myotonic dystrophy) (Udd, 1997), and DM2 (Ranum, 1998, Day, 1999). Collectively with DM1, these multisystemic myotonic disorders are called the myotonic dystrophies. These three disorders differ slightly from each other, but each is characterized by myotonic myopathy, cataracts, cardiac conduction defects, and frontal balding. In contrast to DM1, no mental deficiency or

congenital cases have been observed and the skeletal muscles affected are mainly those proximal rather than distal. The precise mutations for these other myotonic myopathies have yet to be identified and it is not clear whether they represent varying manifestations of the same mutation or whether each represents a discrete gene.

Myotonic Dystrophy and the trinucleotide repeat diseases

Myotonic dystrophy is one of a group of inherited diseases, including Huntington's disease and Fragile X syndrome, that are caused by the expansion of a trinucleotide repeat (Harper, 1997) (Table 2). Like many other triplet repeat diseases, DM1 shows the phenomenon of anticipation, earlier onset of disease and increasing disease severity with each successive generation. The cause of the observed anticipation effect in DM1 was the subject of controversy in the field until the gene was cloned in 1992 (Brook, 1992, Fu, 1992, Harley, 1992, Mahadevan, 1992) and the mutation associated with the disease was determined. The gene encodes a serine/threonine protein kinase, named *dystrophia myotonica* protein kinase, or DMPK. The mutation in the *DMPK* gene was determined to be an expanded CTG repeat in the 3' untranslated region of the gene (3'UTR). So far both the type of triplet (CTG) and its location in the gene are unique to myotonic dystrophy, although a newly discovered form of spinocerebellar ataxia, SCA8, possibly contains an expanded CTG repeat in a noncoding region of its gene, either intronic or in the 5' or 3' untranslated region.

The list of diseases connected with trinucleotide repeat expansions grows larger each year, particularly in the category of the spinocerebellar ataxias. Although they share the phenomenon of anticipation, each disease has its own particular mechanism by which the mutation translates into disease pathology. As Table 2 illustrates, expanded repeats can cause dramatically different pathology, dependent on the specific locus, the type and number of repeats, as well as the location of the repeat within the gene (Wilmot, 1998).

DRPLA, Huntington's disease, and SCA 1, 2, 3, 6, and 7 are autosomal dominant triplet repeat diseases in which expanded CAG repeats occur in the coding region of the genes, producing polyglutamine tracts in the middle of the proteins (Wilmot, 1998). Although the number of repeats is generally small in these diseases, the mutations interrupt the coding region of the gene and cause a complete loss of function. In addition, the polyglutamine tracts exhibit a gain of function effect through self-aggregation and have been shown to have toxic consequences for the cell. Kennedy's disease is the only CAG expansion that appears to be autosomal recessive, resulting from loss of function of the androgen receptor. The degree to which polyglutamine aggregation plays a part in this disease is not yet entirely understood. The full nature of the polyglutamine aggregates in these diseases is currently under investigation.

Triplet repeat diseases involving noncoding repeats are typically multisystem disorders characterized by long expansions in symptomatic individuals. Asymptomatic individuals can carry pre-mutation alleles with an intermediate number of repeats; these repeats can expand upon transmission to the germline and give rise to the full mutation. Fragile X syndrome and fragile XE mental retardation result from loss of function of FMR1 and FMR2, respectively. The expanded CGG repeat in the 5'UTR of both genes results in a CG-rich region that becomes extensively methylated, causing transcriptional silencing. Friedreich's ataxia also results from loss of function as the intronic GAA repeat suppresses expression of the frataxin gene, potentially through inhibition of transcription.

Although all the triplet repeat diseases share the presence of expanded repeat tracts and the phenomenon of anticipation, each disease has dramatically different clinical manifestations. This property illustrates the fact that, in each case, a specific mutation causes the disease pathology through its own particular mechanism.

Disorder	Inheritance	Gene/locus	protein product	expansion type	repeat location	mut. type	parental gender bias
Dentatorubal pallidolusian atrophy/Haw river syndrome	AD	DRPLA	atrophin-1	(CAG) ₅₁₋₈₈	coding	GOF	paternal
Fragile X syndrome	XD	FMR1 (FRAXA)	FMRP	(CGG) ₂₃₀₋₁₀₀₀	5'UTR	LOF	maternal
Fragile XE (mental retardation)	XD	FMR2 (FRAXE)	FMR2 protein	(GCC) ₂₃₀₋₇₅₀	5'UTR	LOF	ND
Friedreich's ataxia	AR	X25	frataxin	(GAA) ₁₁₂₋₁₇₀₀	Intron	LOF	maternal
Huntington's disease	AD	IT15	huntingtin	(CAG) ₃₆₋₁₂₁	coding	GOF	paternal
Myotonic Dystrophy	AD	DMPK (DM1)	DMPK	(CTG) ₅₀₋₅₀₀₀	3'UTR	?	ND/maternal (congenital)
Spinobulbar muscular atrophy (Kennedy's disease)	XR	AR	androgen receptor	(CAG) ₃₈₋₆₆	coding	GOF	ND
Spinocerebellar ataxia type 1	AD	SCA1	ataxin-1	(CAG) ₄₁₋₈₁	coding	GOF	paternal
Spinocerebellar ataxia type 2	AD	SCA2	ataxin-2	(CAG) ₃₅₋₆₄	coding	GOF	paternal
Spinocerebellar ataxia type 3 (Machado-Joseph disease)	AD	SCA3 (MJD1)	ataxin-3	(CAG) ₄₀₋₈₄	coding	GOF	paternal
Spinocerebellar ataxia type 6 /Episodic ataxia type 2	AD	CACNA1A	α_{1A} -voltage-dependent calcium channel subunit	(CAG) ₂₀₋₂₃ (EA2) (CAG) ₂₁₋₂₇ (SCA6)	coding	GOF	ND
Spinocerebellar ataxia type 7	AD	SCA7	ataxin-7	(CAG) ₃₈₋₁₃₀	coding	GOF	paternal
Spinocerebellar ataxia type 8	AD	SCA8	KLHL1	(CTA/CTG) ₁₀₀₋₂₅₀	probably 3'UTR	GOF	maternal
Spinocerebellar ataxia type 12	AD	SCA 12	PPP2R2B	(CAG) ₆₆₋₇₈	5'UTR	GOF?	?

Table 2: Features of triplet repeat diseases AD, autosomal dominant; AR, autosomal recessive; XD, X-linked dominant; XR, X-linked recessive; GOF, gain of function; LOF, loss of function; ND, not detected

The DMPK gene and the triplet repeat expansion

Understanding the relationship between the pathology of myotonic dystrophy and the expanded trinucleotide repeats in the *DMPK* gene may be the biggest challenge for investigators. The extended CTG repeat has been shown to have ramifications at the DNA, RNA, and protein level. Full knowledge of the mechanisms by which the triplet repeat exerts its effects is not yet known. The *DMPK* gene is located on human chromosome 19q13.3 and is flanked by the genes *DMWD* (5') and *SIX5* (3'). *DMWD* encodes a WD-repeat containing protein that terminates less than 1kb from the 5' end of *DMPK*. *SIX5* encodes a homeodomain protein that lies less than 1kb from the 3' end of *DMPK*. The expression of all three of these genes is potentially affected by the CTG expansion (Klesert, 1997). Furthermore, the mRNA from the mutant *DMPK* allele remains sequestered in discrete foci in the nucleus after transcription (Davis, 1997). This has the combined effect of the titration of CUG-repeat-binding proteins from the nuclear matrix, thus producing a dominant negative RNA effect, and, as this allele is never translated, the reduction by 50% of the normal amount of *DMPK*. An analysis of possible mutation mechanisms is discussed later in this section.

CTG triplet repeat instability

Normal alleles of *DMPK* contain less than 50 of the CTG repeats, while mutant alleles have numbers of repeats ranging from greater than 50 to several thousand. The number of repeats in a mutant allele increases with each subsequent passage through the germline. Furthermore, the repeat is not only meiotically unstable but also mitotically unstable, and this instability shows tissue type variance. For example, *DMPK* mRNA from blood cells contains relatively few repeats, whereas mRNA from muscle, heart, and kidney displays the largest expansion. Nevertheless, the number of repeats, usually assessed from skeletal muscle biopsies, correlates to the age of onset and the severity of DM1, especially with regard to the wasting of muscles. Patients with a relatively low number of repeats may experience symptoms such as cataracts or mild muscle weakness late in life, and may be unaware that they have the disease, whereas a patient in a later generation might exhibit more severe symptoms such as myotonia and severe muscle wasting.

Myotonic dystrophy can be transmitted both maternally and paternally, with no gender bias of inheritance except in the case of maternal transmission of congenital DM1. Interestingly, paternal transmission of the mutant allele can produce a single-generation anticipation effect. Older progeny (those born first)

tend to have milder symptoms than do their younger siblings. The hypothesis that may account for this is that germ cells produced later in life have higher number of repeats than those produced earlier due to the somatic instability of the CTG repeat in the testes.

Possible mechanisms through which the CTG repeat causes DM1

After almost ten years since the *DMPK* gene was cloned, it is still unclear how the mutation causes myotonic dystrophy. However, work from our lab and others has shed some light onto the direct effect of the expanded repeat mutation in the cell. These data show that the effect of the expanded repeat at the molecular level is three-fold: it prevents translation of the allele bearing the repeat region, it produces mRNA with extended CUG tracts, and it affects the expression of neighboring genes. Thus the repeats could cause gain of function effects at the RNA level and loss of function at the protein level, as well as affecting the transcription of other genes. Many investigators now believe that DM1 results from a combination of events involving all of these effects of the CTG expansion.

Haploinsufficiency of DMPK

DMPK mutant transcripts that contain the expanded repeat mutations are not translated; rather, the mRNA is sequestered in discrete foci tethered to the

nuclear matrix. As a result, DM1 patients cells contain only 50% of the normal level of DMPK protein (Davis, 1997). Therefore, one hypothesis to explain how the DMPK mutation causes DM1 is that it is the loss of DMPK that is detrimental to the cell.

As is described in the next section, *DMPK* *-/-* mice do not completely recapitulate the myotonic dystrophy phenotype. However, *DMPK* *-/-* mice exhibit the same peripheral muscle degeneration and cardiac conduction defect that is seen in human patients. The fact that mice both heterozygous and homozygous for *DMPK* deletion exhibit this particular phenotype strongly suggests that the cardiac defect is caused by loss of DMPK protein. By analogy, it is possible that haploinsufficiency in human DM1 patients gives rise to the cardiac conduction defects. This hypothesis is supported by the fact that the severity of this defect does not appear to be amplified with increasing CTG repeat number. Although no point mutations have been identified that cause myotonic dystrophy in humans, it has not yet been determined whether point mutations in DMPK are sufficient to cause arrhythmia and cardiomyopathy. Understanding the mechanism through which loss of DMPK leads to the cardiac phenotype will provide important clues about the role of DMPK in this particular tissue.

Gain of function of DMPK mRNA

There have been no reported cases of DM1 that are not associated with the expanded CTG repeat; no point mutations or deletions in the *DMPK* gene are known to cause this disease. This suggests that a reduction in the amount of the myotonic dystrophy protein kinase is not the only cause of myotonic dystrophy. Given the autosomal dominant inheritance and the anticipation effect in DM1, a second hypothesis to explain the effect of the expanded repeats on DMPK proposes a toxic gain of function of the DMPK mRNA.

Davis et. al. have shown that the mutant mRNA transcripts remain sequestered in the nucleus and are not translated (Davis, 1997) Furthermore, Timchenko et. al. have revealed the existence of a CUG-repeat binding protein, CUGBP1 (Timchenko, 2001). This protein is implicated in the regulation and processing of messenger RNA. It is possible that CUGBP1 is being titrated away by the vast numbers of CUG repeats in the DMPK mRNA transcripts and thus is being kept from its normal function for other genes as well as DMPK. This effect could explain the correlation between disease severity and repeat size, since transcripts with higher numbers of repeats would sequester more of the total CUGBP1. Interestingly, a cardiac-specific CUG repeat-binding protein ETR-3 (*elav*-type riboprotein 3) (Lu, 1999) has been discovered recently and may be

sequestered by the mutant transcripts in cardiac tissue. This possibility would raise important questions about the causes of the cardiac phenotype in myotonic dystrophy.

Another group of proteins that appears to be sequestered in the nucleus with mutant DMPK mRNA is the EXP group of proteins (named for triplet repeat expansion proteins). The EXP proteins are homologous to the *Drosophila muscleblind* proteins and, interestingly, are necessary for terminal differentiation of muscle tissue and photoreceptor cells in the fly (Miller, 2000). Additionally, recent *in vitro* studies have shown by electron microscopy that the expanded repeat forms hairpin turns which bind and activate the PKR kinase, which is activated by double-stranded RNA (Tian, 2000).

The discovery of this diverse collection of CUG-repeat binding proteins supports an emerging hypothesis that the expanded CUG repeat exerts a global effect on RNA processing. More research is needed to determine the full function of these various proteins and how they might be affecting myotonic dystrophy patients. Nevertheless, understanding these aspects could reveal important information about the molecular consequences of the DM1 mutation.

Effect of expansion on neighboring genes

In both mice and humans, the *DMPK* gene is located between the genes *DMWD* and *SIX5*. Cells containing the expanded repeat exhibit decreased levels of *DMPK*. Significantly, these cells also show decreased levels of the *DMWD* and *SIX5* proteins (Eriksson, 1999). As a result, changes in the expression levels of the *DMWD* and *SIX5* genes must be taken into account when studying the etiology of DM1, as they are likely to contribute to its pathology. Furthermore, *DMWD*, *DMPK*, and *SIX5* are each regulated in a tissue-specific manner and thus analysis of changes in gene expression must include a careful analysis of the normal expression for any given tissue (Eriksson, 2000)

The 3'UTR of the *DMPK* gene has been shown to contain enhancer elements for the expression of the downstream gene *SIX5* (Eriksson, 1999). Expansion of the triplet repeat has been shown to alter the local chromatin structure and suppress the expression of *SIX5*, although the degree of suppression seems to be tissue-specific. The *SIX5* protein exhibits homology to a family of homeobox proteins that are implicated in the regulation of muscle cell differentiation and sodium ion homeostasis, both of which are disrupted in DM1

(Murakami, 1998). The disruption of one *SIX5* allele in mice is sufficient to cause the formation of cataracts in mice, which suggests that the manifestation of this symptom in humans may result from the disruption of this gene (Sarkar, 2000, Klesert, 2000).

The *DMWD* gene encodes a protein with unknown function containing a proline-rich N-terminus and 4 WD-repeat domains. WD-repeats are ubiquitous in proteins with propeller-like domains (such as the G-protein β subunit) and are found in a variety of types of proteins. This protein is most prominently expressed in brain and testis, and may be involved in the pathology of DM1 in those tissues.

Mouse models of Myotonic Dystrophy

While significant contributions to the etiology of myotonic dystrophy disease have come from patient-derived material, the utility of this approach is limited by several factors. It is difficult to obtain samples from living patients and analysis of post-mortem samples is often complicated by the degenerated condition of the skeletal muscle or cardiac tissue. Other factors complicating generalized analysis include differences in allele sizes (repeat number), genetic background, patient ages, and environmental effects. Mouse models not only provide a way to circumvent these problems but also make *in vivo* experiments possible.

Mouse DMPK is highly homologous to its human counterpart, sharing 93.2% identity and 93.9% similarity at the protein level. The gene encoding murine *DMPK* is located on mouse chromosome 2, within a region syntenic with human chromosome 19q13.3. Indeed, the mouse *DMPK* gene is flanked by the homologs of the same genes that flank human *DMPK*, the *DMWD* and *SIX5* genes. Given the high degree of conservation between the sequence as well as chromosomal arrangement of mouse and human *DMPK* genes, it is therefore valid to address questions regarding mechanisms of DM1 disease pathology in the framework of a mouse model. Several different types of transgenic and knockout mice have been generated (for a summary, see Table 4).

DMPK *-/-* mice

In 1996 two groups attempted to create a myotonic dystrophy mouse model by generating *DMPK* *-/-* mice (Reddy, 1996, Jansen, 1996). Both groups deleted exons one through seven of the *DMPK* gene, which includes most of the kinase domain of DMPK. These mice are viable throughout development although they do show slightly reduced fertility. This phenotype is most likely caused by failure to thrive of the mutant neonates rather than fertility problems similar to those seen in female DM1 patients. Myotonia is notably absent from the phenotype of the *DMPK* *-/-* mice although they do exhibit other symptoms that are similar to human myotonic dystrophy (Table 3) including a progressive

muscle myopathy and cardiac conduction defects. *DMPK* *-/-* mice have no skeletal muscle pathology at three months of age, however, by eleven months these mice have muscle pathology comparable with that seen in DM1 patients. The skeletal muscles of the aging mice exhibit extensive fibrosis and ultrastructural disorganization, reduced muscle strength, and increased regeneration (as measured by *MyoD* expression) (Reddy, 1996).

The mouse phenotype that is most strikingly similar to the human DM condition is the cardiac conduction defect. The fact that this conduction abnormality is sensitive to DMPK dosage has been thoroughly demonstrated in the *DMPK* *-/-* mice. The cardiac conduction defect is reproduced in mice both heterozygous and homozygous for the disrupted *DMPK* allele; these mice show the same elongation of the PR interval of the EKG trace when compared to wild-type controls (Table 3) (Berul, 1999), and much of this delay has been traced to the Bundle of His (Saba, 1999). As the expanded CTG repeat is not present in these mice, it is clear that DMPK is necessary for proper cardiac function, suggesting that the cardiac phenotype in mice results from loss of DMPK protein.

Table 3: Cardiac conduction defect in myotonic dystrophy mouse model			
	DMPK + / +	DMPK + / -	DMPK - / -
PR interval (ms)	34	48	48
Mean Age (weeks)	67.6	73.5	68.5
n	17	11	17

DMPK overexpression mice

In addition to the *DMPK* *-/-* mice, transgenic mice that express elevated levels of DMPK have also been generated (Jansen, 1996). The transgene used in these experiments contained the human *DMPK* gene, with 20 CTG repeats (below the disease-causing threshold in humans) in the 3'UTR as well as the last exon of the gene 5' to the *DMPK* gene, *DMWD*. The *DMPK* transgenic mice had apparently normal skeletal muscle structure and function and no measurable difference in cardiac function. However, histological analysis revealed that these mice developed an abnormal cardiac morphology, including whorling of the myocardium, hypertrophy, and fibrosis. As cardiac function in these mice is normal, the relationship between this phenomenon and DM1 has not been determined.

CTG repeat expansion mice

As the family of triplet repeat diseases expanded in the early 1990s several groups attempted to generate mouse models with expanded repeats, including models for Kennedy's disease, SCA1, Huntington's disease, and Machado-Joseph disease (SCA3). These mouse models failed to exhibit the high levels of expanded repeat instability in human patients. The CTG expansion

transgenic mice described by Monckton, et. al. represented the first successful attempt to create a mouse model that exhibited intergenerational repeat length variation (Monckton, 1997). However, unlike CTG repeat tract transmission in humans, in which the number of repeats always increases, repeat number both increased and decreased in these mice. These experiments were hampered by the fact that the males were infertile due to gross testicular atrophy. Gourdon, et. al. also made CTG repeat mice using a transgene that contained the *DMPK* gene from a mildly affected DM patient (Gourdon, 1997). This 45 kb transgene contained all three genes in the 19q13.3 region, including 55 repeats in the 3'UTR of *DMPK*. No phenotype or genetic instability was demonstrated in these mice; perhaps the low number of repeats is not unstable enough to show dramatic expansion. In fact, mice that were subsequently generated with more than 300 CTG repeats show measurable intergenerational instability of the repeat in tissues and in sperm, similar to that observed in humans. Other aspects of the phenotype have not yet been addressed in these mice and it is unclear whether they develop DM1-like pathology.

Recently, Mankodi et. al. described a mouse that shows expression of a transgene containing 250 repeats. The transgene contained skeletal muscle actin under the control of a skeletal muscle specific promoter and included 250 CTG repeats in the 3'UTR. These mice developed myotonia and skeletal muscle myopathy similar to that seen in DM1. This interesting result argues that mRNA containing 250 CTG repeats is sufficient to cause myotonia and muscle

pathology like that observed in myotonic dystrophy, regardless of the gene in which they occur. These mice do not exhibit cardiac conduction defects and have not been tested for some of the other various symptoms of DM1, such as cataracts.

Table 4: Comparison of human DM1 and mouse models								
	human	mouse						
	DM1	DMPK +/-	DMPK +/-	DMPK over-expressed	55 CTG repeats	162 CTG repeats	250 CTG repeats	300 CTG repeats
increased muscle regeneration	+	+	+	-	-	-	-	
*muscle fiber size variation	+	+	+ / -	-	-	-	+	
*fibrosis	+	+	+ / -	-	-	-		
*central nuclei	+	+	+ / -	-	-	-	+	
*ring fibers	+	+	+ / -	-	-	-	+	
*ultrastructural alterations	+	+	+ / -	n/a	-	n/a	n/a	
muscle weakness	+	+	n/a	-	-	-	n/a	
elevated cytosolic calcium	+	+	n/a	n/a	-	n/a	n/a	
cardiomyopathy	+	+	+	+ / -	-	-	-	
myotonia	+	-	-	-	-	-	+	
congenital variant	+	-	-	n/a	-	n/a	n/a	
cataracts	+	n/a	n/a	-	-	-	n/a	
testicular atrophy	+	-	-	-	-	++	n/a	
Intergenerational instability	+	n/a	n/a	n/a	-	+	+	+

n/a, not addressed or not applicable

*muscle histopathology characteristic of degeneration

Interpretation of mouse models

Table 4 shows a comparison of the phenotype of the various mouse models and symptoms cataloged in human myotonic dystrophy patients. The phenotype of the *DMPK* *-/-* mice supports the hypothesis that dosage of DMPK is important for proper cardiac and skeletal muscle function, and the phenotype of the repeat expansion mice supports the hypothesis that the repeat expansion is a cause of DM1 symptoms. However, while not all mice have yet been thoroughly tested for all the various manifestations of DM1, it is evident that no mouse model to date exactly recapitulates the entire spectrum of DM1 symptoms.

The data from the various mouse models must be interpreted with caution due to potential differences in physiology between mouse and human. These differences can be illustrated by the *mdx* mouse, which is the model for Duchenne's muscular dystrophy. Duchenne's muscular dystrophy patients harbor mutations in the *dystrophin* gene and exhibit symptoms such as extensive progressive wasting of proximal muscles, progressive scoliosis and respiratory difficulties, and severe cardiomyopathy (Harper, 1989). The *mdx* mice, that carry a point mutation in the *dystrophin* gene, show a very mild phenotype of slight muscle fiber necrosis starting at two weeks of age. Unlike humans, these mice maintain skeletal muscle integrity. This is thought to be due to increased regenerative capacity of the mice, as these mice appear hypertrophic in that they have a 25% increase in the number of muscle fibers and a 1.7 fold increase in muscle compared to wild-type mice. It was not until Megeney, et. al. generated

mice that are mutant for both the *dystrophin* gene and the *MyoD* gene, which encodes a muscle specific transcription factor, that the mouse model accurately reproduced the human Duchenne's phenotype (Megenny, 1996). The *mdx/MyoD* *-/-* mice show many of the symptoms of Duchenne's, including severe curvature of the spine, reduction in the number of satellite cells, significant reduction in the mass and number of skeletal muscle fibers, and premature death at twelve months of age due to loss of muscle mass (Megenny, 1996). As these data indicate a difference in muscle regeneration rate or capacity between mice and humans, differences in physiology must be taken into account when comparing the effect of a given gene disruption in mice and humans.

Age span is another factor that may affect the pathology of the knockout mice. Myotonic dystrophy is an adult-onset progressive disease. Symptoms are mild at the beginning and can take years to worsen appreciably (Harper, 1989). The late onset of the disease and the relatively short lifespan (approximately two years) of mice in general may be a factor in the mildness of the muscle myopathy of the *DMPK* *-/-* mice. The mice begin to show measurable deterioration at 11 months to one year of age but are usually dead from old age by two years of age; therefore long term analysis of muscle deterioration is not possible.

Nevertheless, the fact that the *DMPK* *-/-* and transgenic mice do not exactly recapitulate the human disease may eventually help us to determine how

each effect of the repeat expansion contributes to DM1 pathology and give us clues to the role of DMPK in cardiac and skeletal muscle.

DMPK protein

Although the function of DMPK is not known, the phenotype associated with the *DMPK* *-/-* mice clearly indicates that lack of the proper level of DMPK has serious molecular consequences in skeletal and cardiac muscle.

DMPK is most highly expressed in the heart, skeletal muscle type I (slow, oxidative) fibers, smooth muscle, and brain, the tissues most affected in myotonic dystrophy patients. It is also expressed at lower levels in skeletal muscle type II (fast, glycolytic) fibers, lung, kidney, testis, retina, and liver. In the heart, DMPK localizes to intercalated discs, and to the sarcoplasmic reticulum near gap junctions (van der Ven, 1993), (Whiting, 1995, Ueda, 1998).

Immunohistochemistry experiments with various antibodies indicated that DMPK localizes near the sarcoplasmic reticulum lateral cisternae/triads in skeletal muscle (Shimokawa, 1997, Salvatori, 1997) and, for one splice form, to the mitochondria in cultured myotubes (BM Davis, personal communication). The significance of these various observations is yet unknown, although each area of localization represents a site of dense ion channel clustering and this may prove to be significant for the function of DMPK.

Structural Domains

Analysis of the *DMPK* protein sequence predicts a protein with several different domains. These include a 40 amino acid N-terminal leucine-rich region, a serine/threonine kinase catalytic domain, a coiled coil domain, and, in one splice form, a C-terminal hydrophobic domain.

Exons 2-8 encode the catalytic domain of DMPK. This region contains eleven subdomains characteristic for members of the serine/threonine-type subfamily of kinases (Hanks, 1988). Protein kinase A (PKA) and protein kinase C (PKC) show high sequence homology to DMPK. More recently, DMPK has been shown to share significant sequence homology with a novel class of multidomain protein kinases, the Rho-kinases. Members of this family are implicated in regulation of actin-myosin contractility and of cell size and shape in a variety of organisms. Family members include *Neurospora* Cot1, *Drosophila* Wts and Ghengis Khan, rat ROK α , human p160^{ROCK}, human PK418, *Caenorhabditis elegans* LET-502, murine citron Rho-interacting kinase (CRIK) and rat DMPK-related Cdc42-binding kinase (MRCK) (Zhao, 1997) (Shimizu, 2000). Like the homology between PKA and PKC, most of the homology between DMPK and the Rho kinase family members exists in the kinase domain. However, although the regions of homology outside this domain are small, these sequences are significant as they represent the only regions in DMPK outside the kinase domain that are homologous to other known proteins.

Exons 9-12 contain an α -helical region with weak homology to myosin heavy chain and other myofibrillar and filamentous proteins. This region may be involved in the formation of coiled-coil structures or self-association of the enzyme. Exons 12-15 encode a region in which alternative splicing can result in various C-termini (Figure 2). These differing C-termini may convey a different subcellular localization or function to the resultant splice forms of DMPK.

Overall, the analysis of DMPK sequence has provided few clues about DMPK function, substrate specificity, and potential mechanisms of regulation.

Alternative Splice forms

Multiple DMPK variants are produced by alternative splicing of the *DMPK* gene. In humans and in mice there exist multiple isoforms of DMPK (Figure 2) (Fu, 1992, Fu, 1993, Groenen, 2000). To date, the significance and function of each DMPK alternative splice form have not been determined.

Each tissue examined contains the full-length DMPK isoform and one or more alternatively spliced variants of DMPK (Groenen, 2000). One DMPK isoform that occurs with frequency equal to the full-length transcript harbors the deletion of the first four bases in exon 14. This deletion results in a protein

Figure 2. The DMPK exon arrangement and splice forms

DMPK has fifteen exons that can be alternately spliced to produce six isoforms that have been found in both human and mouse. DMPK A and B are the most common isoforms found in skeletal muscle. DMPK C and D appear to be specific to smooth muscle (Groenen et. al. 2000).

	MOUSE	HUMAN
	69.6 kDa pI 4.69	69.4 kDa pI 4.84
	69.3 kDa pI 4.69	69.0 kDa pI 4.84
	70.3 kDa pI 4.67	69.9 kDa pI 4.68
	70.0 kDa pI 4.67	69.9 kDa pI 4.68
	60.2 kDa pI 4.48	5.98 kDa pI 4.55
	59.8 kDa pI 4.48	59.4 kDa pI 4.55



DMPK A
full-length



DMPK B
15 bp exon 8 splice



DMPK C
4 bp exon 14 splice



DMPK D
15 bp exon 8 splice
4 bp exon 14 splice



DMPK E
exon 13/14 splice



DMPK F
15 bp exon 8 splice
exon 13/14 splice

- leucine-rich region
- catalytic domain
- alpha-helical region
- hydrophobic tail A
- tail B
- VSGGG motif
- putative signal peptide

variant with a less hydrophobic C-terminus than in the full-length DMPK protein. Similarly, another alternatively spliced DMPK variant contains a deletion of 15 nucleotides in exon 8. These two alternative forms of exon 8 can be combined with the exon 14 splice forms to produce further variance. Another variant of DMPK, most common in smooth muscle tissue and, to a lesser extent, in heart, arises as a result of splicing that fuses exon 12 directly to exon 15, resulting in the deletion of exons 13 and 14. This causes a frameshift that terminates translation directly at the beginning of exon 15, therefore resulting in a truncated C-terminal end. Deletion of exon 13 alone has also been observed, primarily in brain-specific transcripts.

Potentially, each DMPK splice form may have a specific function in the cell distinct from that of the full-length protein. In support of this hypothesis, the full-length kinase is distributed uniformly throughout the cytoplasm in cultured human myoblasts, while the exon 14 spliced form with the alternate C-terminus localizes to the periphery of mitochondria (BM Davis et. al., manuscript in preparation). The differential localization of DMPK splice form variants suggests that the DMPK isoforms have distinct properties, and potentially distinct substrate specificity. Characterizing the properties of the DMPK variants in each of the tissues where DMPK is expressed is absolutely essential in order to understand fully the *in vivo* role of DMPK and how its mutation leads to myotonic dystrophy.

Substrate Specificity

Currently, only *in vitro* data are available about direct targets of DMPK. DMPK has been shown to phosphorylate a number of different proteins, each with interesting implications for myotonic dystrophy. These include: phospholemman, a membrane substrate for phosphorylation by PKA and PKC (Mounsey, 2000); the myosin-binding subunit of myosin phosphatase, a target of Rho-kinase (Muranyi, 2001); the CUG-repeat binding protein CUGBP1 in a proposed autoregulation mechanism (Roberts, 1997); the β -subunit of the dihydropyridine receptor, which is located at the triads in skeletal muscle and thus co-localizes with DMPK; the tetrodotoxin (TTX) u-conotoxin sensitive skeletal muscle sodium channel, which correlates nicely with the fact that DMPK has been shown to be involved in calcium homeostasis in skeletal muscle (Benders, 1997). Furthermore, it has been demonstrated that DMPK will phosphorylate known targets of PKC, but not those of PKA, and that DMPK activity is inhibited by known inhibitors of PKC, but not those of PKA. These data offer clues about the consensus phosphorylation site of DMPK.

Our group and others have performed assays in order to identify substrates of DMPK. These experiments have demonstrated that expressed recombinant DMPK has a relatively low specific activity compared to other kinases, that is, the protein will phosphorylate most generic kinase substrates *in vitro* at a low level (Dunne, 1994, Bush, 2000). This is true for a number of

different DMPK constructs expressed in bacteria, baculovirus, or mammalian cells. This aspect of DMPK biochemistry could be explained by the fact that for some kinases specificity is conferred by compartmentalization in the cell, that is, substrates are targeted to the kinase rather than the other way around. Once removed from this context such enzymes can behave promiscuously toward other proteins *in vitro*. This has complicated traditional protein-interaction assays such as two-hybrid and co-immunoprecipitation, since high specificity is required. We also attempted screening of a heart expression library with active kinase and radioactive phosphate, an assay that has worked well for CDK/cyclin combinations. The result was low level phosphorylation of many proteins; no one protein stood out as being good substrate candidate. We assume the result would be the same for protein CHIP analysis, although this has not been attempted.

Summary

Myotonic dystrophy is a variable and complex disease in which symptoms are caused by a CTG repeat expansion. No mouse model has yet been produced that successfully duplicates the DM1 phenotype, and the normal function of the myotonic dystrophy protein kinase is currently unknown. The various manifestations of DM1 may be attributed to the combined effect of the disruption by the CTG repeat expansion of a collection of genes and gene products. The picture is not complete, however. Further studies of the effect(s)

of the CTG repeat on the surrounding genes, the effect(s) of the CUG repeat in the nucleus, and the normal function of DMPK are needed.

This chapter has outlined the various ways in which the effects of the CTG repeat are being investigated. Each avenue of research is providing valuable clues to the puzzle of the myotonic dystrophy disease mechanism. To date no single investigative approach can encompass the entirety of the effects of the expanded CTG repeat on the cell.

It has been shown that DMPK has a significant role in maintaining proper skeletal and cardiac function. The next chapter describes experiments to identify proteins with altered biochemical properties in *DMPK* *-/-* mouse tissue. Thorough analysis of the proteome, the full protein complement expressed in an organism or cell type, of *DMPK* *-/-* mutant cells would reveal all the ways in which a cell type or tissue is altered due to the loss of this kinase. In a proteomics-based approach that utilizes two-dimensional SDS-PAGE and mass spectrometry, I will discuss the isolation of two proteins that are affected by the loss of DMPK and their identification as fatty acid binding proteins.

References

1. Harper, P. S., *Myotonic Dystrophy*. 1989, W. B. Saunders Company: London.
2. Meola, G., 2000. Myotonic dystrophies *Curr Opin Neurol* **13**(5): p. 519-525.
3. Ueda, H., M. Shimokawa, M. Yamamoto, N. Kameda, H. Mizusawa, T. Baba, N. Terada, Y. Fujii, S. Ohno, S. Ishiura and T. Kobayashi, 1999. Decreased expression of myotonic dystrophy protein kinase and disorganization of sarcoplasmic reticulum in skeletal muscle of myotonic dystrophy *J Neurol Sci* **162**(1): p. 38-50.
4. Reddy, S., D. B. Smith, M. M. Rich, J. M. Leferovich, P. Reilly, B. M. Davis, K. Tran, H. Rayburn, R. Bronson, D. Cros, R. J. Balice-Gordon and D. Housman, 1996. Mice lacking the myotonic dystrophy protein kinase develop a late onset progressive myopathy *Nature Genetics* **13**: p. 325-335.
5. Nguyen H.H., W. J. T. I., Holmes D. R. Jr., Edwards W. D., 1988. Pathology of the cardiac conduction system in myotonic dystrophy: a study of 12 cases *Journal of the American College of Cardiology* **11**(3): p. 662-671.
6. Berul, C. I., C. T. Maguire, M. J. Aronovitz, J. Greenwood, C. Miller, J. Gehrmann, D. Housman, M. E. Mendelsohn and S. Reddy, 1999. DMPK dosage alterations result in atrioventricular conduction abnormalities in a mouse myotonic dystrophy model *J Clin Invest* **103**(4): p. R1-7.
7. Fragola, P. V., M. Luzi, L. Calo, G. Antonini, M. Borzi, D. Frongillo and D. Cannata, 1994. Cardiac involvement in myotonic dystrophy *Am J Cardiol* **74**(10): p. 1070-1072.
8. Berul, C. I., C. T. Maguire, J. Gehrmann and S. Reddy, 2000. Progressive atrioventricular conduction block in a mouse myotonic dystrophy model *J Interv Card Electrophysiol* **4**(2): p. 351-358.
9. Saba, S., B. A. Vanderbrink, B. Luciano, M. J. Aronovitz, C. I. Berul, S. Reddy, D. Housman, M. E. Mendelsohn, N. A. Estes, 3rd and P. J. Wang, 1999. Localization of the sites of conduction abnormalities in a mouse model of

myotonic dystrophy [see comments] *J Cardiovasc Electrophysiol* **10**(9): p. 1214-1220.

10. Ricker, K., M. C. Koch, F. Lehmann-Horn, D. Pongratz, N. Speich, K. Reiners, C. Schneider and R. T. Moxley, 3rd, 1995. Proximal myotonic myopathy. Clinical features of a multisystem disorder similar to myotonic dystrophy *Arch Neurol* **52**(1): p. 25-31.

11. Udd, B., R. Krahe, C. Wallgren-Pettersson, B. Falck and H. Kalimo, 1997. Proximal myotonic dystrophy--a family with autosomal dominant muscular dystrophy, cataracts, hearing loss and hypogonadism: heterogeneity of proximal myotonic syndromes? *Neuromuscul Disord* **7**(4): p. 217-228.

12. Ranum, L. P., P. F. Rasmussen, K. A. Benzow, M. D. Koob and J. W. Day, 1998. Genetic mapping of a second myotonic dystrophy locus *Muscle Nerve* **21**(7): p. 954-957.

13. Day, J. W., R. Roelofs, B. Leroy, I. Pech, K. Benzow and L. P. Ranum, 1999. Clinical and genetic characteristics of a five-generation family with a novel form of myotonic dystrophy (DM2) *Neuromuscul Disord* **9**(1): p. 19-27.

14. Harper, P. S., 1997. Trinucleotide repeat disorders *J Inherit Metab Dis* **20**(2): p. 122-124.

15. Brook, J. D., McCurrah, M. E., Harley, H.G., Buckler, A. J., Church, D., Aburatani, H., Hunter, K., Stanton, V. P., Thirion, J. P., Hudson, T., Sohn, R., Zemelman, B., Snell, R. G., Rundle, S. A., Crow, S., Davies, J., Shelbourne, P., Buxton, J., Jones, C., Juxenon, V., Johnson, K., Harper, P. S., Shaw, D. J., Housman, D. E., 1992. Molecular basis of myotonic dystrophy: expansion of a triplet (CTG) repeat at the 3' end of a transcript encoding a protein kinase family member *Cell* **68**: p. 799-808.

16. Fu, Y. H., Pizzuti, A., Fenwick, R. G. Jr., King, J., Rajnarayan, S., Dunne, P. W., Dubel, J., Nasser, G. A., Ashizawa, T., De Jong, P., Wieringa, B., Korneluk, R. G., Perryman, B., Epstein, H. F., Caskey, C. T., 1992. An unstable triplet repeat in a gene related to myotonic muscular dystrophy *Science* **255**: p. 1256-1258.

17. Harley, H. G., Brook, J. D., Rundle, S. A., Crow, S., Reardon, W., Buckler, A. J., Harper, P. S., Housman, D. E., Shaw, D. J., 1992. Expansion of an unstable DNA region and phenotypic variation in myotonic dystrophy *Nature* **355**: p. 545-546.
18. Mahadevan, M., Tsilfidis, C., Sabourin, L., Shutler, G., Amemiya, C., Jansen, G., Neville, C., Narang, M., Barcelo, J., O'Hoy, K., LeBlond, S., Earle-MacDonald, J., de Jong, P. J., Wieringa, B., Korneluk, R. G., 1992. Myotonic dystrophy mutation: an unstable CTG repeat in the 3' untranslated region of the gene *Science* **255**(1253-1255): p.
19. Wilmot, G. R., Warren, S. T., *Genetic Instabilities and Hereditary Neurological Diseases*. 1998, Academic Press: San Diego, CA.
20. Klesert, T. R., A. D. Otten, T. D. Bird and S. J. Tapscott, 1997. Trinucleotide repeat expansion at the myotonic dystrophy locus reduces expression of DMAHP *J Muscle Res Cell Motil* **18**(4): p. 429-440.
21. Davis, B. M., M. E. McCurrach, K. L. Taneja, R. H. Singer and D. E. Housman, 1997. Expansion of a CUG trinucleotide repeat in the 3' untranslated region of myotonic dystrophy protein kinase transcripts results in nuclear retention of transcripts *Proc Natl Acad Sci U S A* **94**(14): p. 7394-7399.
22. Timchenko, N. A., Z. J. Cai, A. L. Welm, S. Reddy, T. Ashizawa and L. T. Timchenko, 2001. RNA CUG repeats sequester CUGBP1 and alter protein levels and activity of CUGBP1 *J Biol Chem* **276**(11): p. 7820-7826.
23. Lu, X., N. A. Timchenko and L. T. Timchenko, 1999. Cardiac elav-type RNA-binding protein (ETR-3) binds to RNA CUG repeats expanded in myotonic dystrophy *Hum Mol Genet* **8**(1): p. 53-60.
24. Miller, J. W., C. R. Urbinati, P. Teng-Umnuay, M. G. Stenberg, B. J. Byrne, C. A. Thornton and M. S. Swanson, 2000. Recruitment of human muscleblind proteins to (CUG)(n) expansions associated with myotonic dystrophy *Embo J* **19**(17): p. 4439-4448.

25. Tian, B., R. J. White, T. Xia, S. Welle, D. H. Turner, M. B. Mathews and C. A. Thornton, 2000. Expanded CUG repeat RNAs form hairpins that activate the double-stranded RNA-dependent protein kinase PKR *RNA* **6**(1): p. 79-87.
26. Eriksson, M., T. Ansved, L. Edstrom, M. Anvret and N. Carey, 1999. Simultaneous analysis of expression of the three myotonic dystrophy locus genes in adult skeletal muscle samples: the CTG expansion correlates inversely with DMPK and 59 expression levels, but not DMAHP levels *Hum Mol Genet* **8**(6): p. 1053-1060.
27. Eriksson, M., T. Ansved, L. Edstrom, D. J. Wells, D. J. Watt, M. Anvret and N. Carey, 2000. Independent regulation of the myotonic dystrophy 1 locus genes postnatally and during adult skeletal muscle regeneration *J Biol Chem* **275**(26): p. 19964-19969.
28. Murakami, Y., H. Ohto, U. Ikeda, K. Shimada, T. Momoi and K. Kawakami, 1998. Promoter of mDMAHP/Six5: differential utilization of multiple transcription initiation sites and positive/negative regulatory elements *Hum Mol Genet* **7**(13): p. 2103-2112.
29. Sarkar, P. S., B. Appukuttan, J. Han, Y. Ito, C. Ai, W. Tsai, Y. Chai, J. T. Stout and S. Reddy, 2000. Heterozygous loss of Six5 in mice is sufficient to cause ocular cataracts *Nat Genet* **25**(1): p. 110-114.
30. Klesert, T. R., D. H. Cho, J. I. Clark, J. Maylie, J. Adelman, L. Snider, E. C. Yuen, P. Soriano and S. J. Tapscott, 2000. Mice deficient in Six5 develop cataracts: implications for myotonic dystrophy *Nat Genet* **25**(1): p. 105-109.
31. Jansen, G., P. J. Groenen, D. Bachner, P. H. Jap, M. Coerwinkel, F. Oerlemans, W. van den Broek, B. Gohlsch, D. Pette, J. J. Plomp, P. C. Molenaar, M. G. Nederhoff, C. J. van Echteld, M. Dekker, A. Berns, H. Hameister and B. Wieringa, 1996. Abnormal myotonic dystrophy protein kinase levels produce only mild myopathy in mice *Nat Genet* **13**(3): p. 316-324.
32. Monckton, D. G., M. I. Coolbaugh, K. T. Ashizawa, M. J. Siciliano and C. T. Caskey, 1997. Hypermutable myotonic dystrophy CTG repeats in transgenic mice *Nat Genet* **15**(2): p. 193-196.

33. Gourdon, G., Radvanyi, F., Lia, A. S., Duros, C., Blanche, M., Abitbol, M., Junien, C., and Hofmann Radvanyi, H., 1997. Moderate intergenerational and somatic instability of a 55 CTG repeat in transgenic mice *Nature Genetics* **15**: p. 190-192.
34. Megeney, L. A., B. Kablar, K. Garrett, J. E. Anderson and M. A. Rudnicki, 1996. MyoD is required for myogenic stem cell function in adult skeletal muscle *Genes Dev* **10**(10): p. 1173-1183.
35. van der Ven, P. F., G. Jansen, T. H. van Kuppevelt, M. B. Perryman, M. Lupa, P. W. Dunne, H. J. ter Laak, P. H. Jap, J. H. Veerkamp, H. F. Epstein and et al., 1993. Myotonic dystrophy kinase is a component of neuromuscular junctions *Genomics* **18**(2): p. 340-348.
36. Whiting, E. J., J. D. Waring, K. Tamai, M. J. Somerville, M. Hincke, W. A. Staines, J. E. Ikeda and R. G. Korneluk, 1995. Characterization of myotonic dystrophy kinase (DMK) protein in human and rodent muscle and central nervous tissue *Hum Mol Genet* **4**(6): p. 1073-1076.
37. Ueda, H., N. Kameda, T. Baba, N. Terada, M. Shimokawa, M. Yamamoto, S. Ishiura, T. Kobayashi and S. Ohno, 1998. Immunolocalization of myotonic dystrophy protein kinase in corbular and junctional sarcoplasmic reticulum of human cardiac muscle *Proc Natl Acad Sci U S A* **95**(9): p. 5015-5020.
38. Shimokawa, M., Ishiura, S., Kameda, N., Yamamoto, M., Sasagawa, N., Saitoh, N., Sorimachi, H., Ueda, H., Ohno, S., Suzuki, K., Kobayashi, T., 1997. Novel isoform of myotonin protein kinase: gene product of myotonic dystrophy is located in the sarcoplasmic reticulum of skeletal muscle *American Journal of Pathology* **150**: p. 1285-1295.
39. Salvatori, S., Biral, D., Furlan, S., Marin, O, 1997. Evidence for localization of the myotonic dystrophy protein kinase to the terminal cisternae of the sarcoplasmic reticulum *Journal of Muscle Research and Cell Motility* **18**: p. 1-12.
40. Hanks, S. K., Quinn, A. M., and Hunter, T., 1988. The protein kinase family: conserved features and deduced phylogeny of the catalytic domains *Science* **241**: p. 42-52.

41. Zhao, Y., Loyer, P., Li, H., Valentine, V., Kidd, V., and Kraft, A. S., 1997. *Journal of Biological Chemistry* **272**: p. 10013-10020.
42. Shimizu, M., Wang, E. T., Walch, P. W., Dunne and H. F. Epstein, 2000. Rac-1 and Raf-1 kinases, components of distinct signaling pathways, activate myotonic dystrophy protein kinase *FEBS Lett* **475**(3): p. 273-277.
43. Fu, Y. H., Friedman, S., Richards, J. A., Pearlman, R. A., Gibbs, A., Pizzuti, T., Ashizawa, M. B., Perryman, G., Scarlato, R. G., Fenwick, Jr. and et al., 1993. Decreased expression of myotonin-protein kinase messenger RNA and protein in adult form of myotonic dystrophy *Science* **260**(5105): p. 235-238.
44. Groenen, P. J., Wansink, M., Coerwinkel, W. van den Broek, G. Jansen and B. Wieringa, 2000. Constitutive and regulated modes of splicing produce six major myotonic dystrophy protein kinase (DMPK) isoforms with distinct properties *Hum Mol Genet* **9**(4): p. 605-616.
45. Mounsey, J. P., John, 3rd, S. M., Helmke, E. W., Bush, J., Gilbert, A. D., Roses, M. B., Perryman, L. R., Jones and J. R. Moorman, 2000. Phospholemman is a substrate for myotonic dystrophy protein kinase *J Biol Chem* **275**(30): p. 23362-23367.
46. Muranyi, A., Zhang, F., Liu, K., Hirano, M., Ito, H. F. Epstein and D. J. Hartshorne, 2001. Myotonic dystrophy protein kinase phosphorylates the myosin phosphatase targeting subunit and inhibits myosin phosphatase activity *FEBS Lett* **493**(2-3): p. 80-84.
47. Roberts, R., Timchenko, J. W., Miller, S., Reddy, C. T., Caskey, M. S., Swanson and L. T. Timchenko, 1997. Altered phosphorylation and intracellular distribution of a (CUG)_n triplet repeat RNA-binding protein in patients with myotonic dystrophy and in myotonin protein kinase knockout mice *Proc Natl Acad Sci U S A* **94**(24): p. 13221-13226.
48. Benders, A. A., Groenen, F. T., Oerlemans, J. H., Veerkamp and B. Wieringa, 1997. Myotonic dystrophy protein kinase is involved in the modulation of the Ca²⁺ homeostasis in skeletal muscle cells *Hum Genet* **100**(5-6): p. 611-619.

49. Dunne, P. W., E. T. Walch and H. F. Epstein, 1994. Phosphorylation reactions of recombinant human myotonic dystrophy protein kinase and their inhibition *Biochem Biophys Res Commun* **203**(3): p. 1365-1370.

50. Bush, E. W., S. M. Helmke, R. A. Birnbaum and M. B. Perryman, 2000. Myotonic dystrophy protein kinase domains mediate localization, oligomerization, novel catalytic activity, and autoinhibition *Biochemistry* **39**(29): p. 8480-8490.

**Chapter 2: Proteomic analysis of proteins affected by the absence of the
myotonic dystrophy protein kinase (DMPK) in *DMPK*^{-/-} mice**

Chapter 2: Proteomic analysis of proteins affected by the absence of the myotonic dystrophy protein kinase (DMPK) in *DMPK*^{-/-} mice

Abstract

Myotonic dystrophy type 1 (DM1) patients harbor an expanded CTG repeat in the 3'UTR of the gene encoding the myotonic dystrophy protein kinase (DMPK). This mutation appears to have several mechanistically independent consequences, one of which is a reduction in DMPK protein production. DMPK insufficiency likely accounts for the cardiac pathology associated with DM1, and potentially contributes to pathology in skeletal muscle and brain as well. As the molecular targets of DMPK and the pathway in which DMPK acts have not been identified, it is not known why the absence of this protein results in cardiac abnormalities and a loss of muscle integrity. A proteomics-based approach was utilized to search for targets of DMPK as well as to identify other proteins whose expression is altered in response to DMPK deficiency. The proteins of cardiac tissue from wild-type and *DMPK*^{-/-} mice were compared on 2-dimensional SDS-PAGE gels and several proteins with altered mobility were identified. Two of these proteins were selected for further investigation and were identified by mass spectrometry. Both were identified as fatty acid binding proteins. These proteins may contribute to the pathology of DM1.

Proteomics

The completion of the human genome project, as well as the completion of the genomes of a number of other organisms, provides a resource for understanding physiology. Proteomics utilizes the power of genomics and expands it to ask questions about physiology at a different level, the protein level. The term proteome has been defined as the protein complement expressed by the genome of an organism, or, in multicellular organisms, as the protein complement expressed by a tissue or differentiated cells (Wilkins, 1996). This definition takes into account all of the different protein species present due to tissue-specific expression, levels of expression of individual genes, splice variants, and post-translational modifications. Proteome research involves the combined applications of advanced separation techniques, mass spectrometry, and bioinformatics tools to characterize proteins in complex mixtures.

Separation techniques

Two-dimensional SDS-polyacrylamide gel electrophoresis (hereafter, 2-DE) was first described in 1969 (Macko, 1969), and the slightly altered method that most resembles methods currently in use were described in 1975 (Klose, 1975, O'Farrell, 1975). 2-DE is currently the most widely used method of separating complex protein mixtures, and the only method currently capable of

separating thousands of proteins individually. In the first dimension, isoelectric focusing, proteins are separated according to their isoelectric point (pI). In the second dimension of 2-DE, SDS-PAGE, proteins are separated according to their apparent molecular weight. This technique produces gels in which thousands of individual proteins are separated into discrete protein spots. One such example is found in Figure 1, a 2-DE gel of skeletal muscle proteins. Either dimension is capable of resolving 100-200 protein species, but the resolving power of the combined techniques is approximately the product of the resolving power of the individual techniques. Up to 10,000 individual protein species have been resolved in a single gel (Klose, 1995). By comparing 2-DE protein patterns from different tissues, cell fractions, and developmental stages, proteins can be characterized according to different biological parameters. Any modification that results in a change in apparent molecular weight or pI can be visualized on these gels (Figure 1).

Visualization methods

Coomassie and silver staining, autoradiography, and fluorescent protein stains such as Sypro Red can all be used for visualization of the full range of proteins on a 2-DE gel. Each has its own particular advantages and disadvantages. Coomassie blue staining is preferred for use with proteins to be identified by mass spectrometry as the stain can be entirely removed during preparation of the peptides. However, the detection limit of this technique is

Figure 1. Two dimensional gel electrophoresis (2-DE)

A) 2-DE gel of skeletal muscle (gastrocnemius and soleus) from mouse.

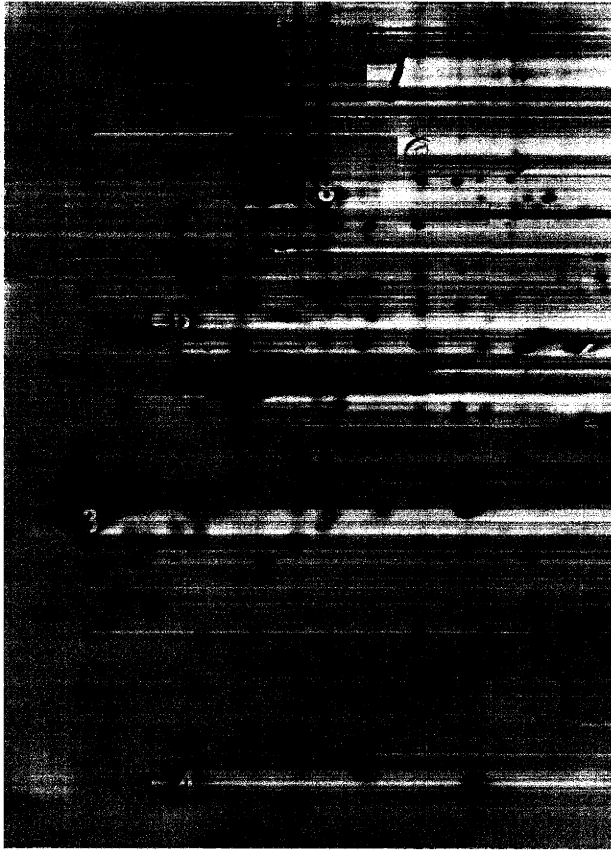
Molecular weight is represented by the vertical direction and pH by the horizontal. Identifications of major muscle proteins are listed based on comparison with online 2D gel databases at

http://ca.expasy.org/cgi-bin/map2/def?MUSCLE_MOUSE

The spot labeled number three was cut out and analyzed by matrix-assisted laser desorption ionization time-of-flight (MALDI-TOF) mass spectrometry and identity was confirmed to be α -tropomyosin.

B) A sample list of modifications causing a change in apparent molecular weight or isoelectric point, including splice variants and post-translational modifications. Differences in levels of expression can also be detected by laser densitometry comparison.

A



1. alpha-actin-1
2. beta-enolase
3. alpha-tropomyosin
4. myosin light chain
5. creatine kinase
6. ATP synthase
7. myosin heavy chain
(approximate area)
8. serum albumin

B

Modifications causing a change in molecular weight (MW) or isoelectric point (pI)

Alternate mRNA editing resulting in multiple isoforms, N-myristoylation, glycosylation, hydroxylation, N-methylation, C-terminal GPI anchor, signal peptidase site, prenylation, phosphorylation, acetylation, alkylation, sulfation, carboxymethylation, carboxylation, sialation.

roughly 100 ng protein, therefore, it is not extremely sensitive and can only be used to visualize proteins that are present in high concentration, such as those from an immunoprecipitation (IP) experiment. Silver staining is a common method for visualizing proteins in complex mixtures. Most silver stain protocols will stain proteins present in concentrations as low as 1ng (Merril, 1987). The disadvantages of silver staining technique are that it does not stain all proteins with equal efficiency, and that it is hard to remove subsequently and thus can create background noise in mass spectrometry analysis.

2-DE gels are often blotted to membrane before visualization. Fluorescent dyes such as Sypro Red can be used to visualize all of the proteins on the blot. Furthermore, if prior knowledge of the identity of the protein exists, antibodies can be used to identify these proteins on blotted gels. 2-DE gel blots can be probed with antibodies that will recognize glycoproteins or tyrosine phosphoproteins, for example, if a particular post-translational modification is of interest.

To examine gels for proteins of interest they can either be compared manually or analyzed by one of the specialized software packages available such as Melanie, Phoretix 2D, or ImageMaster. The software approach includes scanning and normalizing of the gels to be prepared, and then calculation of differences by subtraction. Gels can be compared within a laboratory or via links with online gel databases.

Protein digestion and mass spectrometry

The classical method of identifying an unknown protein from a gel is Edman sequencing. The main disadvantage of Edman sequencing in the context of 2-DE is that it lacks the required sensitivity. The method also requires unblocked amino-termini and so cannot be used for the identification of most 2-DE spots from eukaryotic cells, since proteins in these cells have chemically modified amino termini that makes them resistant to hydrolysis (Brown, 1976). Mass spectrometry is rapidly emerging as the technique that is central to proteomics applications. It has the advantages of high throughput capacity, very high sensitivity (reported to be in the low femtomole range) (Martin, 2000, Gatlin, 1998), and relatively gentle ionization techniques that allow transfer of large molecules into the gas phase with little or no fragmentation. The two mass spectrometric techniques that have provided these advantages are matrix-assisted laser desorption time of flight (MALDI-TOF) and electrospray ionization (ESI). These techniques rely on the highly accurate mass measurement of peptides obtained by specific enzymatic cleavage of a protein, which is commonly named peptide mass fingerprinting (Mann, 1993).

For mass spectrometry analysis proteins are either blotted to PVDF membrane or the protein spot is cut directly out of the 2-DE gel. The selected protein is then digested with a protease, most commonly trypsin. After careful

removal of any contaminants, the masses of the peptides are measured by mass spectrometry. The principle behind identification of proteins via accurate mass measurements of enzymatically derived peptides relies on the frequency of specific cleavage sites within a protein yielding a set of potential peptide masses that are unique to that sequence entry when compared with all of the others in the database. Studies have shown that only four to six peptide masses, measured with a mass accuracy of between 0.1% to 0.01%, are required to identify proteins in searches of a database of more than 100,000 entries (Pappin, 1993).

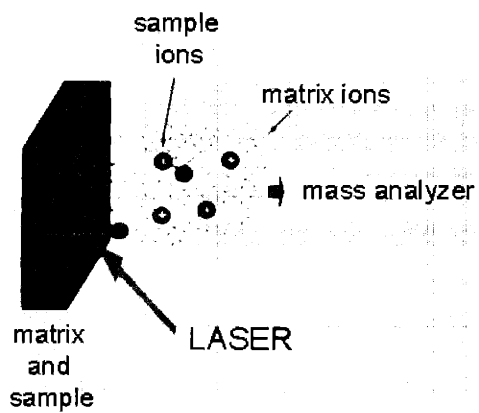
MALDI-TOF mass spectrometry

MALDI-TOF mass spectrometry is the simplest, fastest, and most sensitive mass spectrometric approach. The technique is also suitable for high throughput applications as it can be easily automated. MALDI-TOF creates ions by excitation of molecules that are isolated from solid phase sample surrounded by an ionizing matrix. A laser of specific energy is directed at the sample. The matrix molecules absorb energy from the laser and transfer it to the sample, causing subsequent ejection of the matrix and sample ions into the gas phase. The ions travel to an ion detector at the end of a long vacuum tube, and their mass-to-charge ratio (m/z) is computed as a function of their time of flight (Figure 2).

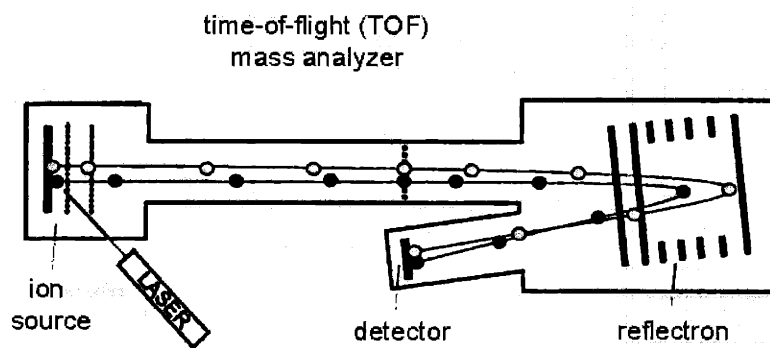
Figure 2 Schematic of MALDI-TOF mass spectrometry

- A) The sample is spotted either in a mixture of matrix solution or on top of dried matrix layer. The high energy laser excites the matrix crystals leading to sublimation and ionization of peptides. These peptides then enter the mass analyzer and travel down the flight tube illustrated in B.
- B) After the laser pulse, a strong acceleration field is switched on. This field causes the peptides to travel down the flight tube with a fixed kinetic energy such that separation occurs solely on the basis of their charge-to-mass (m/z) ratio. Instruments that are equipped with a reflector function can measure mass accuracy to within 0.1 dalton.

A



B



Electrospray Ionization Mass Spectrometry (ESI-MS)

ESI mass spectrometry creates ions by application of an electrical potential to a flowing liquid causing the liquid to charge and subsequently spray. The electrospray creates very small droplets of solvent-containing analyte. Solvent is removed by heat as the droplets enter the mass spectrometer, and multiply-charged ions are formed in the process. In contrast to the use of MALDI-TOF mass spectrometry, sample preparation for electrospray analysis requires a concentration and desalting step, due to the lower sensitivity and lower tolerance to salt and buffer contamination of the ESI technique. Additional drawbacks to this technique include the absolute loss of sample during the desalting/concentration step, the time required for sample handling, and the use of needles, which is not well suited for automation (Figure 3).

Tandem Mass Spectrometry (MS/MS)

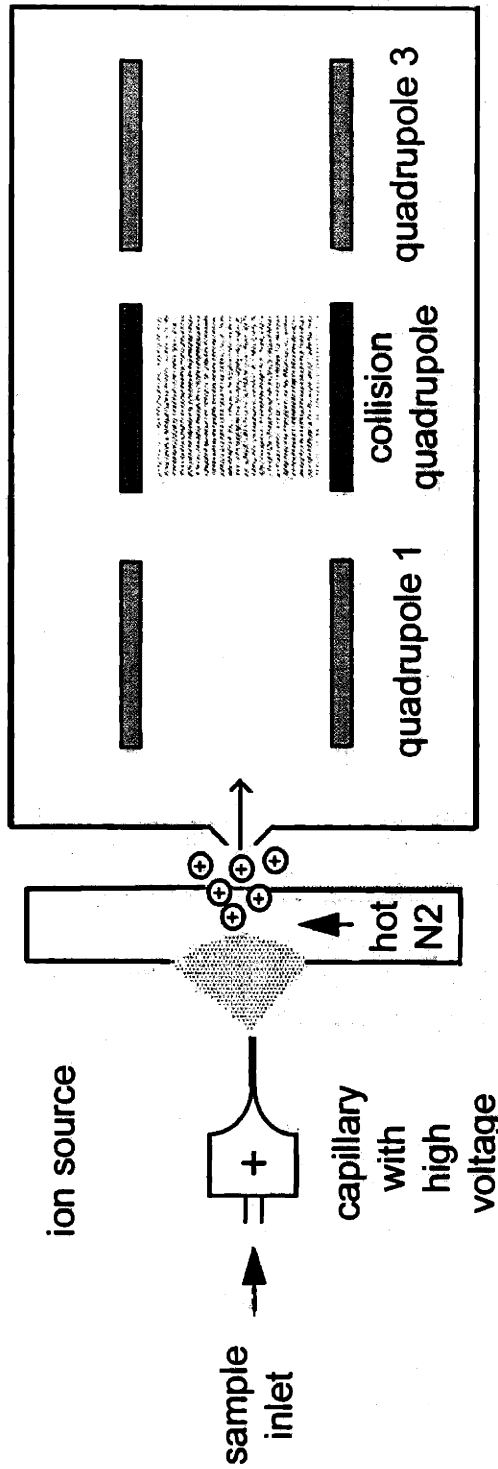
Peptide mapping-based methodologies such as MALDI-TOF and ESI allow only for the identification of a protein that is already in the protein database (Mann, 1996). A complementary mass spectrometric approach based on electrospray tandem mass spectrometric analysis (ESI-MS/MS) has been developed (Mann, 1994) that permits the confirmation of the identity of proteins found in the database. This is particularly useful when the genome for the species being searched is incomplete; sequence confirmation can be used to

Figure 3. Electrospray Ionization Mass Spectrometry (ESI-MS)

Electrospray mass spectrometry combined with a quadrupole mass spectrometer. The quadrupole applies an oscillating electric field that allows only a certain mass to pass through; the other masses are on unstable trajectories and don't reach the detector. A mass spectrum is obtained by scanning the amplitude of the electric field and recording the ions at the detector.

This figure illustrates a triple quadrupole instrument used for tandem mass spectrometry. The first mass separating quadrupole measures the mass of the peptides. The central quadrupole contains the ions during fragmentation. The third quadrupole measures the masses of the peptide fragments.

electrospray ionization (ESI) mass spectrometer



rule out an incorrect match, or, alternatively, can be used to search for a homologous protein from a species whose genome is fully sequenced. Furthermore, online coupling of liquid chromatography (LC) with electrospray MS/MS can overcome the disadvantages, such as sample purity, associated with ESI mass spectrometry. In the collision-induced dissociation (CID) process, peptides fragment in a predictable manner. A fast Fourier transform algorithm, Sequest, has been developed that correlates the experimental data with data predicted from the protein sequences in databases. The “sequence tag” data combined with the mass of the peptide provide a highly specific probe for sequence database searches (Ducret, 1998, Link, 1999).

Protein bioinformatics

The peptide mass fingerprint and sequence tag data can lead to the identification of the original protein by online scanning using various search tools. A large number of programs are available online that include not only peptide mass fingerprint search programs, but protein digest prediction, primary, secondary, and tertiary structure prediction, search of 2D gel databases, and post-translational modification prediction. For a list of programs see <http://www.expasy.ch/tools> (Gras, 1999).

Genomics, proteomics, and human disease

Genomics techniques have identified many genes crucial to our understanding of human disease. However, it is estimated that only 2% of human disease genes are monogenic; the rest are either polygenic in origin, such as heart disease, asthma, or schizophrenia, or epigenetic in nature, such as diseases caused by mutations in mitochondrial genes or imprinted genes, such as the Beckwith-Wiedemann, Prader-Willi, or Angelman Syndromes. The information contained within the proteome, the total protein product in the cell with all its concomitant editing and modification, is critical to the understanding of diseases that have complex pathologies, such as those caused by mutations in multiple genes or by epigenetic changes. This reverse approach is more sensitive than genomic analysis to factors, such as those that exist in disease states, which can change the cellular environment and thus affect the proteome, but not the genome, at the cellular level. In recent years, the techniques mentioned above have been successfully applied in the investigations of proteins involved in cancer, heart, and infectious disease.

A proteomic approach to investigate the role of DMPK

Although the mutation causing myotonic dystrophy is known, the mechanism by which the mutation exerts its effects in DM1 patients is not clear.

As discussed in Chapter 1, several factors make it difficult to analyze the biochemical pathway of DMPK. The reported low specific activity of DMPK has made it impractical for use in well-characterized assays such as 2-hybrid, IP-kinase, and peptide library screening, and protein chip technology, as these assays all rely on a high specific activity of the kinase used. Furthermore, any data resulting from these types of experiments can be considered *in vitro* information. Other groups have used *in vitro* assays that resulted in the identification of various DMPK substrate candidates. However, it is still unclear whether these proteins are in fact the *in vivo* substrates of DMPK. In order to obtain *in vivo* information about the role of DMPK, I used a proteomics-based approach.

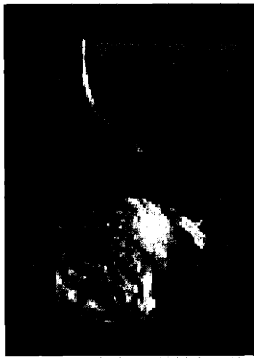
Proteins were isolated directly from either wild-type or *DMPK* *-/-* mouse tissue and the proteomics techniques described earlier were used to identify those proteins that have a difference in gel mobility between protein lysates from the two genotypes. Proteins were isolated from heart, skeletal muscle, and brain, the tissues in which DMPK is expressed most highly. Heart proteins were used for the majority of the experiments, as DMPK is expressed at the highest level in this tissue, and the cardiac phenotype in the *DMPK* *-/-* most closely resembles that of DM1 patients. The 2-DE gels from wild-type and *DMPK* *-/-* tissue were compared, and protein spots that exhibited a shift in mobility between the two gels were cut out, digested with trypsin, and identified by mass spectrometry (for a summary, see Figure 4).

Figure 4. Experimental Overview

Tissues of interest are harvested from sibling or age-matched wild-type and *DMPK* *-/-* mice. Proteins are extracted and either used directly or fractionated. Two-dimensional electrophoresis (2-DE) is performed on wild-type and *DMPK* *-/-* extracts in parallel. Gels are compared and mobility shifts identified (arrows). The protein selected for analysis is cut out of the gel and digested in situ with trypsin, chymotrypsin, or another peptidase. Peptides are eluted from the gel fragment and analyzed by mass spectrometry; peptide mass fingerprinting is performed by MALDI-TOF or ESI mass spectrometry, or peptide fragmentation sequencing is performed by tandem mass spectrometry (MS/MS). Spectrometry results are used to search the databases for the identity of the protein.



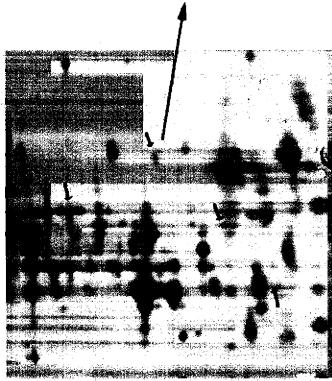
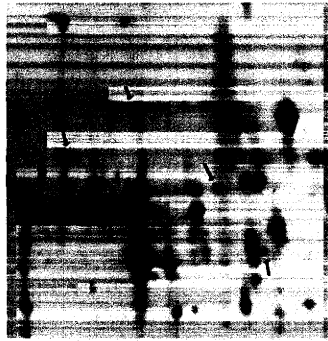
wild-type mouse



mutant mouse

harvest proteins
fractionate

perform 2-DE
compare gels



cut out selected protein

digest with trypsin

analyze by mass spectrometry

bioinformatic identification

Results

In my efforts to establish the *in vivo* function of DMPK, I used a proteomics-based approach to identify cellular proteins that are affected by loss of DMPK. These proteins could potentially constitute *in vivo* substrates of DMPK; alternatively, the proteins could represent downstream consequences of the primary phosphorylation event. Throughout the analysis total cell extracts isolated from wild-type and *DMPK* *-/-* mouse heart were used, thus allowing a direct and physiologically relevant comparison of the effects of loss of DMPK. This approach utilized 2-D gel electrophoresis to separate wild-type and DMPK mutant protein extracts, followed by the comparison of the gels obtained in each case.

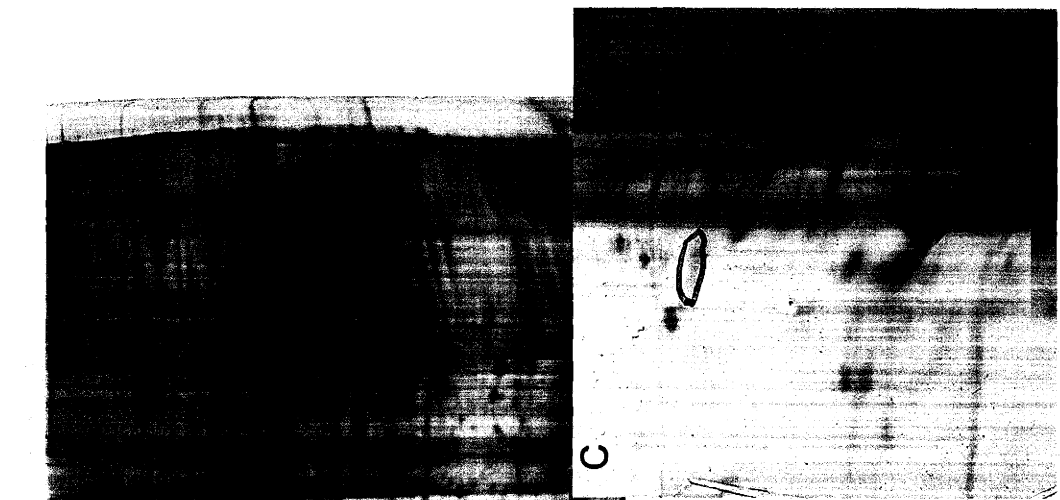
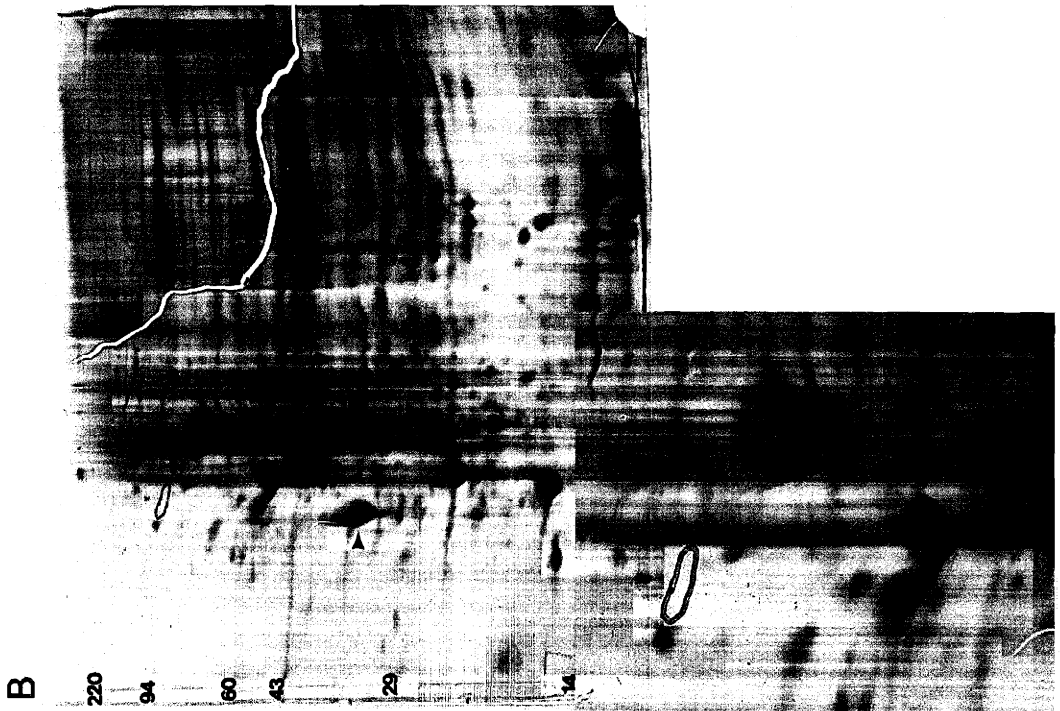
Initial comparison of gels reveals the location of DMPK

First, I sought to determine the efficacy of comparing gels to one another. Total cell extracts from wild-type and *DMPK* *-/-* mouse heart were run on small format, medium resolution gels. These gels were analyzed by laser densitometry comparison and Phoretix 2D full software (version 4.0). The protein profiles of the wild-type and *DMPK* *-/-* tissue had no appreciable differences except for the apparent absence of one protein in the *DMPK* *-/-* cells that had the approximate molecular weight and isoelectric point of DMPK (Figure 5). These experiments showed that gels containing different protein extracts could be successfully

Figure 5. Two dimensional gel electrophoresis (2-DE) comparison of wild-type and *DMPK* ^{-/-} mouse proteins

A) 2-DE separation of 50 micrograms whole cell lysate from wild-type mouse heart. B) 2-DE separation of 50 micrograms whole cell lysate from *DMPK* ^{-/-} mouse heart. C) Expanded region with difference outline from A. D) expanded region with difference outline from B. The region outlined in ink corresponds to an area of pI 5.4 and MW 89,613 daltons. Spot percentages were defined as individual spot density divided by total density of all measured spots. The WT/KO ratio of the circled spot was calculated as 24.00. No other significant differences were detected.

Two-dimensional electrophoresis was performed according to the method of O-Farrell (J. Biol. Chem. 250: 4007-4021, 1975) by Kendrick Labs, Inc. (Madison, WI). Isoelectric focusing was carried out in glass tubes of inner diameter 2.0 mm, using 2% pH 4-8 ampholines for 9600 volt hours. After equilibration each tube gel was sealed to the top of a 10% acrylamide slab gel (0.075 mm thick) and SDS slab gel electrophoresis was carried out for about 4 hours at 12.5 mA per gel. Duplicate gels were scanned with a laser densitometer (Model PDSI, Molecular Dynamics inc., Sunnyvale, CA). The images were analyzed using Phoretix 2D Full software (version 4.0) such that differing spots and all major unchanging spots were outlined. Spots which appeared by eye to be different between the samples were outlined.



compared to one another, thus establishing the feasibility of this proposed experimental approach.

High resolution analysis of the wild-type and *DMPK* ^{-/-} proteomes

Although the gels could be successfully compared, medium resolution small-format gels were not detailed enough to provide the level of information we were looking for. In order to increase the amount of the proteome that could be visualized on a given gel at one time, several techniques were incorporated into the assay to greatly improve the resolution of the gels.

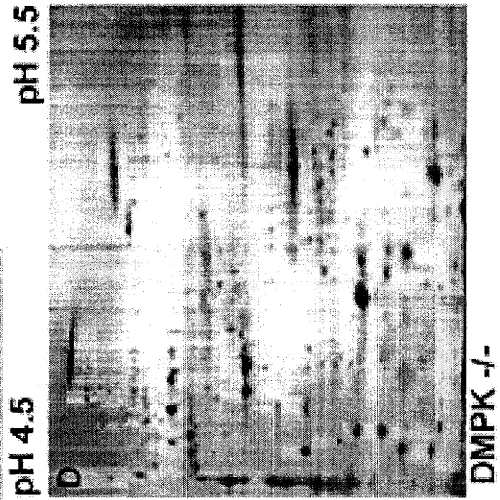
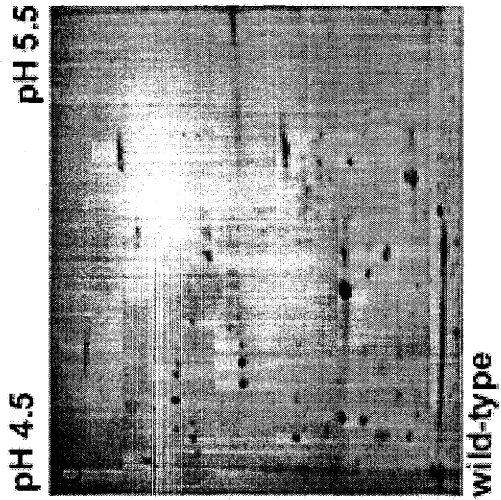
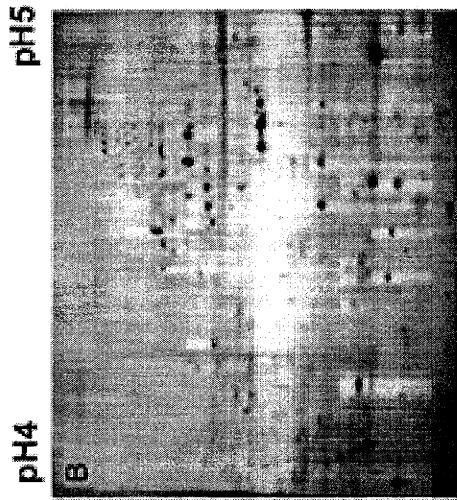
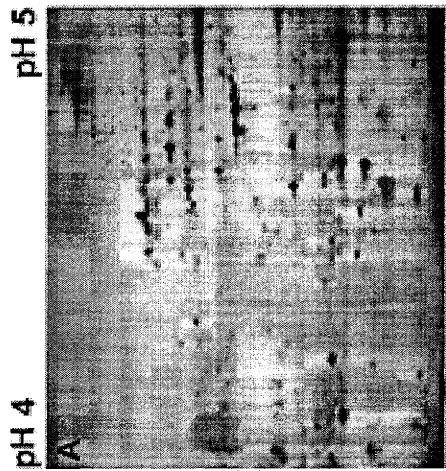
First, the format was changed from small- to large-format gels--18 cm 1st dimension gels and 20 cm 2nd dimension gels. Roughly three times as many proteins can be seen on these large format gels when compared to the earlier 11cm x 11 cm gels. Second, tube gels were replaced with immobilized pH gradient isoelectric focusing (IEF) gels. Tube gels have the advantage of showing superior focusing resolution but have the disadvantages of drifting pH gradient as well as localized stretching and breakage, which severely hampers any efforts to compare two gels precisely. Finally, in addition to wide pH range gels, such as pH 3-10 or 4-7 which have been available for several years, reduced pH range gels have recently become available. Reduced pH gradient gels which cover a short pH range, including pH 3.5-4.5, 4-5, 4.5-5.5, 5-6, 5.5-7, 6-9, and 6-1, can be used to focus in on one particular pH range in the proteome,

and can be staggered to produce a ladder of gels which covers a large pH range (figure 6). In addition, the reduced pH gradient IEF gels offer the advantage of enhancing the representation of a given protein on a gel, which is helpful when analyzing proteins that are typically present at low concentration in the cell. For example, since only proteins with isoelectric points within the pH range of the gel will focus and be visualized, the reduced pH gels in effect filter out the proteins outside the pH range while allowing entry into the gel of a much greater amount of the proteins within the particular pH range. In general, having more protein contained in a given spot on a gel greatly facilitates its subsequent analysis by mass spectrometry.

To further expand the amount of the proteome we were able to visualize at once, and because each IEF gel has a finite loading capacity, protein lysates were separated into three fractions. The fractionation buffers were designed to separate proteins on the basis of their solubility in aqueous solution, since DMPK has been shown by several groups to localize near various membranous structures in the cell. Potential membrane-bound target proteins would therefore be enriched in the fraction that contained membrane-bound proteins. The protocol is adapted from one previously described for the fractionation of bacterial proteins (Molloy, 1998) and mammalian tissues (Klose, 1999). The fractions can be roughly divided into three groups: cytoplasmic proteins that are soluble in tris buffer, membrane-associated proteins that are soluble in a

Figure 6. Reduced pH gradient gels for systematic analysis of the proteome

Panels A-D: 2-dimensional electrophoresis was performed on 120 μ g protein from whole cell lysate of wild-type and *DMPK*^{-/-} mouse heart using reduced pH range Immobiline Drystrips from Amersham Pharmacia Biotech. A) Wild-type pH 4-5. B) *DMPK*^{-/-} pH 4-5. C) Wild-type pH 4.5-5.5. D) *DMPK*^{-/-} pH 4.5-5.5.



buffer of urea and CHAPS, and very hydrophobic proteins that are soluble in an enhanced extraction solution of urea, thiourea, CHAPS, and betaines.

All extracts were prepared from sibling mice when possible to reduce the possibility of genetic background variation giving misleading results. Age-matched groups of half-siblings were also used. Mice of three or four months of age were typically used since these mice showed no muscle deterioration that could have introduced variation between wild-type and *DMPK* *-/-* mice (Reddy, 1996). Samples analyzed represent pools of tissues from three to six mice with a mixture of males and females to control for individual and sex-specific variation. Tissues were never frozen due to potential shearing of the cell membrane that could alter the resultant fraction components. All 2-dimensional gel comparisons were analyzed in duplicate for each of three different extract preparations to control for fraction reproducibility and potential gel artifacts.

Comparison of proteins from wild-type and *DMPK* *-/-* 2-DE gels

This section contains a number of figures that illustrate the types of protein shifts that were observed in the comparison of gels of proteins. A number of mobility shift differences were observed. However, as is demonstrated by the color overlay in Figure 24, for example, the majority of the wild-type and *DMPK* *-/-* proteins behave identically on the gels. This indicates that no gross alteration in the muscle has occurred that would cause global changes in physiology;

therefore, the relatively small number of observed protein shifts in *DMPK* *-/-* tissue represent modifications of the cellular proteome due to the lack of DMPK.

Figure 7 shows the types of mobility differences we see when comparing 2-DE gels of wild-type and *DMPK* *-/-* proteins. The three panels show comparison of unfractionated proteins from skeletal muscle and heart. Arrows indicate spots with either altered mobility (top and middle panels) or, in the case of the bottom panel, spots that are present in gels from one genotype but not in the other.

Figure 8 shows a comparison of unfractionated heart protein. Panels A and C represent wild-type proteins, whereas panels B and D represent proteins from *DMPK* *-/-* tissue. The arrows in C and D indicate three ladders of proteins in the low pH range of the gel. This type of laddering is generally seen with a succession of post-translational modifications, such as glycosylation. The ladder of protein indicated by the center arrow in C and D exhibits a molecular weight shift between wild-type and mutant, suggesting a difference in splicing or a type of post-translational modification that would alter the molecular weight.

In Figure 9 four differences were noted between the two gel comparisons of skeletal muscle whole cell lysate. The topmost arrow points to a set of four proteins that are grouped together vertically appear to be shifted horizontally between wild-type (A) and *DMPK* *-/-* (B) in relation to the other proteins. The

Figure 7. Differences found in comparison of whole cell lysates of wild type and *DMPK* *-/-* mouse heart and skeletal muscle proteins

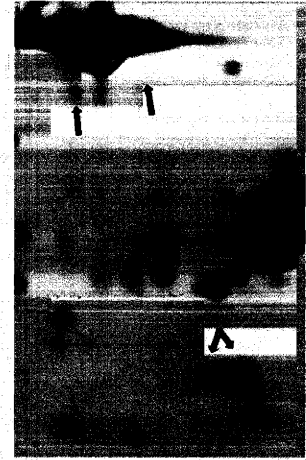
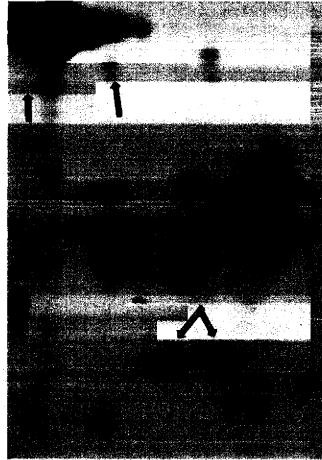
2-DE was performed on unfractionated whole cell lysate from heart and skeletal muscle. Proteins were focused for 22 hours, or 14,200 volt-hours, in 11cm 1.5 mm (inner diameter) tube gels. The second dimension was 10% SDS-PAGE slab gels.

The three sets of panels show the types of mobility differences seen when comparing 2-DE gels of wild-type and *DMPK* *-/-* proteins. Arrows indicate spots with either altered mobility (top and middle panels) or, in the case of the bottom panel, spots that are present in gels from one genotype but not in the other.

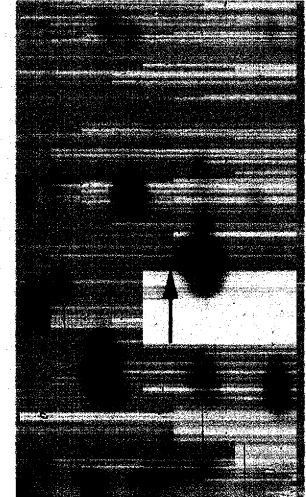
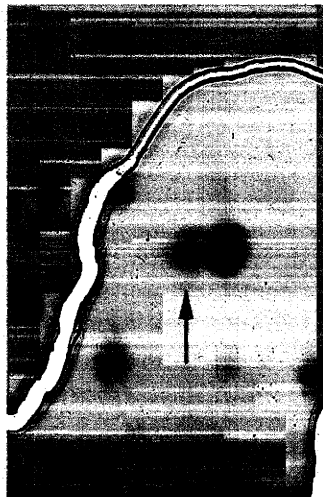
DMPK -/-

DMPK +/+

Skeletal Muscle



Cardiac Muscle



Cardiac Muscle

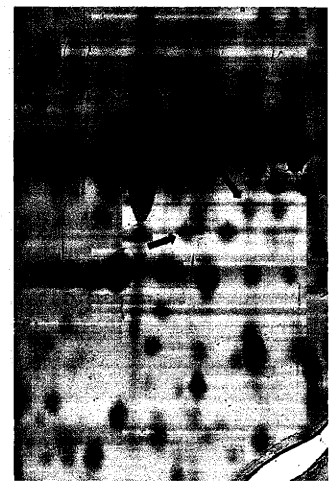
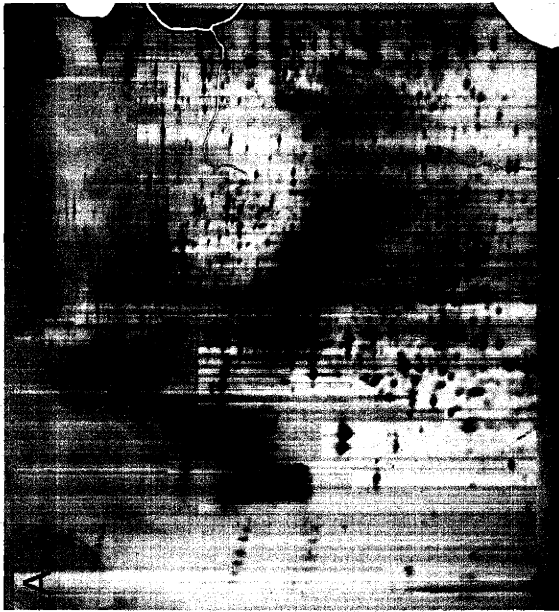
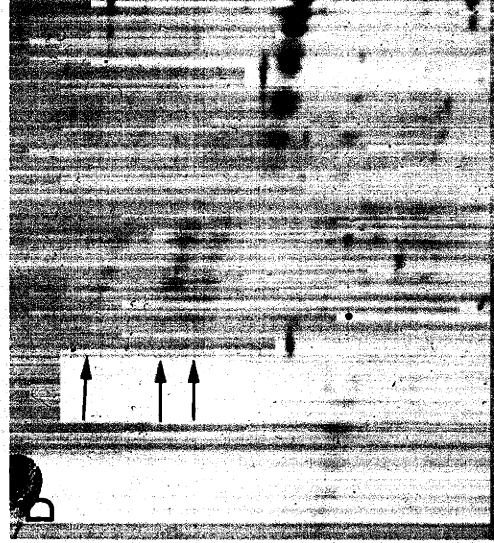
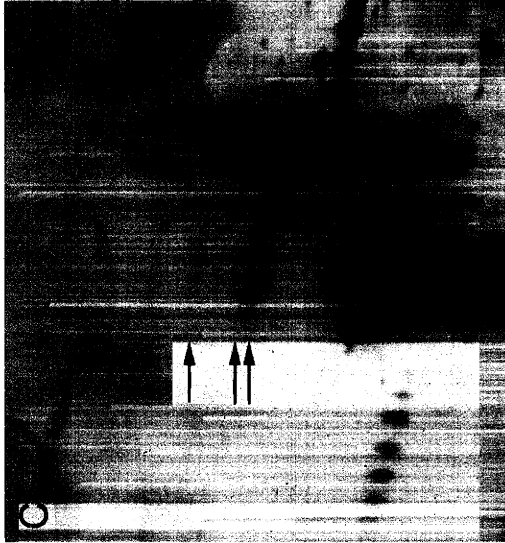


Figure 8. 2-DE gel comparison of whole cell lysate from heart.

Panels A and B represent whole cell heart lysate from three-month-old sibling wild-type and *DMPK*^{-/-} mice, respectively. Protein from one mouse of each genotype were used. The pH range of these gels was from pH 3 to pH 10; 2nd dimension gels were 10% acrylamide. Panels C and D highlight an area in which a ladder of protein spots, indicated by the center arrow, have a mobility difference between the gels. The laddering pattern could be due to a post-translational modification that alters both molecular weight and isoelectric point, such as the addition of sugar or phosphate moieties. The mobility shift difference may be due to a splice variant or some other modification that alters molecular weight.



10

pH

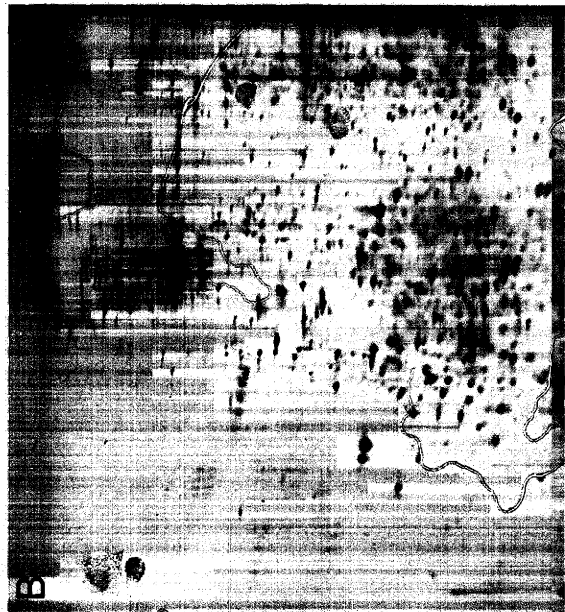
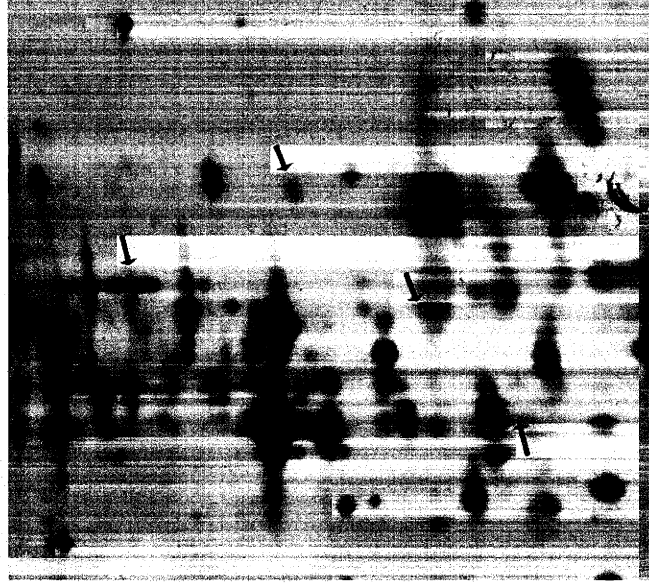


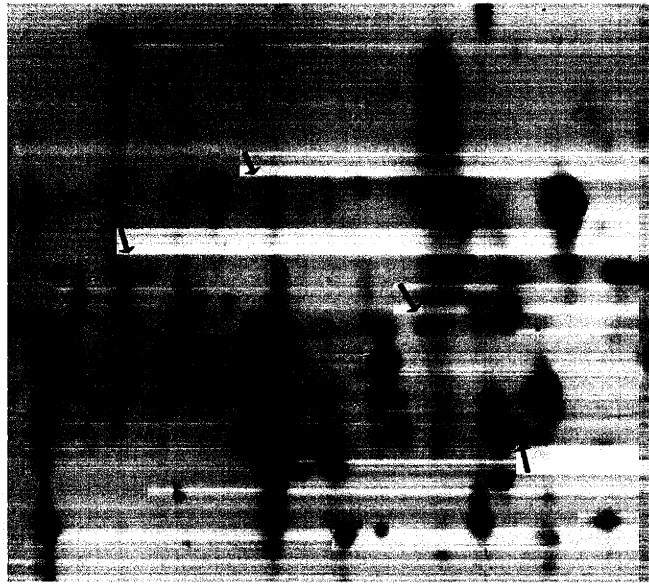
Figure 9. Difference between wild-type and *DMPK* ^{-/-} skeletal muscle proteins

2-DE was performed on unfractionated whole cell lysate from skeletal muscle of three-month-old sibling mice. Proteins were focused for 22 hours, or 14,200 volt-hours, in 11cm 1.5 mm (inner diameter) tube gels. The second dimension was 14 cm 10% SDS-PAGE slab gels.

The topmost arrow points to a set of proteins that all have the same altered mobility in the pH dimension. This set of proteins may represent one protein that is present in several different modified forms that could arise from successive phosphorylations, for example. The arrow farthest to the right indicates a protein that is moved in the molecular weight dimension. The bottom two arrows point at proteins that are present in the wild-type sample but absent in the mutant sample.



B



A

arrow furthest to the right indicates a protein that runs at a lower apparent molecular weight in the *DMPK* *-/-* gel, and the bottom two arrows point at proteins that are present in the wild-type gel but not the *DMPK* *-/-* gel.

Figure 10 shows a comparison of heart proteins representing extract 1 of the fractionation scheme described above. Panels C and D highlight the area of the gels in which the mobility difference can be observed. The arrows point to two protein spots that differ in their distance from each other. Gels were overlaid to determine that it is in fact the left-hand spot that has altered mobility, appearing at a lower pH in the wild-type sample compared to the *DMPK* *-/-* sample. This sort of mobility shift is consistent with a post-translational modification such as phosphorylation.

Figure 11 shows a set of gels that reproduce the mobility shift seen in Figure 10. The proteins of interest are labeled with arrows.

Figure 12 shows a comparison of heart proteins representing extract 2. Panels B and C highlight the area in which the mobility shift occurs. In this case the protein from the *DMPK* *-/-* gel is shifted more toward the acidic end of the pH range.

Figure 13 shows another comparison of extract 2 proteins in the pH 4-7 range. In this case there is an obvious difference in the highlighted area,

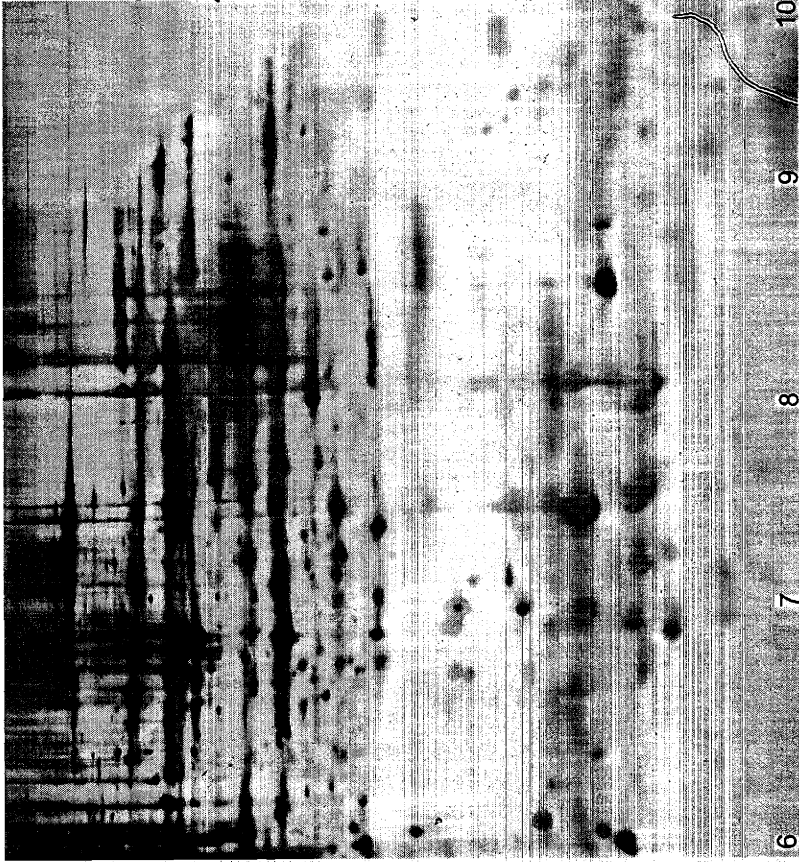
Figure 10. Comparison of fractionated protein samples: extract 1

Proteins were harvested from pooled wild-type and *DMPK* *-/-* age-matched mice and fractionated as described. Extract 1 consists of proteins soluble in 40 mM tris buffer; primarily, this sample contains proteins that are present in the cytosol.

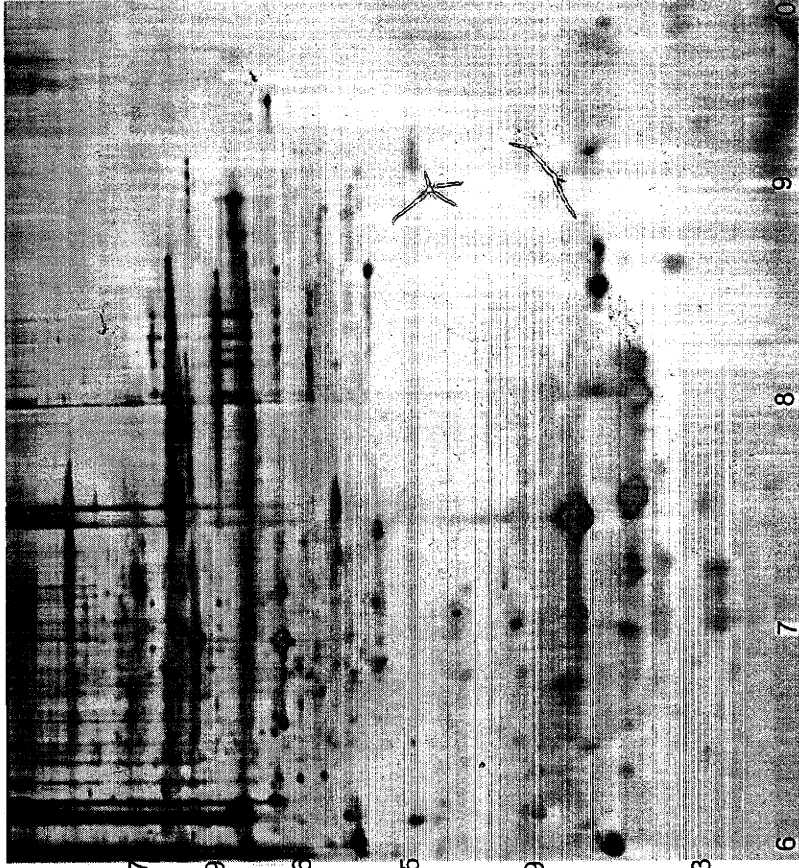
2-DE was performed on extract 1 proteins. Proteins were loaded onto pre-cast 18cm pH 6-11 isoelectric focusing gels. After focusing for 7 hours at 3500 volts, the gels were loaded onto 16% second dimension SDS-PAGE gels. These gels were then fixed and silver stained.

The spacing of the proteins indicated by the arrows is different in the two samples. Direct overlay comparison of the gels revealed the left hand protein to have the altered mobility. The protein from the wild-type sample runs at a more acidic pH than the protein from the mutant sample. This sort of shift is consistent with a post-translational modification difference, such as phosphorylation of the wild-type but not the *DMPK* *-/-* protein.

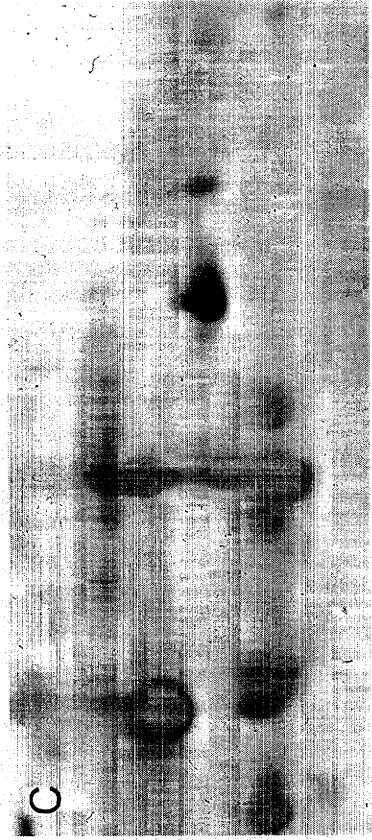
A



B



C



D



Figure 11. Repeat of the Figure 10 gels

A different extract one preparation from another set of three-month-old mice yields gels that show a reproduction of the mobility pattern seen in Figure 10. Again, the protein spots are shown with arrows.

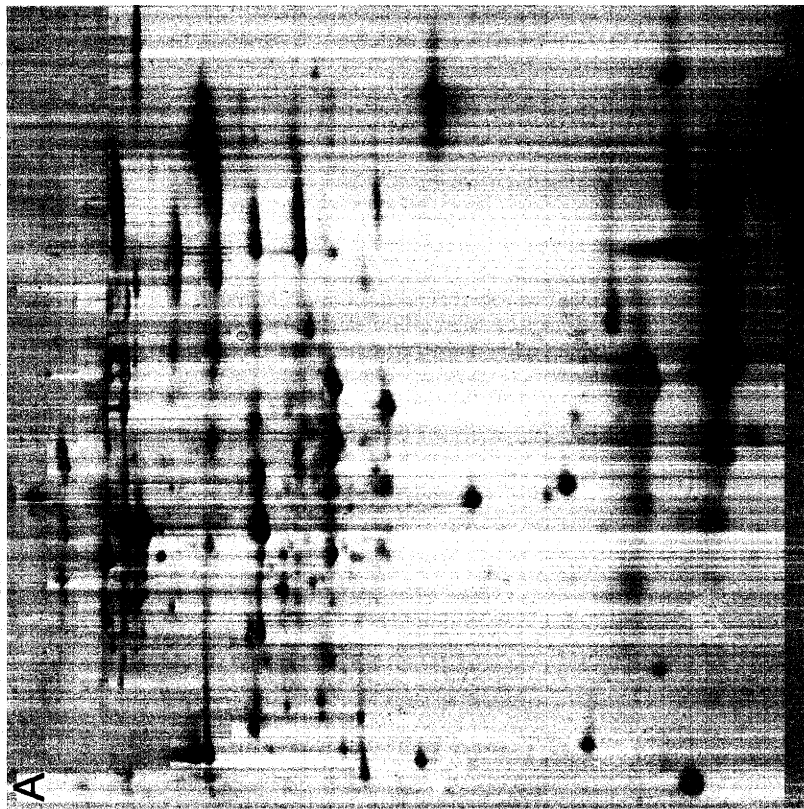


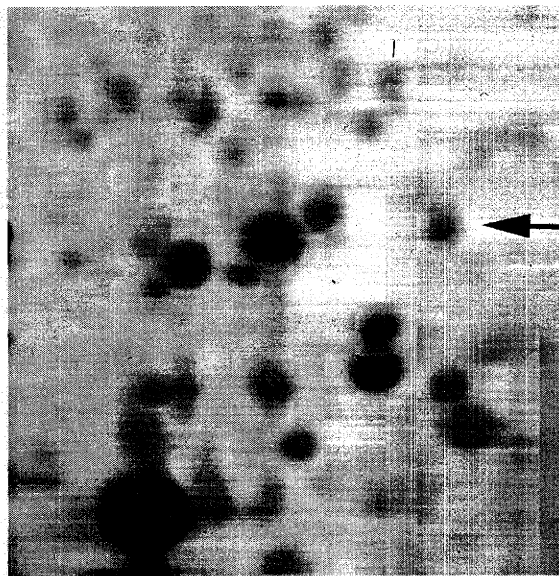
Figure 12. Comparison of fractionated protein samples: extract 2

Proteins were harvested from pooled wild-type and *DMPK* *-/-* age-matched mice and fractionated as described. To prepare extract 2, whole cell protein lysates were pre-fractionated and then solubilized in a buffer consisting of 8M urea, 4% chaps, 0.5% ampholytes, and 100 mM DTT.

2-DE was performed on extract 2 proteins. Proteins were loaded onto pre-cast 18cm pH 4-7 isoelectric focusing gels. After focusing for 7 hours at 3500 volts, the gels were loaded onto 13% second dimension SDS-PAGE gels. These gels were then fixed and silver stained.

Panel A represents the full gel of the wild-type protein sample. The area outlined by the black square appears larger in panel B. Panel C is the same area from the gel of *DMPK* *-/-* proteins. The arrows in panels B and C indicate one protein spot whose mobility is altered in the isoelectric focusing dimension.

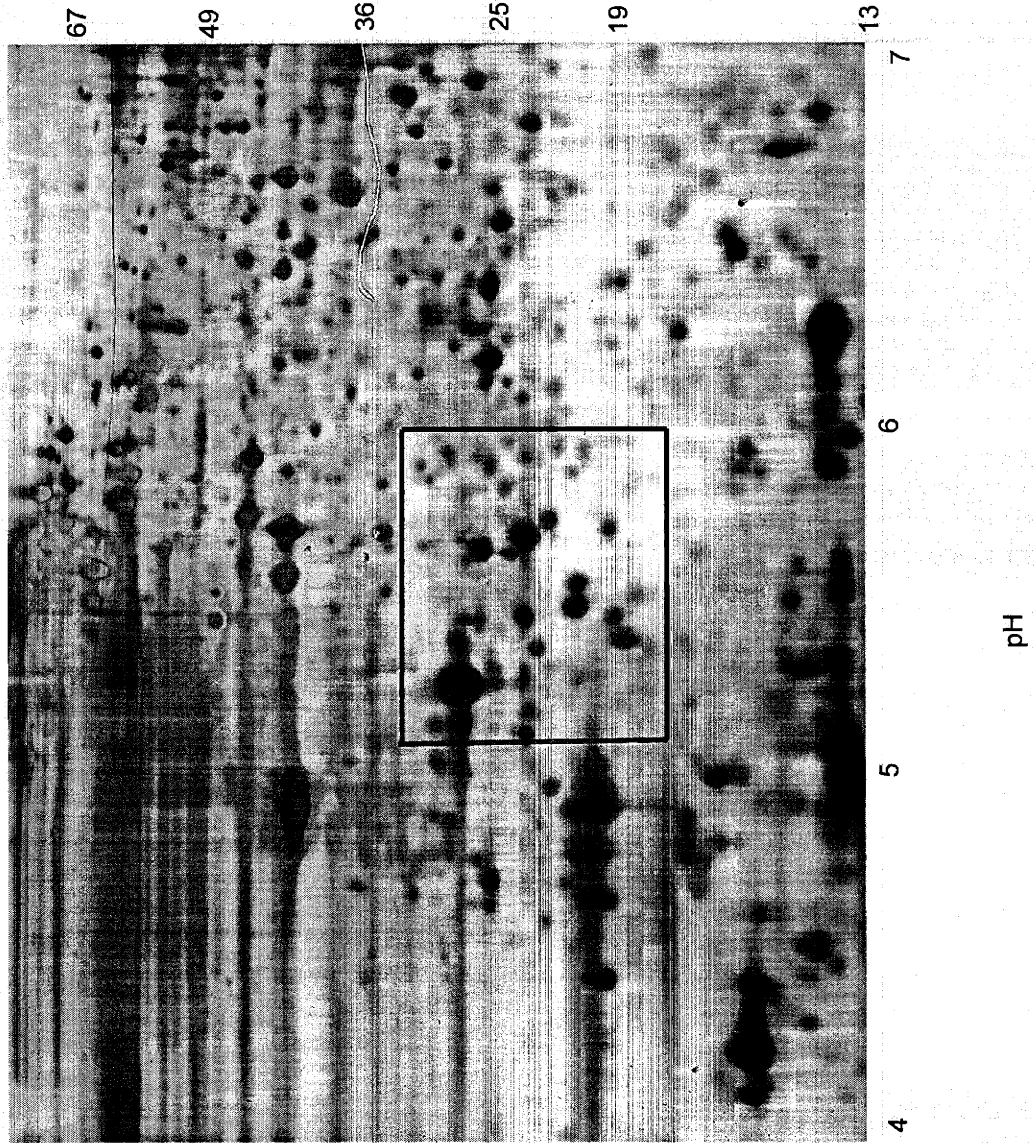
B wild-type



C *DMPK*^{-/-}



A



67

49

36

25

19

13

7

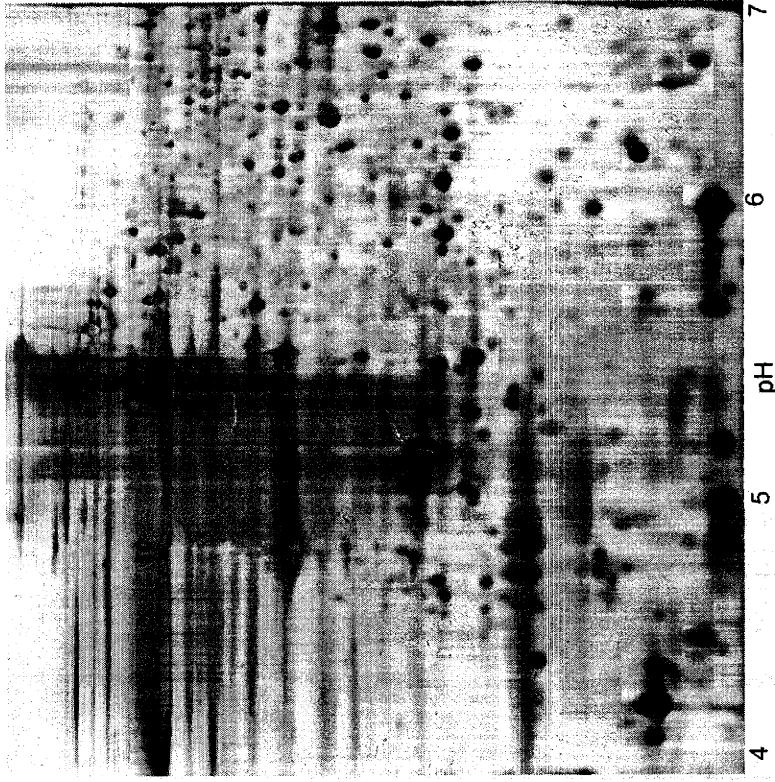
Figure 13. Comparison of fractionated protein samples: extract 2

Proteins were harvested from pooled wild type and *DMPK* *-/-* age-matched mice and fractionated as described. To prepare extract 2, whole cell protein lysates were pre-fractionated and then solubilized in a buffer consisting of 8M urea, 4% chaps, 0.5% ampholytes, and 100 mM DTT.

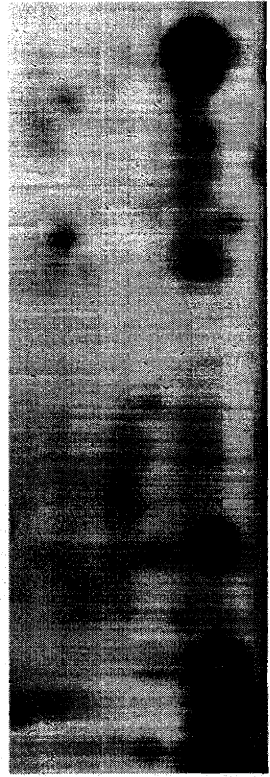
2-DE was performed on extract 2 proteins. Proteins were loaded onto pre-cast 18cm pH 4-7 isoelectric focusing gels. After focusing for 7 hours at 3500 volts, the gels were loaded onto 13% second dimension SDS-PAGE gels. These gels were then fixed and silver stained.

Panels A and C represent the wild type gel and panels B and D represent the mutant gel. In C and D the arrows indicate where one spot appears to be absent in the *DMPK* *-/-* sample.

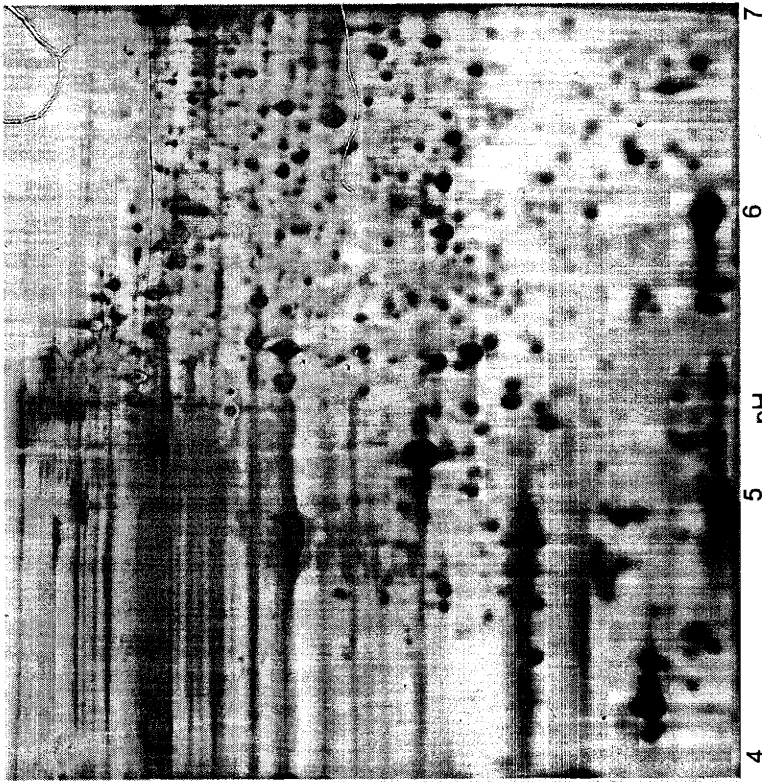
DMPK $-/-$



67
49
36
25
19



wild type

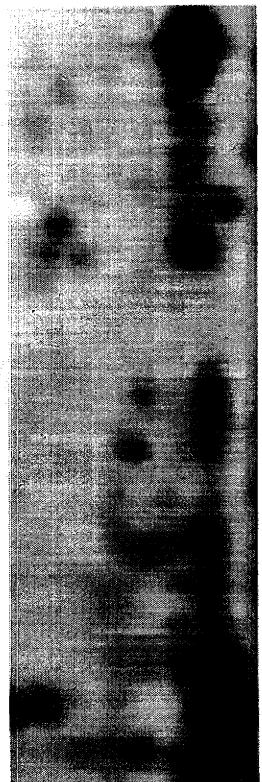


4

5

6

7



however, it is not clear whether the protein labeled with the arrow has moved or disappeared in the *DMPK*^{-/-} sample. In order to examine the area more closely, extract 2 was run on pH 4.5 – 5.5 gels (Figure 14). These gels clearly show that the protein from the wild-type gel appears at a more acidic pH than the protein from the *DMPK*^{-/-} gel. The proteins used in Figures 13 and 14 were prepared from tissues harvested from three-month-old mice. Interestingly, when this experiment was done with proteins prepared from the hearts of eight-month-old mice, the pattern made by these proteins was slightly different (Figure 15). This phenomenon was seen in two different preparations of extract two from eight-month-old mice and may represent an age-related modification of these proteins.

MALDI-TOF analysis of two selected proteins

To determine whether proteins from these gels could successfully be identified, two spots were selected for mass spectrometry analysis. These two were chosen as they were present in the highest concentration of all the mobility shifted proteins. One spot “Sample A” was from gels representing extract one (Figures 10-11) and the other, “Sample B”, was from gels representing extract two (Figures 13-15). Protein spots were excised from gels of wild-type proteins and digested *in situ* with trypsin. The tryptic peptides were eluted from the gel fragment and analyzed by MALDI-TOF mass spectrometry.

Figure 14. Comparison of fractionated protein samples: extract 2

In order to examine the difference seen in Figure 13 more closely, the same sample was run on a reduced pH gradient gel. Samples were loaded onto 18 cm pH 4.5-5.5 precast isoelectric focusing gels. After focusing for 17 hours at 3500 volts, the gels were loaded onto 13% second dimension SDS-PAGE gels. They were then fixed and silver stained.

What appeared to be an absent spot in the *DMPK* *-/-* sample in Figure 13 is in fact a mobility difference. The protein from the wild-type sample runs at a more acidic pH than does the protein from the *DMPK* *-/-* sample.

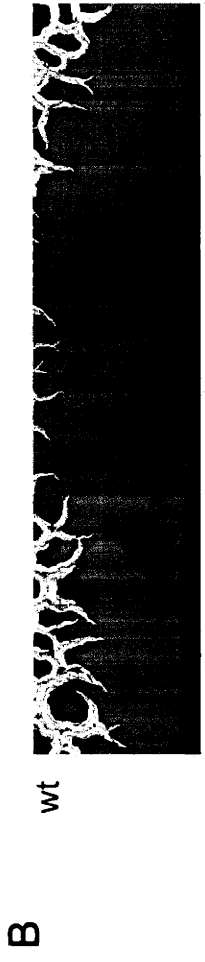
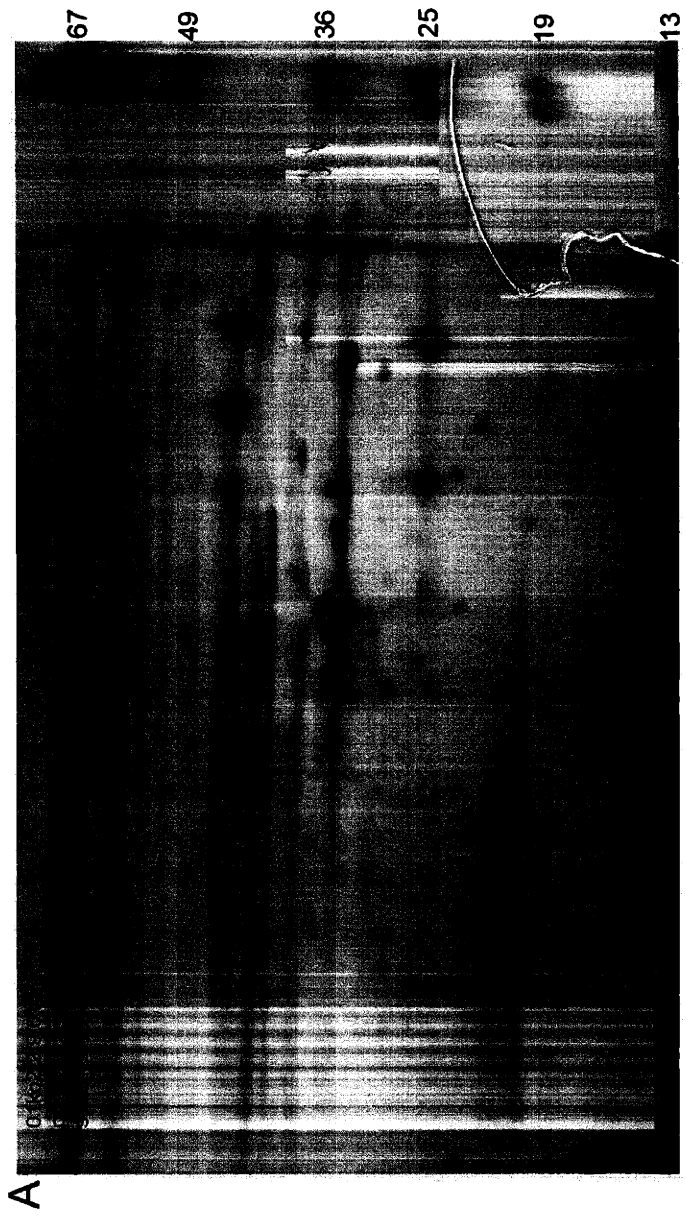
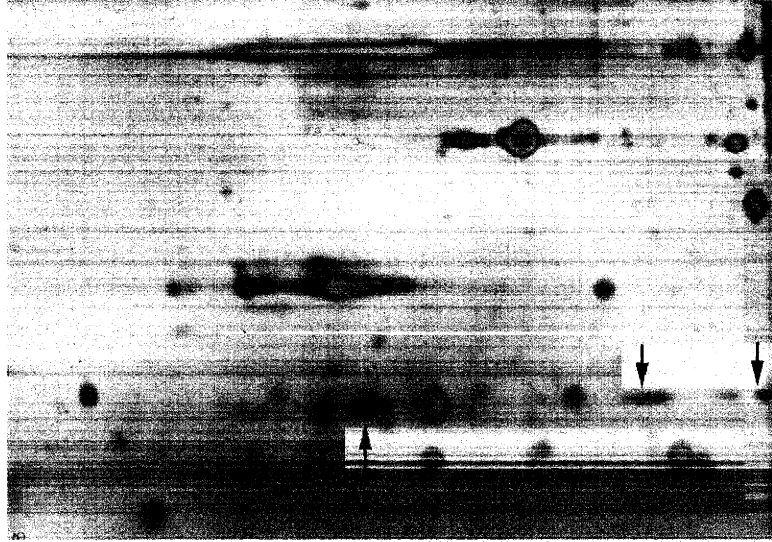


Figure 15. Comparison of fractionated protein samples from eight-month-old mice: extract 2

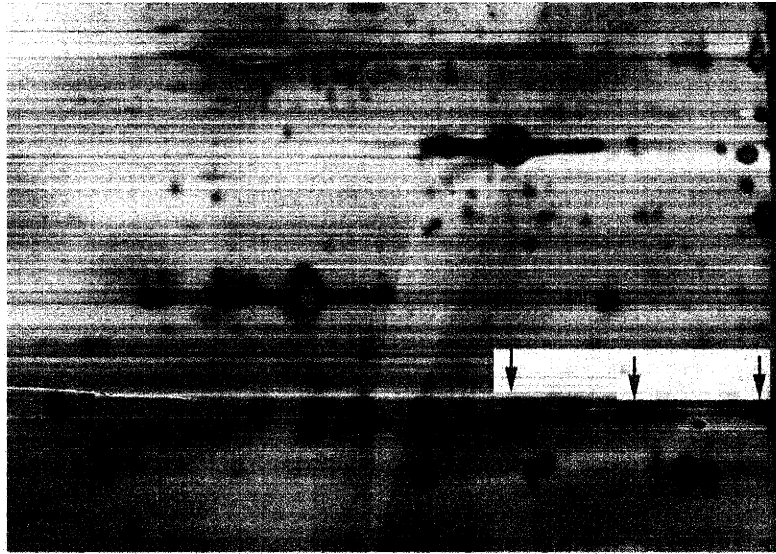
Extract 2 was prepared as described from the heart tissue of eight-month-old mice. Samples were loaded onto 18 cm pH 4.5-5.5 precast isoelectric focusing gels. After focusing for 17 hours at 3500 volts, the gels were loaded onto 13% second dimension SDS-PAGE gels. They were then fixed and silver stained.

Panel A represents the gel of wild type proteins and panel B represents the gel of *DMPK* *-/-* proteins. Arrows indicate proteins that have altered mobility between the two gels. The pattern is more complex than in the samples from three month old mice and it is not clear in which direction the spots have shifted.

A



B



MALDI-TOF analysis of Sample A resulted in a spectrum showing peaks corresponding to peptides various molecular mass. The collection of peptide masses represents the mass fingerprint of the protein; these were used to search the NCBI and SWISSPROT databases using the program MS-FIT at the Protein Prospector website run by UCSF. The result was the identification of Sample A as a fatty acid binding protein, adipocyte isoform (Figures 16-17).

The same procedure was followed for Sample B as for Sample A. In this case, however, the search did not identify one particular protein as a definite match. The MS-FIT program gave a list of several proteins as possible matches. More information was needed for the positive identification of this protein (Figure 18).

LC-MS/MS analysis of two selected proteins

Because the mouse genome is not fully sequenced, we considered the possibility that the protein of interest is not yet entered into the sequence database. Therefore, any identification must be carefully reviewed to be sure that it is a true match and not merely a match with an identified protein that contains a number of similar tryptic peptides. For example, misidentifications can occur in database searches involving tryptic peptide masses of proteins that have a motif common to many proteins of its class, such as the EF-hand calcium binding proteins. Furthermore, searching with peptide masses from mouse

Figure 16. MALDI-TOF identification of Sample A, adipocyte isoform fatty acid binding protein A-FABP

Figure 16 shows the search result of the SwissProt database with peptide masses obtained in MALDI-TOF MS of Sample A. The peptide masses are listed; masses in italics were not matched and are likely to be from keratin contamination.

Peptide masses searched (Da): 620.66, 637.44, 707.13, 833.34, 839.35, 936.74, 1037.83, 1063.49, 1065.19, 1126.47, 1235.5, 1244.84, 1401.45, 1448.3, 1578.67, 1610.01, 1679.15, 1792.98, 2025.97, 2187.01, 2197.03, 2287.82, 2326.63, 2362.1, 2378.18, 2382.26, 2384.322492.69, 3610.72, 4970.2, 5469.3, 5543.6
 masses in italics were not matched

Sample ID (comment): **Sample 3**
 Database searched: **SwissProt.7.2.2001**
 Molecular weight search (**9000 - 19000 Da**) selects **19338** entries.
 Full pI range: **99359** entries.
 Species search (**HUMAN MOUSE**) selects **11676** entries.
 Combined molecular weight, pI and species searches select **1612** entries.
 Pre searches select **1612** entries.
 MS-Fit search selects **2** entries.

Parameters Used in Search

Considered modifications: | Peptide N-terminal Gln to pyroGlu | Oxidation of M | Protein N-terminus Acetylated |

Min. # Peptides to Match	Peptide Mass Tolerance (+/-)	Peptide Masses are	Digest Used	Max. # Missed Cleavages	Cysteines Modified by	Peptide N terminus	Peptide C terminus
20	0.750 %	monoisotopic	Trypsin	1	carbamidomethylation	Hydrogen (H)	Free Acid (O H)

Result Summary

Rank	MOWSE Score	# (%) Masses Matched	Protein MW (Da)/pI	Species	Accession #	Protein Name
1	8.68e+010	24/32 (75%)	14650.0 / 8.53	MOUSE	<u>P04117</u>	FATTY ACID-BINDING PROTEIN, ADIPOCYTE (AFABP) (ADIPOCYTE LIPID-BINDING PROTEIN) (ALBP) (P2 ADIPOCYTE PROTEIN) (MYELIN P2 PROTEIN HOMOLOG) (3T3-L1 LIPID BINDING PROTEIN) (422 PROTEIN) (P15)
2	3.14e+009	20/32 (62%)	14719.0 / 6.59	HUMAN	<u>P15090</u>	FATTY ACID-BINDING PROTEIN, ADIPOCYTE (AFABP) (ADIPOCYTE LIPID-BINDING PROTEIN) (ALBP) (A-FABP)

Figure 17. MALDI-TOF identification of Sample A, adipocyte isoform fatty acid binding protein A-FABP

Figure 17 shows the coverage map of A-FABP, the protein identified by MALDI-TOF mass spectrometry. The portion of the protein that represents matched peptides is underlined. The program MS-Digest was used to predict all the peptides that result from a trypsin digest of A-FABP. Eight out of ten of the predicted peptides were detected by mass spectrometry.

A-FABP
coverage map

MCDAFVGTWK LVSSNFDDYMYK EVGVGFATR K VAGMAK
PNMIISVNGDLVTIR SESTFK NTEISFK LGVEFDEITADDRKVK
SIITLDGGALVQVQK WDGK STTIK R K R DGDK LVVECVMK
GVTSTR VYER A

Coverage: 92%
8/10 predicted peptides
PI 8.53, MW 14,650 Da

Figure 18. MALDI-TOF identification of Sample B: ambiguous results

Figure 18 shows the search result of the SwissProt database with peptide masses obtained in MALDI-TOF MS of Sample B. The search never yielded identification of a single protein, even when search parameters were significantly narrowed. The five proteins that represent the closest match are listed. Interestingly, two of these are also isoforms of fatty acid binding proteins.

Press stop on your browser if you wish to abort this MS-Fit search prematurely.

Sample ID (comment): **Sample B**

Database searched: **SwissProt.7.2.2001**

Molecular weight search (**9000 - 19000 Da**) selects **19338** entries.

Full pI range: **99359** entries.

Species search (**HUMAN MOUSE**) selects **11676** entries.

Combined molecular weight, pI and species searches select **1612** entries.

Pre searches select **1612** entries.

MS-Fit search selects **6** entries (results displayed for top **5** matches).

Parameters Used in Search

Considered modifications: | Peptide N-terminal Gln to pyroGlu | Oxidation of M | Protein N-terminus Acetylated |

Min. # Peptides to Match	Peptide Mass Tolerance (+/-)	Peptide Masses are	Digest Used	Max. # Missed Cleavages	Cysteines Modified by	Peptide N terminus	Peptide C terminus
15	0.750 %	monoisotopic	Trypsin	1	carbamidomethylation	Hydrogen (H)	Free Acid (O H)

Result Summary

Rank	MOWSE Score	# (%) Masses Matched	Protein MW (Da)/pI	Species	Accession #	Protein Name
<u>1</u>	<u>1.09e+009</u>	<u>19/31 (61%)</u>	<u>16890.9 / 4.30</u>	<u>HUMAN</u>	<u>P27482</u>	CALMODULIN-RELATED PROTEIN NB-1 (CALMODULIN-LIKE PROTEIN) (CLP)
<u>2</u>	<u>1.57e+008</u>	<u>16/31 (51%)</u>	<u>14889.0 / 5.40</u>	<u>HUMAN</u>	<u>Q15540</u>	FATTY ACID-BINDING PROTEIN, BRAIN (B-FABP) (BRAIN LIPID-BINDING PROTEIN) (BLBP) (MAMMARY DERIVED GROWTH INHIBITOR RELATED)
<u>3</u>	<u>2.9e+007</u>	<u>15/31 (48%)</u>	<u>14820.0 / 5.68</u>	<u>MOUSE</u>	<u>P11404</u>	FATTY ACID-BINDING PROTEIN, HEART (H-FABP) (MAMMARY-DERIVED GROWTH INHIBITOR) (MDGI)
<u>4</u>	<u>1.54e+007</u>	<u>15/31 (48%)</u>	<u>17490.4 / 9.19</u>	<u>MOUSE</u>	<u>Q62386</u>	INTERLEUKIN-17 PRECURSOR (IL-17) (CYTOTOXIC T LYMPHOCYTE-ASSOCIATED ANTIGEN 8) (CTLA-8)
<u>5</u>	<u>2.29e+006</u>	<u>15/31 (48%)</u>	<u>18505.9 / 8.06</u>	<u>HUMAN</u>	<u>P18282</u>	DESTRIN (ACTIN DEPOLYMERIZING FACTOR) (ADF)

proteins against a database of human proteins is not practical unless the proteins are identical, as any one amino acid change will alter the mass of a particular peptide. Due to these facts, and since the identification of Sample B was ambiguous, we analyzed the proteins by high performance liquid chromatography coupled to tandem mass spectrometry (LC-MS/MS). This analysis was coupled to tandem mass spectrometry in which the peptides are fragmented and the fragments are analyzed by the program Sequest to obtain sequence data. The confirmed peptide sequences can then be used to positively identify the protein through sequence homology. This analysis led to the confirmation of the identity of Sample A as A-FABP (Figures 19-20) and the identification of Sample B as another FABP isoform, the cardiac isoform H-FABP (Figures 21-22).

LC-MS/MS analysis of H-FABP from *DMPK* $-/-$ gels

To ascertain whether the shifted proteins from the corresponding *DMPK* $-/-$ gels were indeed the same proteins with altered mobilities rather than a different protein altogether, the proteins from the gels of *DMPK* $-/-$ tissue were also analyzed by mass spectrometry and confirmed by peptide sequencing. Furthermore, we analyzed both the spots from the gel of the 8-month-old *DMPK* $-/-$ mice to confirm that they were mobility forms of H-FABP. The identity of each of these spots was confirmed by LC-MS/MS to be a mobility form of H-FABP.

Figure 19. LC-MS/MS analysis of Sample A.

Tandem mass spectrometry confirms the MALDI-TOF identification of Sample A as A-FABP. Figure 19 lists the peptide sequences obtained in LC-MS/MS that yielded this result.

A gi|119782

20 MS/MS spectra tTot: 7.3e8

FATTY ACID-BINDING PROTEIN, ADIPOCYTE (AFABP) (ADIPOCYTE LIPID-BINDING PROTEIN) (ALBP) (P2 ADIPOCYTE PROTEIN) (MYELIN P2 PROTEIN HOMOLOG) (3T3-L1 LIPID BINDING PROTEIN) (422 PROTEIN) (P15)
gi|293695|gb|AAA39416.1| (K02109) lip-d-binding protein [Mus musculus] gi|12833

Sequence	Reference	TIC	Ions	Scans
(K) LGVEFDEITADDR	gi 119782 +8	1.7e8	18/24	1405-1410
(R) SESTFKNTEISFK	gi 119782 +11	2.2e7	17/24	1256-1265
(R) KRDKLVVEECVM*K	gi 119782 +4	1.6e6	29/52	1169
(R) DGDKLVVEECVM*KGVSTR	gi 119782 +5	9.5e6	29/68	1307-1312
(K) LVSSNFDDYM*KEVGVFATR	gi 119782 +14	1.5e7	36/80	1461-1466
(R) DGDKLVVEECVMK	gi 119782 +5	9.5e7	18/22	1284-1291
(K) LVSSNFDDYMK	gi 119782 +17	3.8e7	19/22	1330-1333
(R) KRDKLVVEECVMK	gi 119782 +4	1.1e7	30/52	1277-1298
(R) DGDKLVVEECVM*K	gi 119782 +5	7.7e7	24/44	1118-1125
(K) LVSSNFDDYM*K	gi 119782 +17	2.1e7	18/22	1165-1172
(K) LVSSNFDDYM*KEVGVFATR	gi 119782 +14	8.4e5	18/40	1470
(R) KRDKLVVEECVM*K	gi 119782 +4	2.5e6	15/26	1160
(K) LGVEFDEITADDRK	gi 119782 +8	7.5e7	27/52	1363-1368
(K) EVGVGFATR	gi 119782 +14	1.0e8	15/16	1130-1137
(K) LVVEECVMK	gi 119782 +9	2.1e7	13/14	1225-1228
(K) LGVEFDEITADDRKVK	gi 119782 +8	9.9e6	20/60	1384
(K) GVTSTRVYERA	gi 119782 +10	4.1e6	11/20	1046
(K) LVVEECVMK	gi 119782 +9	2.8e6	9/14	1230
(K) NTEISFK	gi 119782 +34	4.0e7	9/12	1104-1109
(K) EVGVGFATR	gi 119782 +14	9.0e6	11/16	1134

Single Sequences (No Groups)

2 MS/MS spectra tTot: 1.4e7

Sequence Reference TIC Ions Scans
(K) VTLVSAAPEK gi|12832118 7.8e6 16/18 1074-1085
(AK002261) putative [Mus musculus] gi|2842924|dbj|BAB25786.1| (AK008624) putative [Mus musculus]

(R) SSFFVNGTLGGQK gi|6755040 +3 6.2e6 18/26 1524-1531
profilin 1 [Mus musculus] gi|130980|sp|P10924|PRO1_MOUSE PROFILIN I gi|91197|pir|S04067 profilin - mouse
gi|53782|emb|CAA32586.1| (X14425) profilin (AA 1-140) [Mus musculus] gi|12805237|gb|AAH02080.1|AAH02080 (BC002080)
profilin 1 [Mus musculus] gi|12846945|dt|BAB27373

Legend:

Sequence: The isobaric residue pairs Leu/Ile, Gln/Lys and Phe/Msx are displayed with the assignment as in the known sequence. Either residue within the pair may be possible: the displayed assignment does not connote a defined assignment to one or the other. The amino acid N-terminal to the known sequence is displayed in parentheses ().

Ions: The number of fragment ions (b-, y- and/or a-ions) experimentally observed / number of fragment ions possible. This fraction is a crude estimate of the minimum percentage of the sequence represented by the spectrum.

Reference: The database reference which contains the displayed sequence. A reference followed by a plus sign and number (e.g. +2) indicates the displayed sequence is also present in that number of additional database references

TIC: The intensity (total ion current) of the the MS/MS spectrum. This is a unitless number. Note: mass spectrometry of different peptide analytes is not quantitative. This value should not be used to ascertain a major versus a minor component.

Scans: The scan number(s) of the acquired MS/MS spectrum.

Modifications: * = +16.000 modifier of preceding amino acid. C=160.038

Dir: blucianosam3-gt
Enz: Trypsin_Strict

Files: 0313Zblsam3-gt (03/14/2001-03/14/2001)
Oper: jma

Report: SAM3-GTsnr (wsl)

MR: 3 PTT: +
R22/D7/C15

Figure 20. Coverage map of LC-MS/MS identification of A-FABP

Figure 20 shows the coverage map of A-FABP, the protein identified by MALDI-TOF mass spectrometry. The portion of the protein that represents matched peptides is underlined. The program MS-Digest was used to predict all the peptides that result from a trypsin digest of A-FABP. Five out of ten of the predicted peptides were detected by mass spectrometry.

A-FABP
coverage map

MCDAFVGTWK LVSSNFDDYMYK EVGVGFATR K VAGMAK
PNMIISVNGDLVTIR SESTFK NTEISFK LGVEFDEITADDRKVK
SIITLDGGALVQVQK WDGK STTIK R K R DGDK LVVECVMK
GVTSTR VYER A

Coverage: 58%
5/10 predicted peptides
PI 8.53, MW 14.7 kDa

Figure 21. LC-MS/MS analysis of Sample B confirms its identity as H-FABP, the heart-type fatty acid binding protein

Tandem mass spectrometry yielded positive, unambiguous identification of Sample B as H-FABP. Figure 21 lists the peptide sequences obtained in LC-MS/MS that yielded this result. These data show the reason for the ambiguity in the MALDI-TOF analysis: two contaminating proteins that apparently run in the same location on the gel.

A gi|1706758 15 MS/MS spectra tTot: 6.1e8
 FATTY ACID-BINDING PROTEIN, HEART (H-FABP) (MAMMARY-DERIVED GROWTH INHIBITOR) (MDGI)

Sequence	Reference	TIC	Ions	Scans
(R) QVAMTKPTTIIIEKNGDTITIK	gi 1706758 +4	5.1e6	28/84	1169-1172
(K) LILTLTHGSVVSTR	gi 1706758 +2	4.4e7	27/52	1237-1244
(R) QVASM*TKPTTIIIEK	gi 1706758 +11	4.4e7	17/26	0913-0920
(R) QVAMTKPTTIIIEK	gi 1706758 +11	5.9e7	14/26	0950-0955
(K) SLVTLDDGGK	gi 1706758 +4	6.9e7	14/16	0964
(K) SLGVGFATR	gi 1706758 +16	1.8e8	13/16	1046-1053
(K) NGDTITIK	gi 1706758 +5	6.4e7	12/14	0850-0857
(K) NFDDYMK	gi 1706758 +16	3.2e7	11/12	1008-1011
(K) SLVTLDDGGK	gi 1706758 +4	3.4e7	11/16	0969-0976
(R) QVASM*TKPTTIIIEK	gi 1706758 +11	1.6e6	17/52	0945
(K) NGDTITIK	gi 1706758 +5	2.1e7	10/14	0766-0824
(R) TYEKEA	gi 1706758 +11	2.1e6	8/10	0614-0628
(K) SLGVGFATR	gi 1706758 +16	5.7e5	9/16	1806-1813
(K) TQSTFK	gi 1706758 +10	9.9e6	8/10	0644-0649
(R) QVAMTKPTTIIIEK	gi 1706758 +11	4.1e7	20/52	1032-1039

B gi|117097 4 MS/MS spectra tTot: 9.7e6
 CYTOCHROME C OXIDASE POLYPEPTIDE VA gi|66277|pir|CABO cytochrome-c oxidase (EC 1.9.3.1) chain Va [validated]
 - bovine gi|5822168|pdb|1OCR|E Chain E, Bovine Heart Cytochrome C Oxidase In The Fully Reduced State
 gi|5822181|pdb|1OCR|R Chain R, Bovine Heart Cytochrome C

Sequence	Reference	TIC	Ions	Scans
(K) GM*N*TLVGYDLVPEPK	gi 117097 +4	1.7e6	20/28	1258-1263
(-) SHGSHEDEEFDFAR	gi 117097	6.1e6	32/52	0852
(R) RLNDFASAVR	gi 117097 +4	1.2e6	13/18	1078
(K) ITDAALR	gi 117097 +5	6.3e5	9/12	0936

C gi|135762 2 MS/MS spectra tTot: 3.7e6
 3-KETOACYL-COA THIOLASE, MITOCHONDRIAL (BETA-KETOTHIOLASE) (ACETYL-COA ACYLTRANSFERASE)
 (MITOCHONDRIAL 3-OXOACYL-COA THIOLASE) gi|66509|pir|XURT acetyl-CoA C-acyltransferase (EC 2.3.1.16),
 mitochondrial - rat gi|55544|emb|CAA28952.1| (X05341) thiolase (AA 1-397) [Rattu]

Sequence	Reference	TIC	Ions	Scans
(R) VGVPTETGALTLNR	gi 135762	2.0e6	16/26	1123
(R) GVFIWAAK	gi 135762	1.7e6	12/14	1076-1081

Single Sequences (No Groups) 1 MS/MS spectra tTot: 1.9e6

Sequence	Reference	TIC	Ions	Scans
(K) AVAQGNLSSADVQAAK	gi 418146 +2	1.9e6	21/30	0868

UBIQUINOL-CYTOCHROME C REDUCTASE COMPLEX CORE PROTEIN 2 PRECURSOR (COMPLEX III SUBUNIT II)
 gi|320069|pir|S29510 ubiquinol-cytochrome-c reductase (EC 1.10.2.2) core protein II precursor - rat

Legend:

- Sequence:** The isobaric residue pairs Leu/Ile, Gln/Lys and Phe/Msx are displayed with the assignment as in the known sequence. Either residue within the pair may be possible: the displayed assignment does not connote a defined assignment to one or the other. The amino acid N-terminal to the known sequence is displayed in parentheses ().
- Ions:** The number of fragment ions (b-, y- and/or a-ions) experimentally observed / number of fragment ions possible. This fraction is a crude estimate of the minimum percentage of the sequence represented by the spectrum.
- Reference:** The database reference which contains the displayed sequence. A reference followed by a plus sign and number (e.g. +2) indicates the displayed sequence is also present in that number of additional database references
- TIC:** The intensity (total ion current) of the the MS/MS spectrum. This is a unitless number. Note: mass spectrometry of different peptide analytes is not quantitative. This value should not be used to ascertain a major versus a minor component.
- Scans:** The scan number(s) of the acquired MS/MS spectrum.
- Modifications:** * = +16.000 modification of preceding amino acid. C=160.038

Figure 22. Coverage map of LC-MS/MS identification of H-FABP

Figure 22 shows the coverage map of H-FABP. The portion of the protein that represents matched peptides is underlined. The program MS-Digest was used to predict all the peptides that result from a trypsin digest of H-FABP. Seven out of thirteen of the predicted peptides were detected by mass spectrometry.

H-FABP

MADAFVGTWKLVDSKNFDDYMKSLGVGFATRQVASMTKPTTIIKNGDTITI
KTQSTFKNTEINFQLGIEFDEVTADDRKVKSLVTLDGGKLIHVQKWDGQETTL
TRELVDGKLILTLTHGSVVSTRTYE KEA

coverage: 55%

7/13 predicted possible peptides

pI 5.38, MW 14.8 kDa



Figure 23. 2-DE analysis of extract 2 proteins from skeletal muscle shows proteins with altered mobility similar to those found in heart

Skeletal muscle proteins from the gastrocnemius and soleus of wild-type and *DMPK*^{-/-} mice were analyzed by 2-DE. First dimension: pH 4.5-5.5 isoelectric focusing. Second dimension, 14% SDS-PAGE slab gel. Panels A and C represent the wild-type sample; panels B and D represent the *DMPK*^{-/-} sample. In panels C and D the outlined portions of the full gels are enlarged to illustrate the shifted proteins, indicated by arrows.

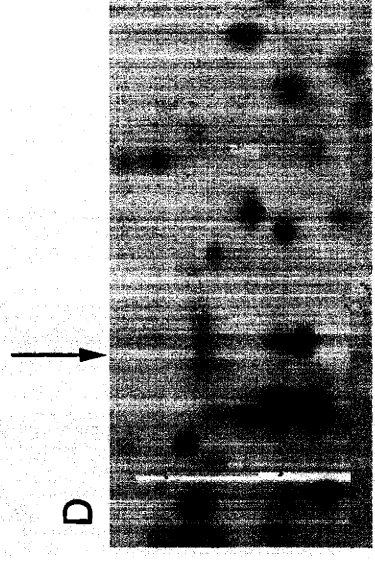
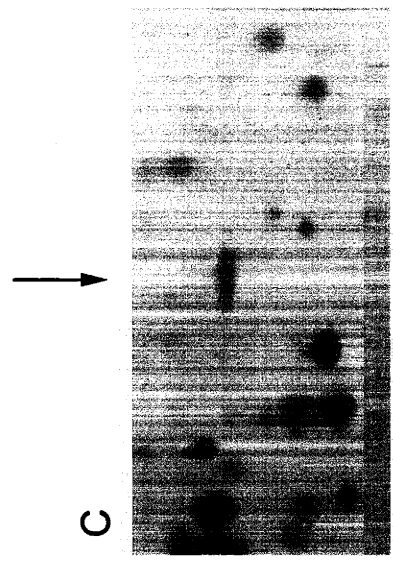
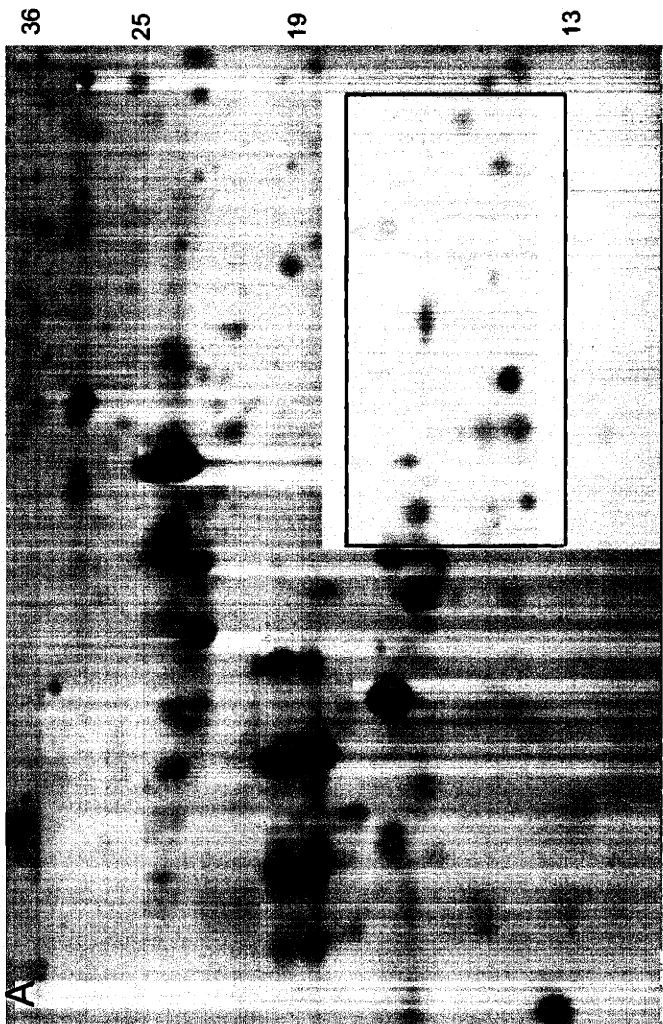
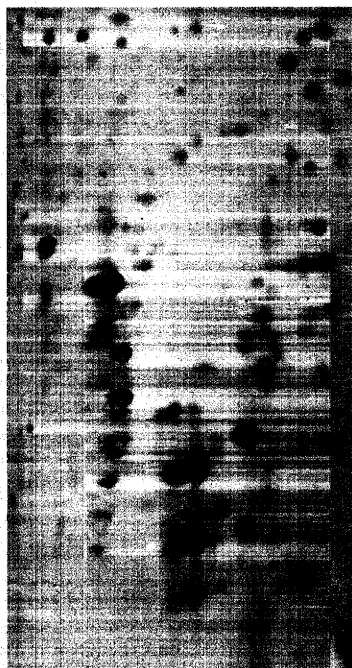


Figure 24. 2-DE analysis of extract 2 proteins: color overlay

In an attempt to make the mobility shift described in Figure 23 more visible, the gels have been colorized and overlaid. Wild-type (green, panel A) and *DMPK* *-/-* (red, panel B) gels are overlaid in C. The boxed area of C is enlarged in panel D. The portions that are clearly green or red in D represent areas of the gel that do not align.



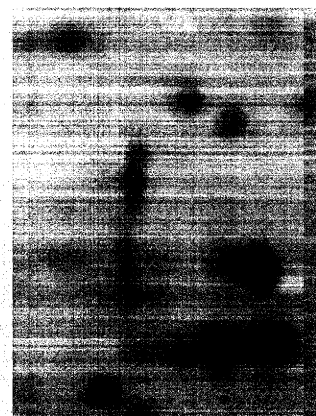
B



A



C



D

Figure 25. Comparison of fractionated protein samples: extract 2 from skeletal muscle

2-DE was performed on extract 2 skeletal muscle proteins. Proteins were loaded onto pre-cast 18cm pH 4.5-5.5 isoelectric focusing gels. After focusing for 17 hours at 3500 volts, the gels were loaded onto 14% second dimension SDS-PAGE gels. These gels were then fixed and silver stained.

Panel A and C represent the wild-type protein sample; panels B and D represent the mutant sample. Mobility difference is indicated by arrows; the highlighted protein appears at a more acidic pI than the corresponding protein from the *DMPK* ^{-/-} sample.

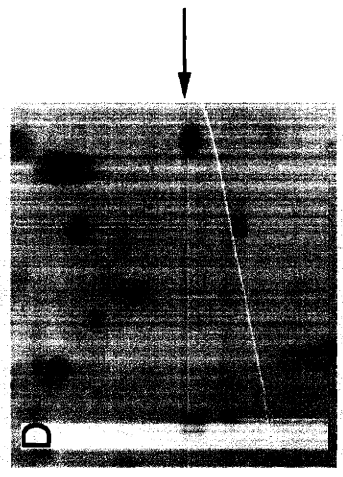
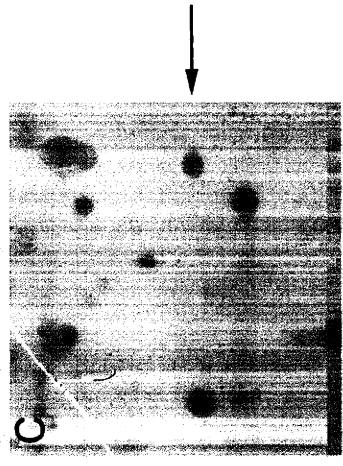
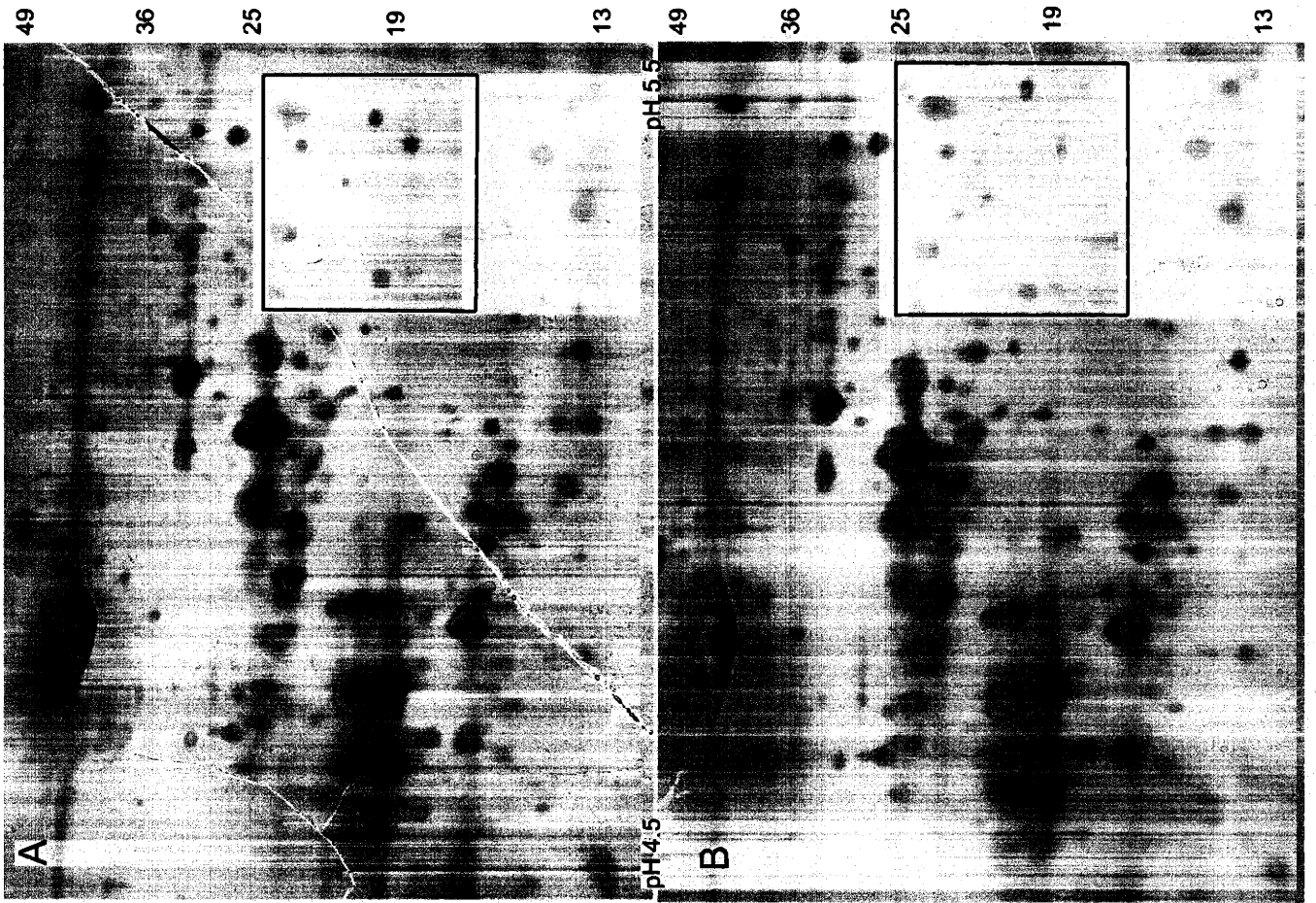
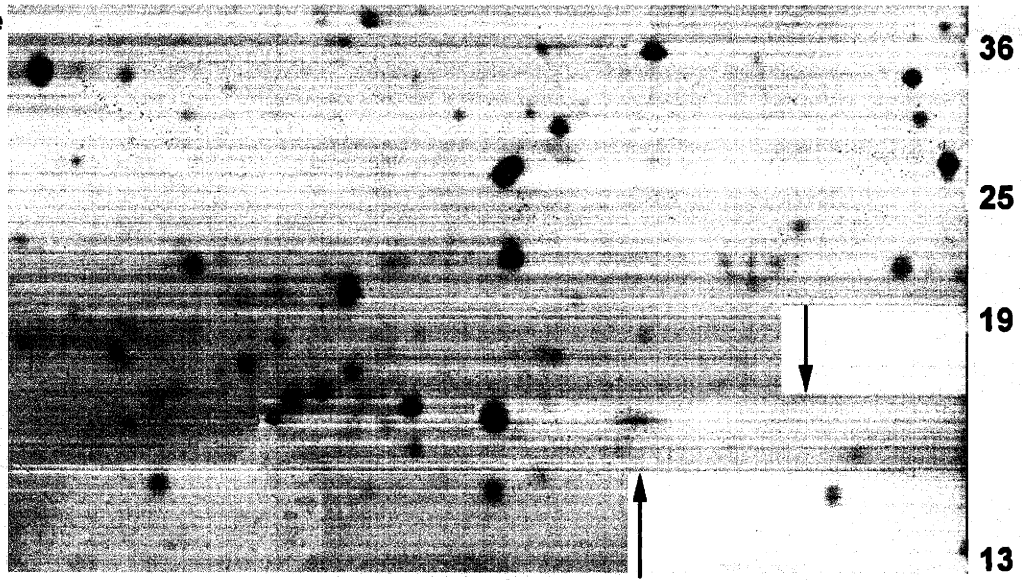


Figure 26. Comparison of fractionated protein samples: extract 2 from brain

2-DE was performed on extract 2 brain proteins. Proteins were loaded onto pre-cast 18cm pH 4.5-5.5 isoelectric focusing gels. After focusing for 17 hours at 3500 volts, the gels were loaded onto 14% second dimension SDS-PAGE gels. These gels were then fixed and silver stained.

Panel A represents the wild-type protein sample, whereas panel B represents the mutant sample. Mobility differences are indicated by arrows; at least two proteins show altered mobility in the comparison of these two gels.

A
wild-type



B
DMPK -/-

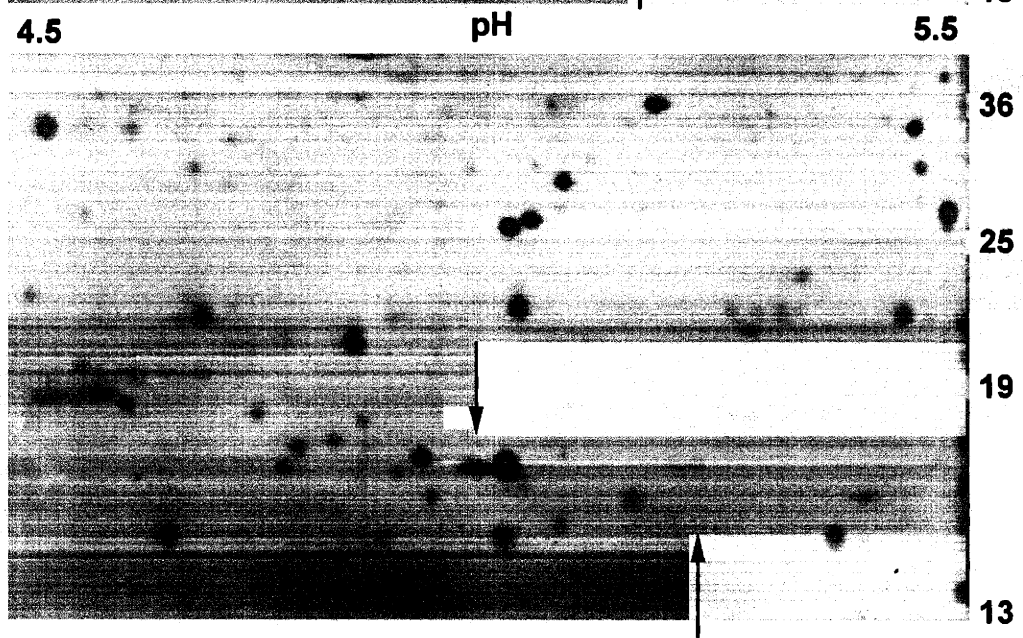
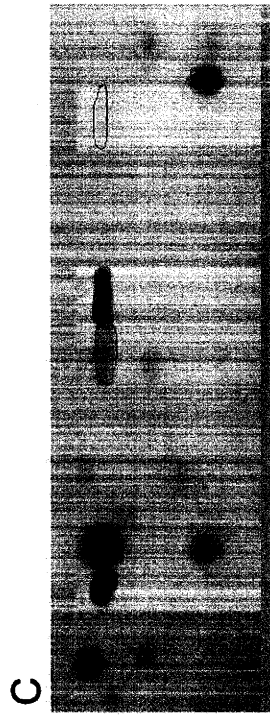
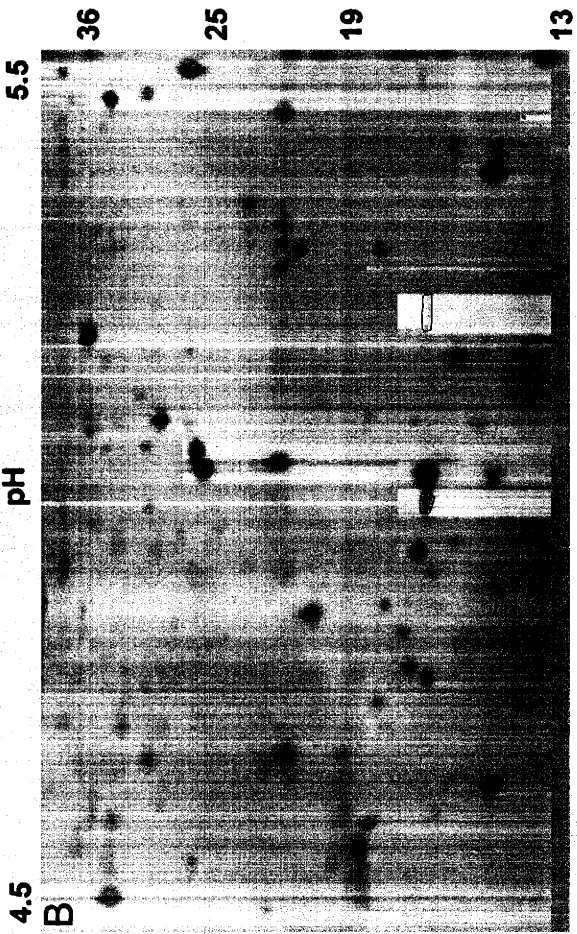
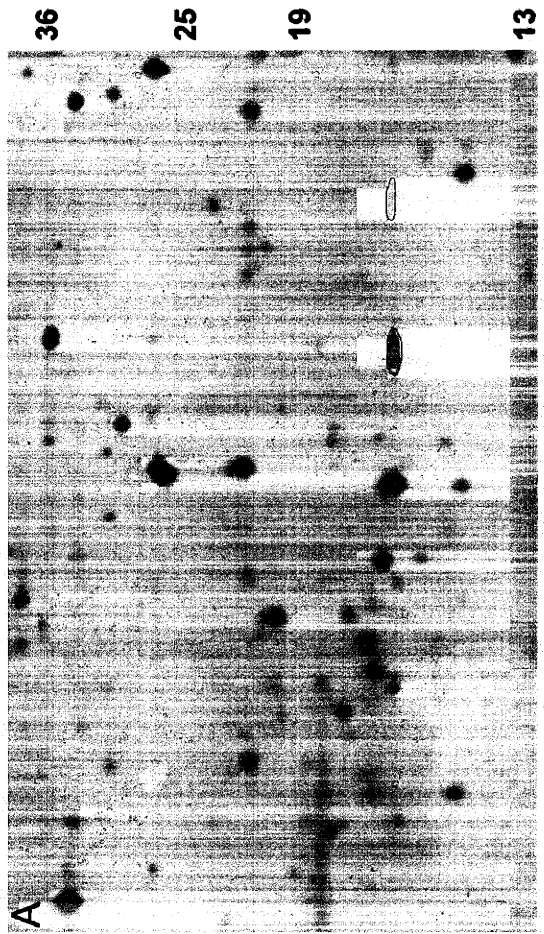


Figure 27. Comparison of fractionated protein samples: color overlay of extract 2 from brain

The 2-DE gels of brain proteins seen in Figure 27 have been colorized and overlaid to illustrate the differences in relation to each other. The spots with altered mobility have been outlined; those from wild-type gel are colored green, those from the *DMPK* *-/-* gel are colored red.



mobility shift. Figure 27 is an overlay of the gels in Figure 16 that is meant to illustrate the position of the spot differences in relation to each other.

Further analysis

Fatty acid binding proteins in skeletal muscle and brain

As Figures 23 and 26 illustrate, we found a mobility shift in a 2-DE comparison of extract 2 proteins from wild-type and *DMPK*^{-/-} skeletal muscle and brain. The shifted proteins correspond to the same isoelectric point and molecular weight area as the H-FABP from heart extract 2. The pattern in brain is somewhat complicated, as there seem to be two FABP-like proteins on each gel (Figure 26). However, it seems that the proteins are shifted in the same manner as those from heart, that is, the proteins in the wild-type sample have a more acidic pI than those from the *DMPK*^{-/-} sample. Interestingly, the opposite pattern is seen in the gels from skeletal muscle (Figure 23). These experiments will need to be repeated and each of the proteins with altered mobility analyzed before conclusions can be drawn as to the meaning of these patterns.

Phosphorylation state of Sample A

To determine whether the altered mobility of the fatty acid binding proteins was due to a difference in phosphorylation state in the absence of DMPK, we investigated the phosphorylation state of the proteins in two different ways. First

we sought to determine whether treatment of the Sample A extracts with phosphatase was sufficient to abolish its mobility difference. The wild-type and *DMPK* *-/-* samples were treated with phosphatase and then run on 2-DE gels in parallel with untreated samples. Sample A from the phosphatase-treated extracts still retained its differential mobility, suggesting that the difference in mobility was not due to phosphorylation. Furthermore, mass spectrometry was used to search for phosphorylated peptides and none were found. As is typical for this type of analysis, not all the peptides were recovered during mass spectrometric analysis of the tryptic digest products. It is possible that a phosphorylated peptide existed but was not recovered. However, taken together these data indicate once again that the observed mobility shift is not due to phosphorylation. This would suggest that the fatty acid binding proteins are not direct targets of DMPK, but are affected by lack of DMPK downstream of the primary phosphorylation event.

Summary

In my efforts to understand the molecular basis for the pathology of myotonic dystrophy, I sought to elucidate the function of DMPK, a serine threonine protein kinase encoded by the gene *DMPK* that is mutated in DM1 patients. To accomplish this goal I undertook a proteomics-based approach. The strategy of using proteomic techniques circumvents many of the issues of

biological relevance and specificity commonly observed in cell culture and *in vitro* studies.

This approach evaluated the effect of loss of DMPK on cellular proteins. For this analysis, protein extracts from wild-type mice were compared to those from mice that are deficient in DMPK (*DMPK -/-*) using proteomics techniques such as 2D gel analysis and mass spectrometry.

The results show that it is possible to identify differences in mobility shift between proteins from wild-type and *DMPK -/-* tissues in 2-dimensional SDS-PAGE gels. To date, a number of different reproducible mobility shifts have been identified. Two of these were selected for analysis by MALDI-TOF mass spectrometry. Due to difficulty in analyzing one of the samples, and to the fact that the mouse genome is not yet completely sequenced (and thus not all the proteins are present in the database), these samples were analyzed further by LC-MS/MS, an approach that provides peptide sequence as well as fingerprint data. Both of these proteins that had altered mobility in the mutant tissues were identified as isoforms of fatty acid binding proteins, by both MALDI-TOF and LC-MS/MS. A mobility shift in the same molecular weight and isoelectric point range was seen in the skeletal muscle and brain 2-DE gel comparisons as well, suggesting that perhaps the loss of DMPK affects fatty acid binding protein mobility in these tissues.

These experiments have demonstrated that proteomic analysis is a useful approach for investigation of mouse models of human disease, and that it is possible to find reproducible differences between mice of different genotype. Investigation of the cellular or subcellular proteomes of other mouse models could provide much needed insight into the mechanisms of various other diseases. In the next chapter we discuss these data and their potential relationship to myotonic dystrophy.

Materials and Methods

Sample Preparation

Age-matched or sibling wild-type and *DMPK*^{-/-} mice were sacrificed using carbon dioxide asphyxiation, and the desired tissues (heart, brain, and skeletal muscle) dissected and removed. When possible, 3-month-old sibling mice were used. To avoid contamination of results by blood proteins, hearts were perfused immediately after dissection to remove traces of blood. The skeletal muscles used were the gastrocnemius and soleus; these muscles are not severely affected in human myotonic dystrophy and thus are less likely to show complicating differences due to accelerated tissue degeneration in the mutant mice. Also, DMPK is most highly expressed in slow twitch muscle fibers, and the soleus muscle represents the largest concentration of slow twitch fibers that is easily dissected cleanly.

Tissue samples were used immediately after dissection since, when fractionating, freezing can alter the sample of proteins in each extract. The extraction protocol was based on those previously described (Molloy, 1998, Klose, 1999). Heart and skeletal muscle were chopped thoroughly and then all three tissues were homogenized in ice-cold 40 mM tris pH 9.5 using a Polytron PT 2100 (Brinkman) for 4 x 5 seconds at medium speed. Homogenates were incubated 10 minutes on ice with 150U endonuclease in the presence of

protease and phosphatase inhibitors. The samples were clarified by centrifugation at 12000g for 10 minutes at 4°C in a Sorval RC-5 centrifuge. The supernatant, extract #1, was lyophilized and resuspended in CHAPS I buffer (below). The pellet was rinsed with ice-cold 40mM, homogenized, and spun again. The washed pellet was resuspended in CHAPS II buffer (see below) and homogenized. The 2nd homogenate was clarified by centrifugation at 12000g for 10 minutes at 10°C and the resultant supernatant, extract #2, was aliquoted and frozen at -80°C. The pellet was washed as before in CHAPS II buffer, homogenized, and spun again. The pellet was resuspended in CHAPS III and homogenized by manual pipetting. The homogenate was spun at 12000g at room temperature and the supernatant, extract #3, was carefully removed from the glassy pellet and frozen at -80°C. CHAPS I: 8M urea, 4% CHAPS, 2 mM tributylphosphine, 40 mM tris pH 9.5, 0.5% carrier ampholytes, 50 µM sodium orthovanadate, 5 mM sodium fluoride, 5 mM β-glycerophosphate, and Complete™ protease inhibitor mix. CHAPS II: 8M urea, 4% CHAPS, 100 mM DTT, 40 mM Tris pH 9.5, 0.5% carrier ampholytes, 50 µM sodium orthovanadate, 5 mM sodium fluoride, 5 mM β-glycerophosphate, and Complete™ protease inhibitor mix. CHAPS III: 5 M urea, 2% thiourea, 2% CHAPS, 2% caprylyl sulfobetaine, 2 mM tributylphosphine, 40 mM Tris pH 9.5, 0.5% carrier ampholytes, 50 µM sodium orthovanadate, 5 mM sodium fluoride, 5 mM β-glycerophosphate, and Complete™ protease inhibitor mix.

2-dimensional gel electrophoresis

Most equipment and supplies for 2-dimensional electrophoresis were purchased from Amersham/Pharmacia Biotech. All 2D gels were run using 18 cm Immobiline of various pH ranges. First dimension gels were run on a Multiphor II flatbed electrophoresis apparatus. DryStrips were rehydrated overnight in rehydrating buffer containing protein sample (8M Urea, 100mM DTT, 4% CHAPS, 0.5% carrier ampholytes, 40mM Tris and trace bromophenol blue). Strips were focused according to prescribed protocol. For example, pH 4.5-5.5 gels were run at 20°C: ramp to 500V for 0:01hr, ramp to 3500V for 1:30hr, hold at 3500V for 16:20 hr. 2nd dimension SDS-PAGE was run on 20 x 23 cm gel cassettes in a Hoefer DALT electrophoresis tank at 75V overnight.

Silver Staining

Silver staining of gels was performed as described previously (Schevchenko, 1996). Briefly, the gels were fixed with 50% methanol / 5% acetic acid for 20 minutes. After a 10 minute wash in 50% methanol followed by a wash in water for 1-12 hr, the gels were sensitized by incubating in 0.2% sodium thiosulfate followed by two brief water washes. The gels were then incubated in 0.15% silver nitrate for 40 minutes followed by two water washes. The gels were developed in 0.04% formalin in 2% sodium carbonate and the reaction was terminated with 1% acetic acid. Gels were either stored at 4°C overnight, or

spots were cut out immediately, washed 2 x 5 minutes in 50% acetonitrile, and stored at -20°C or processed as described below.

Sample Preparation for MALDI-TOF MS

Sample preparation was performed as described (Jensen, 1999).

Reduction and alkylation: gel fragments containing the protein were cut from the silver-stained gels and were swollen in 10 mM DTT/100 mM ammonium carbonate, and then incubated for 45 minutes at 56°C. Tubes were chilled to room temperature, excess liquid was removed and replaced with freshly prepared 55 mM iodoacetamide/100 mM ammonium bicarbonate, then incubated for 30 minutes at room temperature in the dark.

Washing: gel pieces were washed twice with water and 1:1 water/acetonitrile for 15 minutes each. Solvent volumes equaled roughly 2 times the gel volume. Gel fragments were then covered with acetonitrile. After 30 minutes they were rehydrated in 100 mM ammonium carbonate for 5 minutes. An equal volume of acetonitrile was added to make a 1:1 solution and the mixture was incubated for 15 minutes. Gel fragments were then dried in a vacuum centrifuge.

In-gel digestion: Gel fragments were rehydrated in enough digestion buffer (50 mM ammonium carbonate, 5 mM calcium chloride, 12.5 ng/μl of trypsin (Roche Biochemicals, sequencing grade)) to cover the gel pieces and incubated 45 minutes on ice. At this time the supernatant containing the trypsin was removed and replaced with 5-20 μl of the same buffer without trypsin to keep the gel

pieces wet during the enzymatic cleavage, which was carried out at 37°C overnight.

Extraction of peptides from gel: After overnight digestion, a sufficient volume of 25mM ammonium carbonate was added to cover the gel pieces and incubated for 15 minutes. An equal volume of acetonitrile was added and incubated for 15 minutes and the supernatant recovered. The extraction was repeated two times with 5% formic acid and acetonitrile (1:1, v/v). All extracts were pooled and DTT was added to a final concentration of 1mM to prevent oxidation of peptides. The sample was dried in a vacuum centrifuge.

MALDI-TOF MS

Peptides were dissolved in 0.1% trifluoroacetic acid in a volume of 10 μ l and bound to a Zip Tip_{C18} pipette tip containing 10 μ l of Poros R2 resin (Millipore, Bedford, MA). Tips with bound peptide were washed twice with 0.1% trifluoroacetic acid. To eliminate the appearance of polymer contamination peptides were fractionated by eluting with 2%, 5%, 10%, 25%, 50%, and 80% acetonitrile. 6 μ l of each extraction solution was drawn over the resin 10 times and then spotted directly on the gold plated MALDI-TOF probe plate previously spotted with matrix solution, either α -cyano-4-hydroxycinnamic acid or 3,5-dimethoxy-4-hydroxycinnamic acid. Samples were run on a Voyager Elite MALDI-TOF mass spectrometer (Perseptive Biosystems, Bedford, MA) and calibrated by an internal standard (Sequazyme Mass Standards Kit, PE Biosystems, Foster City, CA).

Each extract was analyzed separately and the resultant spectra results combined. Contaminating polymer was seen in the first eluate only.

Analysis of MALDI-TOF MS spectra

Spectra obtained from the MALDI-TOF mass spectrometer were manually analyzed by comparing the sample run with a sample taken from a blank area from the same gel near the selected spot. Any matching peptide peaks were subtracted from the sample fingerprint and the edited peaks were analyzed using the online program MS-Fit at the Protein Prospector website (<http://prospector.ucsf.edu>) sponsored by UCSF. Both NCBI and Swissprot databases were searched for either human and mouse or exclusively mouse protein matches. Results were compared with predicted digest patterns calculated by the MS-Digest program at the Protein Prospector website. If the results indicated a protein that had been previously identified on a 2-dimensional gel the results were compared with the information available at one of the online 2D databases (<http://www.expasy.ch/>). The position of the analyzed spot and nearby reference proteins was compared with that seen in published gels.

MS-MS Peptide Sequencing

The direct sequence analysis by ion trap mass spectrometry was performed on peptides resulting from the in-gel reduction, S-

carboxyamidomethylation, and tryptic digestion of the silver-stained proteins isolated by 2D SDS-PAGE. The resulting mixture was introduced directly into the electrospray ionization (ESI) source of a quadrupole ion trap mass spectrometer (Finnigan LCQ) by a reverse phase microcapillary column packed in-house with POROS R2 (Perseptive Biosystems) (Nash, 1996). Peptides were eluted at a nominal flow rate of 500 nL/min with a gradient of 0 to 50% acetonitrile in 0.05M acetic acid over the course of 25 min. The ion trap's online data-dependent scans allowed the automatic acquisition of high-resolution spectra for determining charge state and exact mass and MS/MS spectra for peptide sequence information. Identification of the spectra corresponding to known peptide sequences in the NCBI (National Center for Biotechnology Information) nr and dbest databases was facilitated using the algorithm Sequest (Eng, 1994) and then confirmed by manual inspection.

References

1. Wilkins, M. R., J. C. Sanchez, A. A. Gooley, R. D. Appel, I. Humphery-Smith, D. F. Hochstrasser and K. L. Williams, 1996. Progress with proteome projects: why all proteins expressed by a genome should be identified and how to do it *Biotechnol Genet Eng Rev* **13**: p. 19-50
2. Macko, V. and H. Stegemann, 1969. Mapping of potato proteins by combined electrofocusing and electrophoresis identification of varieties *Hoppe Seylers Z Physiol Chem* **350**(7): p. 917-919.
3. Klose, J., 1975. Protein mapping by combined isoelectric focusing and electrophoresis of mouse tissues. A novel approach to testing for induced point mutations in mammals *Humangenetik* **26**(3): p. 231-243
4. O'Farrell, P. H., 1975. High resolution two-dimensional electrophoresis of proteins *J Biol Chem* **250**(10): p. 4007-4021.
5. Klose, J. and U. Kobalz, 1995. Two-dimensional electrophoresis of proteins: an updated protocol and implications for a functional analysis of the genome *Electrophoresis* **16**(6): p. 1034-1059.
6. Merril, C., *Detection of proteins separated by electrophoresis*, in *Advances in Electrophoresis*, Chrambach, A., Dunn, M., and Radolla, B., Editor. 1987, VCH: New York, NY. p. 111-140.
7. Brown, J. L., and Roberts, W. K., 1976. Evidence that approximately eighty percent of the soluble proteins from Ehrlich cells are N-acetylated *Journal of Biological Chemistry* **251**: p. 1009-1014
8. Martin, S. E., J. Shabanowitz, D. F. Hunt and J. A. Marto, 2000. Subfemtomole MS and MS/MS peptide sequence analysis using nano-HPLC micro-ESI fourier transform ion cyclotron resonance mass spectrometry *Anal Chem* **72**(18): p. 4266-4274.
9. Gatlin, C. L., Kleeman, G. R., Hays, L. G., Link, A. J., and Yates, J. R. III, 1998. Protein identification at the low femtomole level from silver-stained gels

using a new fritless electrospray interface for liquid chromatography-microspray and nanospray mass spectrometry *Analytical Biochemistry* **263**: p. 93-101

10. Mann, M., P. Hojrup and P. Roepstorff, 1993. Use of mass spectrometric molecular weight information to identify proteins in sequence databases *Biol Mass Spectrom* **22**(6): p. 338-345.

11. Pappin, D. J. C., Hojrup, P., and Bleasby, A. J., 1993. Rapid identification of proteins by peptide-mass fingerprinting *Current Biology* **3**: p. 327-332

12. Mann, M., 1996. A shortcut to interesting human genes: peptide sequence tags, expressed- sequence tags and computers *Trends Biochem Sci* **21**(12): p. 494-495.

13. Mann, M. and M. Wilm, 1994. Error-tolerant identification of peptides in sequence databases by peptide sequence tags *Anal Chem* **66**(24): p. 4390-4399.

14. Ducret, A., I. Van Oostveen, J. K. Eng, J. R. Yates, 3rd and R. Aebersold, 1998. High throughput protein characterization by automated reverse-phase chromatography/electrospray tandem mass spectrometry *Protein Sci* **7**(3): p. 706-719.

15. Link, A. J., J. Eng, D. M. Schieltz, E. Carmack, G. J. Mize, D. R. Morris, B. M. Garvik and J. R. Yates, 3rd, 1999. Direct analysis of protein complexes using mass spectrometry *Nat Biotechnol* **17**(7): p. 676-682.

16. Gras, R., M. Muller, E. Gasteiger, S. Gay, P. A. Binz, W. Bienvenut, C. Hoogland, J. C. Sanchez, A. Bairoch, D. F. Hochstrasser and R. D. Appel, 1999. Improving protein identification from peptide mass fingerprinting through a parameterized multi-level scoring algorithm and an optimized peak detection *Electrophoresis* **20**(18): p. 3535-3550

17. Molloy, M. P., B. R. Herbert, B. J. Walsh, M. I. Tyler, M. Traini, J. C. Sanchez, D. F. Hochstrasser, K. L. Williams and A. A. Gooley, 1998. Extraction of membrane proteins by differential solubilization for separation using two-dimensional gel electrophoresis *Electrophoresis* **19**(5): p. 837-844.

18. Klose, J., *Fractionated extraction of total tissue proteins from mouse and human for 2-D electrophoresis*, in *Methods in Molecular Biology, 2-D Proteome Analysis Protocols*, Link, A. J., Editor. 1999, Humana Press: Totowa, NJ. p. 67-85.
19. Reddy, S., D. B. Smith, M. M. Rich, J. M. Leferovich, P. Reilly, B. M. Davis, K. Tran, H. Rayburn, R. Bronson, D. Cros, R. J. Balice-Gordon and D. Housman, 1996. Mice lacking the myotonic dystrophy protein kinase develop a late onset progressive myopathy *Nat Genet* **13**(3): p. 325-335.
20. Schevchenko, A., Jensen, O., Podtelejnikov, A. V., Saggllocco, F., Wilm, M., Vorm, P., Mortensen, P., Shevchenko, A., Boucherie, H., Mann, M., 1996. *Proc. Natl. Acad. Sci. USA* (93): p. 14440-14445
21. Jensen, O. N., Wilm, M., Shevchenko, A., and Mann, M., *Methods in Molecular Biology: 2D Proteome Analysis Protocols*. 1999, Humana Press. p. 513-530.
22. Nash, H. M., S. D. Bruner, O. D. Scharer, T. Kawate, T. A. Addona, E. Spooner, W. S. Lane and G. L. Verdine, 1996. Cloning of a yeast 8-oxoguanine DNA glycosylase reveals the existence of a base-excision DNA-repair protein superfamily *Curr Biol* **6**(8): p. 968-980.
23. Eng, J. K., McCormick, A. L., and Yates, J. R., III, 1994. *Journal of the American Society of Mass Spectrometry* **5**: p. 976-989

Acknowledgements

All work described in this chapter including mouse handling, 2-DE gel analysis, and peptide preparation was done by Brenda Luciano except for the following:

1. The gels in Figure 5 were run at Kendrick Laboratory of Madison, WI.
2. The gels in Figure 8 were run by Dr. Nick Bizios at Cold Spring Harbor Laboratory.
3. MALDI-TOF mass spectrometry was performed under the instruction of Dr. Bing Wang of Variagenics, Inc., Cambridge, MA.
4. LC-MS/MS analysis was performed by Dr. William S. Lane and his laboratory staff at the Harvard Microchemistry Facility, Cambridge, MA.

Chapter 3: Discussion

Part 1: Fatty acid binding proteins and their potential role in DM1

Part 2: Proteomic analysis in models of human disease

Chapter 3: Discussion

Part 1: Fatty acid binding proteins and their potential role in DM1

The previous chapter describes a proteomics-based approach to investigate the *in vivo* function of DMPK. 2-dimensional SDS-PAGE (2-DE) gels were used to compare several tissue-specific proteomes of wild-type and *DMPK* *-/-* mice. A number of proteins were identified that differed between wild-type and *DMPK* *-/-* tissue with respect to their isoelectric point or apparent molecular mass. Two of these proteins were selected for further investigation and identified by mass spectrometry. Both of these proteins were subsequently determined to be isoforms of fatty acid binding proteins (FABPs).

The proteomics-based approach has the advantage of allowing a direct analysis of the entire cellular proteome. Furthermore, through this method, the proteomes of wild-type and *DMPK* *-/-* cells can be compared directly. This approach is not limited by the need for any prior knowledge about what might be found, nor does is this analysis limited to identifying proteins that are directly bound to DMPK. However, although the proteomics approach can lead to the identification of proteins that are altered by DMPK loss, it does not discriminate between whether the identified proteins are direct substrates of DMPK, whether they are further downstream in the DMPK pathway, or whether their alteration occurs as a secondary consequence of DMPK's role in the cell. Nevertheless,

this analysis creates a molecular fingerprint of *DMPK* *-/-* cells and provides important clues about the cellular consequences of DMPK loss. This information is critical for understanding the *in vivo* function of DMPK and how mutation of DMPK leads to DM1.

The identification of altered mobility of fatty acid binding proteins in the comparison of 2-DE gels of wild-type and *DMPK* *-/-* mice indicates that a loss of DMPK may contribute to the insulin resistance seen in DM1 patients. Insulin is a polypeptide hormone that, along with glucagon, controls the body's energy metabolism. The direction of energy flux, toward either storage or energy production, is mainly controlled by a balance between these two hormones. Energy production varies in different tissues; however, most organs use free fatty acids for energy. Fatty acid binding proteins function as fatty acid transporters in the cell in response to metabolic stimuli. The altered mobility of the fatty acid binding proteins suggests that the function of these proteins is altered in cells lacking DMPK. This argues that proper DMPK dosage may be necessary for normal metabolic function. The concentration of serum insulin and the function of fatty acid binding proteins are both controlled by the metabolic state of the organism, suggesting that the lack of DMPK disrupts an aspect of energy metabolism that affects the behavior of each.

Proteins that are altered by DMPK loss: the fatty acid binding proteins

As shown in the previous chapter, we demonstrated that two proteins that show altered mobility between heart protein extracts from wild-type and *DMPK*^{-/-} cells are both isoforms of fatty acid binding proteins, the heart-type isoform H-FABP, and the adipocyte-type isoform A-FABP, which is also present in heart. Altered mobility of these proteins may also occur in skeletal muscle and brain.

Fatty Acid Metabolism

Fatty acid (FA) metabolism in mammalian cells depends on a flux of fatty acids, between the plasma membrane and mitochondria or peroxisomes for β -oxidation, and between other cellular organelles for lipid synthesis. Fatty acid oxidation, also known as β -oxidation, is the sequential breakdown of fatty acid chains into the two carbon metabolite acetyl coenzyme A. Oxidation of fatty acids occurs in peroxisomes or in the mitochondria, in which it is coupled to energy production. In most cells, FA oxidation is regulated by the availability of fatty acids, which is in turn controlled hormonally.

Fatty acid metabolism is triggered by insulin signaling in response to the nutritional state. In the fed state, insulin signals an increase in cell permeability to glucose in liver, brain and skeletal muscle type II fibers, and the synthesis of

triacylglycerol from fatty acids in adipose tissue; in the heart and skeletal muscle type I fibers, insulin signals the import of fatty acids for β -oxidation metabolism. Between meals, heart as well as both types of skeletal muscle fibers metabolize fatty acids for energy production.

Fatty acid binding proteins (FABPs)

Fatty acid binding proteins (FABPs) were described for the first time in 1972 (Ockner, 1972). The FABPs are part of a family of small intracellular hydrophobic ligand-binding proteins along with proteins that bind retinoids and bile acid binding proteins. These proteins are all 14-15 kDa proteins that bind fatty acids with high affinity. The FABPs are mainly present in tissues with active lipid metabolism; they are thought to function as fatty acid transporters in response to the body's physiological requirements. There are at least nine different fatty acid binding proteins so far described; each was named according to the tissue from which it was first isolated (Table 1).

Table 1: FABP isoforms

Isoform	Tissue Distribution	Possible Function
L-FABP	liver-about 3% of cytoplasmic protein in hepatocytes and enterocytes	fatty acid metabolism
I-FABP	intestine	
H-FABP	2-4% of cytoplasmic protein in cardiac myocytes, testis, mammary gland, skeletal muscle (soleus 63%*, psoas 17%) kidney (5%) brain (10%) adrenal gland (5%) also detected on myofibrils and in the mitochondrial matrix *percentages represent comparison with abundance of H-FABP found in heart	fatty acid metabolism, differentiation, signal transduction possibly phosphorylated downstream of insulin receptor
E-FABP	epidermis	
A-FABP	adipocytes, cardiac tissue	fatty acid metabolism possibly phosphorylated downstream of insulin receptor
Ex-FABP	extracellular matrix expressed in forming myotubes both <i>in vivo</i> and <i>in vitro</i> , expressed in developing myocardium	extracellular transport of long-chain fatty acids
B-FABP	brain	
O-FABP	lens, retina	implicated in cataract formation
M-FABP	peripheral nerve myelin	

FABP mobility forms

The tissue-specific FABP isoforms can also have several mobilities on 2-DE gels or ion exchange columns due to differences in isoelectric points. In the interest of clarity the FABPs that exhibit different apparent isoelectric points are referred to as mobility forms rather than isoforms, to distinguish them from the tissue-specific isoforms. FABPs of different isoelectric point were identified from isoelectric focusing and ion exchange chromatography (Jagschies, 1985),(Offner, 1986),(Jones, 1988,Myers-Payne, 1996a). The exact nature of the different

mobilities is for the most part unclear, however, these mobility forms do not represent a difference in the presence or absence of bound ligand (Table 2).

H-FABP is the only isoform for which an actual amino acid sequence difference has been reported. Two H-FABP forms have been isolated, one containing asparagine at position 98 (form I) and one containing aspartic acid at position 98 (form II). Both these forms of H-FABP have been found in bovine heart and mammary gland (Borchers, 1997) and mouse brain H-FABP isoform (Myers-Payne, 1996b). One of the bovine H-FABP forms appears to be targeted to mitochondria, suggesting that perhaps each form has a specific function in fatty acid metabolism (Unterberg, 1990).

Protein	Species	Tissue	# of mobility forms	
			Native	Delipidated
H-FABP	Bovine	Heart	2	2
H-FABP	Rat	Heart	2	
H-FABP	Rat	Mammary	2	2
H-FABP	Rat	Heart	2	2
H-FABP	Mouse	Brain	2	2
A-FABP	Rat	Adipose	2	

H-FABP

Most of the FABPs are tissue-specific; however, the heart FABP isoform (H-FABP) is found in various tissues (Table 1). If we look at the distribution of H-

FABP, we can see that the concentration of H-FABP correlates with the β -oxidative capacity of each tissue type. For example, slow-twitch red muscle fibers such as those in the soleus muscle have relatively high oxidative capacity when compared to fast-twitch white muscle fibers, and the level of H-FABP is much higher in the soleus. Therefore, as stated earlier, it seems likely that H-FABP is involved in β -oxidation of fatty acids by binding and transporting them to the mitochondria.

This possible role of H-FABP in the oxidation of fatty acids is at odds, however, with the fact that H-FABP is found in the mammary gland and in the brain. In the mammary gland fatty acid metabolism is directed more toward triglyceride synthesis, and the brain does not oxidize fatty acids for energy production. However, this apparent contradiction could be reconciled by the fact that there is some evidence that FABPs may perform more than one function in the cell. The two mobility forms identified for H-FABP may have different subcellular locations and functions. A large portion of H-FABP is cytosolic. However, a portion of H-FABP has been shown by electron microscopy to be localized on myofibrils and in the mitochondrial matrix. The relative proportions of bovine heart H-FABP mobility forms I and II were reported to be near 15% (pI 5) and 85% (pI 4.9), respectively whereas mouse brain H-FABP mobility forms I and II represent 75% (pI 7.4) and 25% (pI 6.4), respectively (Jagschies, 1985). Thus, for H-FABP, the pattern of mobility form distribution in brain and heart were

opposite. These data suggest that different forms of H-FABP are dominant depending on the metabolic needs of the tissue in which they are expressed.

A-FABP

The adipocyte FABP isoform is expressed in adipose tissue and in heart and interacts directly with hormone-sensitive lipase. It has the capacity to bind a range of fatty acids and in adipose tissue its role is to transport fatty acids away from the triglyceride after hydrolysis. The destinations of these fatty acids are not yet clear; they could be bound for internal membranes, or to the plasma membrane for efflux. The role of A-FABP in the heart is less well studied. However, A-FABP has been connected to the relationship between obesity and insulin resistance (Hotamisligil, 2000). The fact that both H-FABP and A-FABP can be tyrosine phosphorylated in response to insulin signaling suggests that these molecules function together to regulate various aspects of fatty acid metabolism.

The alteration of H-FABP and A-FABP in the absence of DMPK

The precise nature of the altered mobility of the FABP isoforms in the DMPK mutant cells is unknown. As figures 2-10 and 2-14 show, the FABP isoforms from the *DMPK* *-/-* mouse heart appear at a gel location corresponding to a more acidic isoelectric point than the FABP isoforms from the wild-type mouse heart. Although the direction of this shift is consistent with that expected to arise from lack of phosphorylation in the *DMPK* *-/-* cells, we believe this is not likely to be the case for several reasons. No phosphopeptides were detected by mass spectrometry, and phosphatase treatment of the extract containing A-FABP produced no difference in the mobilities of these spots. Furthermore, it has been reported that although both H-FABP and A-FABP can occur in phosphorylated form, this form represents less than 1% of the total FABP protein (Nielsen, 1993). As the proteins we isolated from the 2D gels were fairly abundant, and since we only observed one form as opposed to both phosphorylated and unphosphorylated species, we believe the observed mobility difference is not due to phosphorylation. The fact that we saw differences in the location of the entire protein spot argues that some other modification is causing the altered mobility. Furthermore, it is likely that silver stain visualization of the proteins on these gels is not sensitive enough to reveal a species of protein that represents such a small fraction of the total and is present at such a low level. As a result, we cannot fully rule out that loss of DMPK does result in changes in the phosphorylation of H-FABP and A-FABP.

Understanding the difference between the wild-type and *DMPK*^{-/-} heart proteomes would provide valuable insight into the molecular consequences of *DMPK* loss. Since the altered mobility of the FABPs in the absence of *DMPK* is not likely to be caused by phosphorylation, it must therefore be due to some other post-translational modification or alteration in conformation, either of which would cause a change in isoelectric point. As shown in Table 2, both H-FABP and A-FABP have several mobility forms. Although the nature of these mobility forms is not entirely understood, the difference in isoelectric point of these mobility forms does not appear to be due to the presence of bound fatty acid ligand. Further characterization of the different mobility forms is needed before the nature of the mobility shift can be determined.

Our data indicate that H-FABP and A-FABP are not likely to be direct substrates for *DMPK*, as we have seen no evidence that their altered mobility is due to phosphorylation differences. However, the fact that these proteins are altered in the absence of *DMPK* offers important information about the cellular consequences of *DMPK* loss. Specifically, the change in the FABPs suggests that the fatty acid metabolism of these cells could be affected by *DMPK* loss. This possibility is entirely consistent with the insulin resistance of DM1 patients.

DM1 and insulin resistance

Insulin resistance is a cardinal feature of myotonic dystrophy. An estimated 1.6% of DM1 patients exhibit clinical diabetes; an estimated 16% exhibit pronounced glucose intolerance and 63% develop hyperinsulinemia or insulin resistance (Harper, 1989). Insulin production in these patients is normal, as is the character of the insulin molecule itself.

As in many other patients with insulin resistance, patients with DM1 have an increased body fat mass, increased circulating triglyceride levels, hyperleptinemia (excess serum leptin, product of the *ob* gene), disturbed cortisol regulation and elevated 24-hr levels of TNF- α . (Harper, 1989, Piccardo, 1991, Brook, 1992, Jaspert, 1995). DM1 patients also show defects in the fibrinolytic system (Johansson, 2001). However, few DM1 patients become glucose intolerant, the incidence of diabetes mellitus is low, and the blood pressure is not elevated as in diabetic patients.

Typically the serum insulin concentration will reach a level of about two to five times that found in normal age- and sex-matched subjects (Moxley, 1980). In DM1 patients, insulin is present in serum at 2-5 times the normal amount. Interestingly, this increase does not signal a concomitant increase in glucose uptake in the cells. Although muscle wasting is prevalent in DM1, previous data show that muscle wasting is not the cause of exaggerated insulin release

(Moxley, 1983), and forearm studies of glucose transport indicate that fat and skin have insulin-stimulated glucose uptake similar to normal values (Moxley, 1978). This holds true for cultured DM myotubes. The addition of insulin to these cells produced no increase in glucose uptake except when it was administered at very high levels, and even in this case the increase of glucose uptake was small. Furthermore, glucose uptake was stimulated successfully with IGF-1, further evidence that there is no defect in the mechanism of glucose uptake (Furling, 1999),(Hudson, 1987). Studies have shown that the insulin molecule produced by DM patients is normal, as is its binding to the insulin receptor. Taken together, these data are indicative of a biochemical malfunction downstream of insulin binding to its receptor.

Adipose tissue is only mildly insulin resistant in DM1 patients, and these less affected target tissues for insulin action are likely to contribute to the normal glucose tolerance in DM1 patients with hyperinsulinemia, as glucose uptake in adipose tissue can proceed normally.

Conclusions

In our comparison of the tissue-specific proteomes of wild-type and *DMPK* ^{-/-} mice we have observed a number of proteins with altered mobility. Two of

these proteins were identified by MALDI-TOF and tandem mass spectrometry as fatty acid binding protein isoforms H-FABP and A-FABP.

The fact that the FABPs are altered in the absence of DMPK provides important clues about the molecular consequences of DMPK loss. Although it is still unclear whether the FABPs are altered as a direct consequence of DMPK loss, characterizing the nature of the altered mobility is crucial for understanding how these proteins are changed in the absence of DMPK. An asparagine to aspartic acid change has been observed for H-FABP, and this could easily account for the observed difference in isoelectric point. However, it is not clear why *DMPK* *-/-* mice would express one form and wild-type mice would express the other form. A further possibility is that the mobility shift represents a difference in post-translational modification. Although we have ruled out that the altered mobility is caused by a difference in phosphorylation state, we are currently in the process of investigating further the possible nature of the mobility difference.

Both A-FABP and H-FABP have been shown to be phosphorylated in response to insulin stimulation in cultured 3T3 cells. This suggests a link between insulin and fatty acid metabolism. Cardiac tissue utilizes β -oxidation of fatty acids as its primary energy source, as do the type I fibers in skeletal muscle, the two cell types in which DMPK is most highly expressed. Fatty acid binding proteins are thought to act as fatty acid transporters in the cell, potentially

mediated by phosphorylation signaling. Although we have found no evidence for a difference in phosphorylation of FABPs between wild-type and *DMPK* *-/-* mice, we cannot rule out that there are differences in phosphorylation that are too faint to be seen by silver staining, since only a small percentage of these proteins is phosphorylated at one time. Furthermore, the signalling mechanism that activates fatty acid binding protein activity is not known, therefore, it is possible that these proteins might also have a role in this process that is not regulated by phosphorylation. The mechanism behind the insulin processing defect in DM1 is not currently known, although both the production, integrity of, and receptor for insulin are known to be normal. Therefore, the defect in the DM1 patients is believed to occur at some point after insulin binds to its receptor and the receptor becomes phosphorylated.

Future experiments

The *DMPK* *-/-* mice have not been examined to see if they exhibit the same insulin resistance as is seen in the majority of DM1 patients. In order to determine whether the altered behavior of fatty acid binding proteins *DMPK* *-/-* mice is due to an insulin-resistant phenotype, several different types of assays could be attempted. An ELISA assay to determine blood insulin levels of mice at various ages would be the simplest and most straightforward approach toward answering this question. However, this assay is not extremely sensitive and subtle variations might not be seen. Another experiment that could be attempted

is the analysis of the phosphorylation state of the insulin receptor substrate in these mice. An immunoprecipitation of this protein followed by a western blot probing for phosphotyrosine would indicate if signaling from the insulin receptor is disrupted.

The FABP pattern on the 2-DE gels was at times complex, and the proteins were hard to see, especially in skeletal muscle and brain. Immunoprecipitation of FABPs from fractions or whole cell lysates would greatly reduce the complexity of the gels and allow a more careful analysis of the altered mobility of these spots.

Part 2: Proteomic analysis in models of human disease

Chapter two illustrates that standard proteomics techniques, when applied to a mouse model, can be a valuable tool in the investigation of human disease. We successfully identified two proteins that are biochemically altered when comparing the tissue proteomes of wild-type and *DMPK* *-/-* mice. We hope that this information will lead to further understanding of DM1. Furthermore, we believe that this approach can be used to deconstruct the phenotypes of other mouse models of human disease.

At the time these experiments were begun no attempt had yet been made to analyze a mouse model by proteomics. Since then, the popularity of proteomics has increased as a tool for investigation of the cause or treatment of human disease. For example, in 1997 a comparison of the proteomes of colorectal carcinoma tissue versus tissue samples from normal colonic epithelia has resulted in the identification of a protein, calgranulin B, that is thought to function in the malignant transformation of colon mucosa (Stulik, 1997). Since then this technique has been applied to other cancers as well (Jungblut, 1999, Zeindl-Eberhart, 1994a, Zeindl-Eberhart, 1994b). Proteomics has successfully been applied to detect proteins associated with cardiomyopathy, and extensive cardiac 2-dimensional gel databases are available on the internet (Jungblut, 1994, Corbett, 1995, Pleissner, 1997a, Pleissner, 1996, 1997b). Proteomics has also become a valuable tool for drug discovery. Recently, a

proteomics based approach was used to identify proteins that respond to therapeutic drug treatment in the liver of *ob/ob* mice, a mouse model for insulin resistant diabetes and obesity (Edvardsson, 1999).

The experiments discussed in Chapter 2 represent the first case in which proteomic analysis has been applied to comparison of whole tissue lysates of genetically mutant mice and their wild-type counterparts. This technique could provide important insight into other human diseases, in addition to myotonic dystrophy. For example, Huntington's disease is another triplet repeat disease for which both knockout and repeat transgenic mice have been generated (Bates, 1997, Mangiarini, 1997). The CAG repeat expansion in the gene encoding huntingtin result in a translated polyglutamine tract that not only results in loss of function of the protein but also a gain of function effect as the polyglutamine-containing proteins aggregate in the nucleus of the cell. The cause of the aggregation as well as the biochemistry of this interaction is not currently known. However, it is suspected that other proteins besides huntingtin are present within the aggregates and these proteins could potentially play a role in Huntington's disease pathology. A comparison of the subcellular proteomes could identify proteins that are titrated from the nucleus in cells that contain these aggregates.

Future directions and technological advances

The field of proteomics, the child of genomics, is a relatively new field. When this project was first begun, tube gels were more commonly used than pre-cast immobilized pH gradient gels. The potential of MALDI-TOF and ESI mass spectrometry was just beginning to be realized; however, the database resources at that time were few. It was not until 1995 that the first prokaryotic genome, that of *Haemophilus influenzae*, was fully sequenced (Fleischmann, 1995) and the sequence of the first eukaryotic genome, that of *Sacharomyces cerevisciae*, was completed in 1997 (1997).

Proteomics as a science is rapidly maturing and becoming a valuable tool for many diverse areas of research. Several technological innovations have advanced the field enormously. The use of immobilized pH gradient strips has allowed 2-DE to become reproducible and standardized; the use of these, along with analysis software, facilitates the comparison of gels within the laboratory or against the online gel databases. Mass spectrometry has become the core of proteome research; its sensitivity has increased tremendously, and tandem mass spectrometry now allows sequence tag identification. Web resources have also expanded dramatically. As of June 24, 2001, sixty-six fully sequenced genomes were available to the public, including ten archaeobacterial genomes, forty-one bacterial genomes, and fifteen eukaryotic genomes including *Caenorhabditis*

elegans, *Drosophila melanogaster*, *Arabidopsis thaliana*, and *Homo sapiens*, among others.

Furthermore, the staggering amount of proteome research underway is helping to bridge the gap between protein entries in databases versus the entries in protein sequence databases resulting from DNA sequencing. In 1997, the difference was 507 versus 428,814, respectively (Hancock, 1999). Annotation of the sequenced human genome with information from proteomic experiments, such as the identification or verification of open reading frames, molecular weights, hydrophobicity values, isoelectric points, peptide masses, and secondary structure, aid in the predictive methods used to assign new protein sequences to known protein families. The Human Proteomics Initiative (HPI) is a major effort that was begun by the Swiss Institute of Bioinformatics and the European Bioinformatics Institute with the goal of annotating all human sequences according to the standards of SwissProt (for further information see <http://www.expasy.ch/sprot/hpi/>).

Further application of proteomics to the study of *DMPK* *-/-* mice

In our blanket comparison of the proteome of *DMPK* *-/-* mice we found a number of proteins with altered mobility between wild-type and mutant samples. We believe many more altered proteins will be identified with further

investigation. Here we discuss certain ways in which this project can be extended to take a more directed approach.

Fractionating to enrich for phosphoproteins

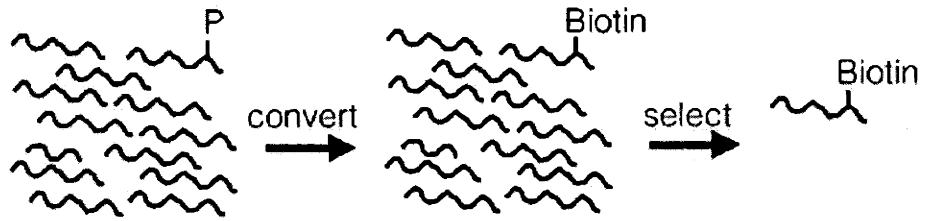
In the previous section we discussed a strategy for enriching a protein fraction for fatty acid binding proteins, thus greatly enhancing their representation on a 2-DE gel and their subsequent analysis. A similar approach could be taken to enrich a sample for phosphoproteins. Anti-phosphotyrosine antibodies have been used with great success to either immunoprecipitate tyrosine phosphoproteins from whole cell lysates or to visualize tyrosine phosphoproteins on an electroblotted 2-DE gel. Unfortunately, there currently exist no reagents of similar quality for serine or threonine phosphoproteins. Radioactive orthophosphate labeling of proteins is one common way to visualize phosphoproteins in cultured cells. However, it is technically difficult to label whole tissue. Recently, a new technique has emerged for the isolation of phosphoproteins from whole cell protein lysate. The method involves chemical replacement of the phosphate moieties by biotin affinity tags. An avidin column can cleanly separate the labeled proteins and these can be identified by mass spectrometry (Figure 1). Tandem mass spectrometry can reveal the localization of the biotinylated residue, thus identifying the site of phosphorylation as well (Oda, 2001).

Figure 1. Fractionation scheme for isolating and enriching phosphoproteins in whole cell lysates or fractions

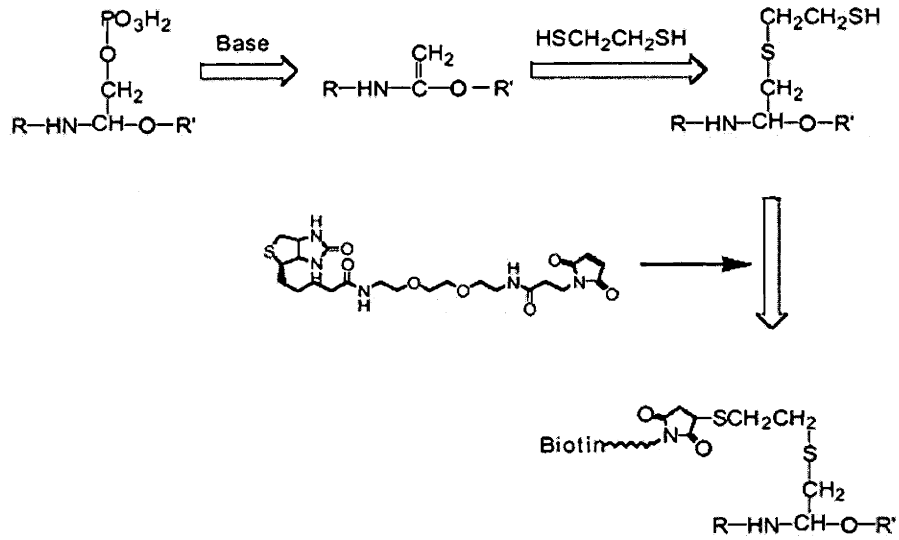
Panel A outlines a scheme for site-specific modification of phosphoseryl/phosphothreonyl residues of proteins with biotin affinity tags, as described in Oda, et. al 2001.

Panel B details the chemical conversion of the phosphoprotein. The scheme is based on the property that the phosphate moiety on serines and threonines is labile at high pH. Oxidized proteins are incubated in a solution containing 4M LiOH and ethanedithiol ($\text{HSCH}_2\text{CH}_2\text{SH}$, or EDT). Under these basic conditions, the phosphoseryl residue undergoes β -elimination to form a dehydroalanyl residue, which readily reacts with EDT. The EDT residue is easily biotinylated, and the biotinylated species may then be enriched by use of an avidin column.

A



B



Identifying the site of phosphorylation and the kinase consensus sequence that surrounds it can yield information about the identity of the phosphate donor. Another recently developed way to identify the site of phosphorylation by serine/threonine protein kinases is the use of immobilized metal affinity chromatography (IMAC). Gallium- or iron-chelated affinity columns are used to bind the negatively charged phosphate ions. This technique conveys a significant advantage for the identification of the phosphorylated peptide by mass spectrometry, as it effectively separates the phosphorylated peptide species from its unphosphorylated counterpart. One drawback to this technique is that the column can bind negatively charged glutamic and aspartic acid as well, causing a certain fraction of background peptides to be included in the sample (Mann, 2001).

Gel imaging software

In our initial experiments we chose not to employ 2-DE analysis software because of the difficulty in analyzing faint proteins spots that contain relatively little protein. However, for a comprehensive analysis of differences between the wild-type and *DMPK* *-/-* proteome, these programs would be essential. The sensitivity of mass spectrometry analysis has increased dramatically in recent years; fractionation schemes could be devised for those protein spots deemed to contain too little protein for analysis. Some common gel imaging software programs are Melanie (<http://www.expasy.ch/melanie/>) [Li, 1999], Phoretix 2D

(<http://www.phoretix.com>) (O'Dell, 2000), ImageMaster (http://www.imsupport.com/2d_body.htm) or Flicker (<http://www-lecb.ncifcrf.gov/flicker/>) (Lemkin, 1999). Use of this software could facilitate detection of differences in faint proteins, such as the phosphorylated forms of FABPs.

Visualization Methods

Coomassie blue staining and silver staining are common ways to visualize proteins, each having advantages and drawbacks (see chapter 2). A recently developed method of visualizing proteins on gels is the application of the fluorescent dyes cy3 and cy5. These cyanine dyes have been synthetically modified and contain succinimidyl esters as reactive groups that can be readily conjugated to antibodies, avidin, modified DNA, and proteins. (Mujumdar, 1996). These dyes can be used in difference gel electrophoresis, a single gel method of comparing proteins (Unlu, 1999). Samples to be compared are each labeled with a different dye conjugate and then run together on the same gel. This method involves running fewer gels and has the additional advantage of eliminating confusion due to individual gel artifact. Currently the use of these dyes is proprietary; small amounts are available from Amersham Pharmacia Biotech <http://www.apbiotech.com/>.

Summary

In the analysis of the proteomes of wild-type and *DMPK* $-/-$ mice, a number of proteins were found to have altered mobility in 2-DE analysis. Each of these proteins could play a role in the etiology of myotonic dystrophy type 1. Their identification will expand the information we have of DMPK and its role in the cell. Further analysis of these proteins, and the identification of others using the techniques described above, will inevitably lead to the understanding of DMPK function and how its mutation leads to DM1.

References

1. Ockner, R. K., Manning, J. A., Poppenhausen, R. B., and Ho, W. K. L., 1972. A binding protein for fatty acids in cytosol of intestinal mucosa, liver, myocardium, and other tissues *Science* **177**: p. 56-58
2. Jagschies, G., M. Reers, C. Unterberg and F. Spener, 1985. Bovine fatty acid binding proteins. Isolation and characterisation of two cardiac fatty acid binding proteins that are distinct from corresponding hepatic proteins *Eur J Biochem* **152**(3): p. 537-545.
3. Offner, G. D., R. F. Troxler and P. Brecher, 1986. Characterization of a fatty acid-binding protein from rat heart *J Biol Chem* **261**(12): p. 5584-5589.
4. Jones, P. D., A. Carne, N. M. Bass and M. R. Grigor, 1988. Isolation and characterization of fatty acid binding proteins from mammary tissue of lactating rats *Biochem J* **251**(3): p. 919-925.
5. Myers-Payne, S. C., T. Hubbell, L. Pu, F. Schnutgen, T. Borchers, W. G. Wood, F. Spener and F. Schroeder, 1996a. Isolation and characterization of two fatty acid binding proteins from mouse brain *J Neurochem* **66**(4): p. 1648-1656.
6. Borchers, T., C. Hohoff, C. Buhlmann and F. Spener, 1997. Heart-type fatty acid binding protein - involvement in growth inhibition and differentiation *Prostaglandins Leukot Essent Fatty Acids* **57**(1): p. 77-84.
7. Myers-Payne, S. C., R. N. Fontaine, A. Loeffler, L. Pu, A. M. Rao, A. B. Kier, W. G. Wood and F. Schroeder, 1996b. Effects of chronic ethanol consumption on sterol transfer proteins in mouse brain *J Neurochem* **66**(1): p. 313-320.
8. Unterberg, C., T. Borchers, P. Hojrup, P. Roepstorff, J. Knudsen and F. Spener, 1990. Cardiac fatty acid-binding proteins. Isolation and characterization of the mitochondrial fatty acid-binding protein and its structural relationship with the cytosolic isoforms *J Biol Chem* **265**(27): p. 16255-16261.
9. Hotamisligil, G. S., 2000. Molecular mechanisms of insulin resistance and the role of the adipocyte *Int J Obes Relat Metab Disord* **24 Suppl 4**: p. S23-27.

10. Nielsen, S. U. and F. Spener, 1993. Fatty acid-binding protein from rat heart is phosphorylated on Tyr19 in response to insulin stimulation *J Lipid Res* **34**(8): p. 1355-1366.
11. Harper, P. S., *Myotonic Dystrophy*. 1989, W. B. Saunders Company: London.
12. Piccardo, M. G., G. Pacini, M. Rosa and R. Vichi, 1991. Insulin resistance in myotonic dystrophy *Enzyme* **45**(1-2): p. 14-22
13. Brook, J. D., McCurrah, M. E., Harley, H.G., Buckler, A. J., Church, D., Aburatani, H., Hunter, K., Stanton, V. P., Thirion, J. P., Hudson, T., Sohn, R., Zemelman, B., Snell, R. G., Rundle, S. A., Crow, S., Davies, J., Shelbourne, P., Buxton, J., Jones, C., Juxenon, V., Johnson, K., Harper, P. S., Shaw, D. J., Housman, D. E., 1992. Molecular basis of myotonic dystrophy: expansion of a triplet (CTG) repeat at the 3' end of a transcript encoding a protein kinase family member *Cell* **68**: p. 799-808
14. Jaspert, A., Fahsold, R., Grel, H., Claus, D., 1995. Myotonic dystrophy: correlation of clinical symptoms with the size of the CTG trinucleotide repeat. *Journal of Neurology* **242**: p. 99-104
15. Johansson, A., K. Boman, K. Cederquist, H. Forsberg and T. Olsson, 2001. Increased levels of tPA antigen and tPA/PAI-1 complex in myotonic dystrophy *J Intern Med* **249**(6): p. 503-510.
16. Moxley, R. T., R. C. Griggs and D. Goldblatt, 1980. Muscle insulin resistance in myotonic dystrophy: effect of supraphysiologic insulinization *Neurology* **30**(10): p. 1077-1083.
17. Moxley, R. T., R. C. Griggs, G. B. Forbes, D. Goldblatt and K. Donohoe, 1983. Influence of muscle wasting on oral glucose tolerance testing *Clin Sci (Colch)* **64**(6): p. 601-609.
18. Moxley, R. T., III, R. C. Griggs, D. Goldblatt, V. VanGelder, B. E. Herr and R. Thiel, 1978. Decreased insulin sensitivity of forearm muscle in myotonic dystrophy *J Clin Invest* **62**(4): p. 857-867.

19. Furling, D., A. Marette and J. Puymirat, 1999. Insulin-like growth factor I circumvents defective insulin action in human myotonic dystrophy skeletal muscle cells *Endocrinology* **140**(9): p. 4244-4250.
20. Hudson, A. J., M. W. Huff, C. G. Wright, M. M. Silver, T. C. Lo and D. Banerjee, 1987. The role of insulin resistance in the pathogenesis of myotonic muscular dystrophy *Brain* **110**(Pt 2): p. 469-488.
21. Stulik, J., H. Kovarova, A. Macela, J. Bures, P. Jandik, F. Langr, A. Otto, B. Thiede and P. Jungblut, 1997. Overexpression of calcium-binding protein calgranulin B in colonic mucosal diseases *Clin Chim Acta* **265**(1): p. 41-55.
22. Jungblut, P. R., U. Zimny-Arndt, E. Zeindl-Eberhart, J. Stulik, K. Koupilova, K. P. Pleissner, A. Otto, E. C. Muller, W. Sokolowska-Kohler, G. Grabher and G. Stoffler, 1999. Proteomics in human disease: cancer, heart and infectious diseases *Electrophoresis* **20**(10): p. 2100-2110.
23. Zeindl-Eberhart, E., P. R. Jungblut, A. Otto and H. M. Rabes, 1994a. Identification of tumor-associated protein variants during rat hepatocarcinogenesis. Aldose reductase *J Biol Chem* **269**(20): p. 14589-14594.
24. Zeindl-Eberhart, E., P. Jungblut and H. M. Rabes, 1994b. Expression of tumor-associated protein variants in chemically induced rat hepatomas and transformed rat liver cell lines determined by two-dimensional electrophoresis *Electrophoresis* **15**(3-4): p. 372-381.
25. Jungblut, P., A. Otto, E. Zeindl-Eberhart, K. P. Plessner, M. Knecht, V. Regitz-Zagrosek, E. Fleck and B. Wittmann-Liebold, 1994. Protein composition of the human heart: the construction of a myocardial two-dimensional electrophoresis database *Electrophoresis* **15**(5): p. 685-707.
26. Corbett, J. M., C. H. Wheeler and M. J. Dunn, 1995. Coelectrophoresis of cardiac tissue from human, dog, rat and mouse: towards the establishment of an integrated two-dimensional protein database *Electrophoresis* **16**(8): p. 1524-1529.

27. Pleissner, K. P., P. Soding, S. Sander, H. Oswald, M. Neuss, V. Regitz-Zagrosek and E. Fleck, 1997a. Dilated cardiomyopathy-associated proteins and their presentation in a WWW-accessible two-dimensional gel protein database *Electrophoresis* **18**(5): p. 802-808.
28. Pleissner, K. P., S. Sander, H. Oswald, V. Regitz-Zagrosek and E. Fleck, 1996. The construction of the World Wide Web-accessible myocardial two-dimensional gel electrophoresis protein database "HEART-2DPAGE": a practical approach *Electrophoresis* **17**(8): p. 1386-1392.
29. Pleissner, K. P., S. Sander, H. Oswald, V. Regitz-Zagrosek and E. Fleck, 1997b. Towards design and comparison of World Wide Web-accessible myocardial two-dimensional gel electrophoresis protein databases *Electrophoresis* **18**(3-4): p. 480-483.
30. Edvardsson, U., M. Alexandersson, H. Brockenhuus von Lowenhielm, A. C. Nystrom, B. Ljung, F. Nilsson and B. Dahllof, 1999. A proteome analysis of livers from obese (ob/ob) mice treated with the peroxisome proliferator WY14,643 *Electrophoresis* **20**(4-5): p. 935-942.
31. Bates, G. P., L. Mangiarini, A. Mahal and S. W. Davies, 1997. Transgenic models of Huntington's disease *Hum Mol Genet* **6**(10): p. 1633-1637
32. Mangiarini, L., K. Sathasivam, A. Mahal, R. Mott, M. Seller and G. P. Bates, 1997. Instability of highly expanded CAG repeats in mice transgenic for the Huntington's disease mutation *Nat Genet* **15**(2): p. 197-200.
33. Fleischmann, R. D., Adams, M. D., White, O., Clayton, R. A., Kirkness, E. F., Kerlavagte, A. R., Bult, C. J., Tomb, J. F., Dougherty, B. A., Merrick J. M., McKenney, K., Sutton, G., FitzHugh, W., Fields, C., Gocayne, J. D., Scott, J., Shirley, R., Liu, L., Glodek, A., Kelley, J. M., Weidman, J. F., Phillips, C. A., Spriggs, T., Hedblom, E., Cotton, M. D., Utterback, T. R., Hanna, M. C., Nguyen, D. T., Saudek, D. M., Brandon, R. C., Fine, L. D., Fritchman, J. L., Fuhrmann, J. L., Geoghagen, N. S. M., Gnehm, C. L., McDonald, L. A., Small, K. V., Fraser, C. M., Smith, H. O., and Ventner, J. C., 1995. Whole-genome random sequencing and assembly of *Haemophilus influenzae* Rd. *Science* **269**(5223): p. 496-512
34. 1997. The yeast genome directory *Nature* **387**(6632 Supplement): p. 5

35. Hancock, W., Apffel, A., Chakel, J., Hahnenberger, K., Choudhary, G., Traina, J. A., Pungor, E, 1999. Integrated Genomic/Proteomic Analysis *Analytical Chemistry* **71**(21): p. 742A-748A
36. Oda, Y., T. Nagasu and B. T. Chait, 2001. Enrichment analysis of phosphorylated proteins as a tool for probing the phosphoproteome *Nat Biotechnol* **19**(4): p. 379-382.
37. Mann, M., R. C. Hendrickson and A. Pandey, 2001. Analysis of Proteins and Proteomes by Mass Spectrometry *Annu Rev Biochem* **70**: p. 437-473
38. Li, X. P., K. P. Pleissner, C. Scheler, V. Regitz-Zagrosek, J. Salnikow and P. R. Jungblut, 1999. A two-dimensional electrophoresis database of rat heart proteins *Electrophoresis* **20**(4-5): p. 891-897.
39. O'Dell, S. D., T. R. Gaunt and I. N. Day, 2000. SNP genotyping by combination of 192-well MADGE, ARMS and computerized gel image analysis *Biotechniques* **29**(3): p. 500-504, 505-506.
40. Lemkin, P. F. and G. Thornwall, 1999. Flicker image comparison of 2-D gel images for putative protein identification using the 2DWG meta-database *Mol Biotechnol* **12**(2): p. 159-172.
41. Mujumdar, S. R., Mujumdar, R. B., Grant, C. M., and Waggoner, A. S., 1996. Cyanine-labeling reagents: sulfobenzindocyanine succinimidyl esters *Bioconjugate Chemistry* **7**(3): p. 356-362
42. Unlu, M., 1999. Difference gel electrophoresis *Biochem Soc Trans* **27**(4): p. 547-549.

Appendix A: Generation of *DMPK*^{-/-}: *MyoD*^{-/-} Mice

Appendix A: Generation of *DMPK*^{-/-}: *MyoD*^{-/-} Mice:

Analysis of Phenotype

Myotonic dystrophy (DM1) is caused by a trinucleotide expansion in the 3'UTR of the *DMPK* gene. Although it is not known how this mutation leads to DM1, one possible mechanism is through disruption of *DMPK* gene expression. To determine the direct effect of *DMPK* loss, we mutated the *DMPK* gene in mice (Reddy, et al., 1996). Surprisingly, *DMPK*^{-/-} mice show a significant but incomplete DM1 phenotype, with symptoms including cardiac conduction defects and mild skeletal muscle myopathy. The skeletal muscle myopathy is extremely variable in *DMPK* heterozygotes, and mild in nature and late in onset even in the homozygous null mice. Histological examination of muscle sections indicates that muscles are normal at three to four months of age but begin to show deterioration before 11 months of age. This deterioration is characterized by fibrosis, increased activation of satellite cells to form new muscle tissue (as measured by *MyoD* expression), ultrastructural disorganization, central nuclei, and muscle fiber size variation. One possible explanation for the mild phenotype of the *DMPK* mutant mice is that loss of *DMPK* only causes a subset of DM1 symptoms (see Chapter 1). However, it is also possible that the discrepancy between DM1 symptoms and the *DMPK* mutant phenotype is caused by aspects of muscle physiology that are distinct between humans and mice.

In order to generate a mouse model that more fully reiterates the phenotype of human DM1, we designed experiments to produce a mouse model that would have more acute muscle pathology. In this section we describe the generation and characterization of *DMPK*^{-/-}:*MyoD*^{-/-} mice.

The Duchenne's muscular dystrophy mouse model: another incomplete phenotype

Duchenne's muscular dystrophy patients harbor mutations in the *dystrophin* gene and exhibit symptoms such as extensive progressive wasting of proximal muscles, progressive scoliosis and respiratory difficulties, and severe cardiomyopathy (Harper, 1989). The *mdx* mice are mutant for *dystrophin* and were generated in an attempt to create a mouse model for Duchenne's muscular dystrophy. However, in contrast to the human patients, the *mdx* mice show a very mild phenotype of slight muscle fiber necrosis starting at two weeks of age. Furthermore, unlike humans, these mice maintain skeletal muscle integrity. These data show that disruption of the *dystrophin* gene had very distinct consequences in mice and humans. The relatively mild phenotype of the *mdx* mice was thought to be due to increased regenerative capacity of the mice. Indeed, *mdx* mice are hypertrophic and have a 25% increase in the number of muscle fibers and a 1.7 fold increase in muscle compared to wild-type mice.

***mdx/MyoD* ^{-/-} mice have a Duchenne's-like phenotype**

Megeney, et. al. generated mice that are mutant for the *dystrophin* gene as well as for the *MyoD* gene, which encodes a muscle specific transcription factor. The *mdx/MyoD* double mutant mice more accurately reproduce the human Duchenne phenotype. These mice show many of the symptoms of Duchenne's including severe curvature of the spine, severe cardiomyopathy, reduction in the number of satellite cells, significant reduction in the mass and number of skeletal muscle fibers, and premature death at twelve months of age due to loss of muscle mass (Megeney, et al., 1996, Megeney, et al., 1999).

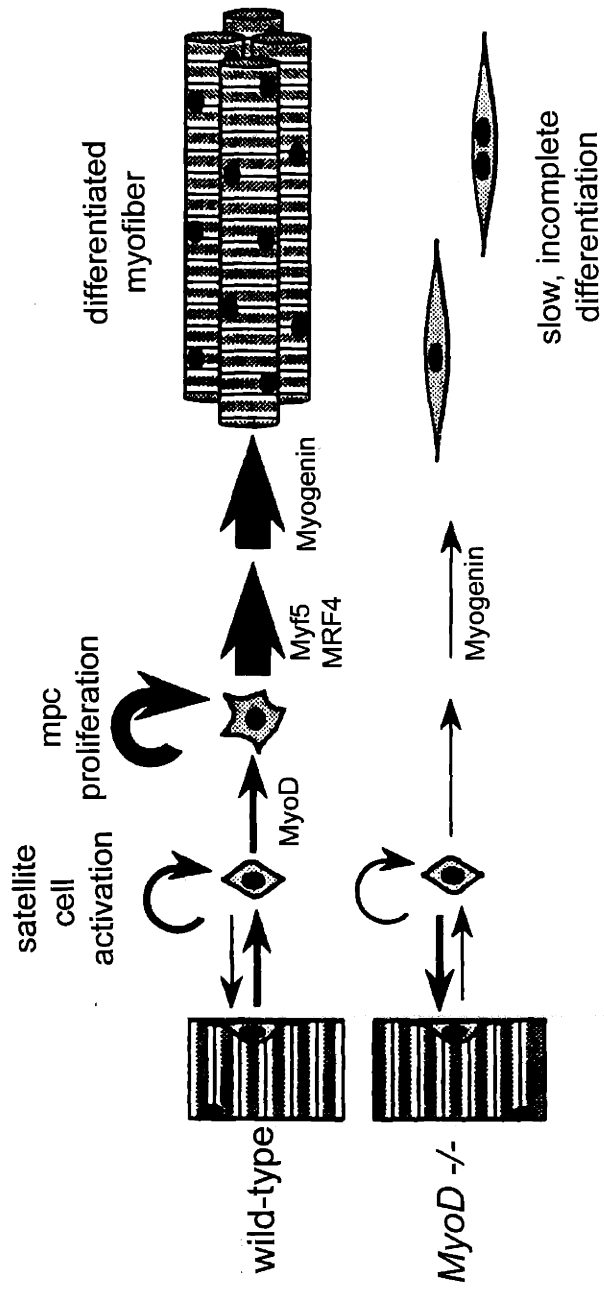
MyoD compensates for muscle degeneration in mice

The more severe, Duchenne-like phenotype of the *mdx/MyoD* mice can be explained by the fact that MyoD loss has impaired the regenerative capacity of muscle in these mice. MyoD is a muscle-specific transcription factor involved in both muscle development and regeneration. *MyoD* ^{-/-} mice are born with no abnormal muscle pathology due to compensation by the another muscle-specific transcription factor, Myf-5. However, analysis of *MyoD* ^{-/-} mice has shown that MyoD is important for muscle regeneration (Figure 1). Damaged muscle can be repaired through the activation of satellite cells present in the basal lamina of skeletal muscle. These undifferentiated cells are activated to differentiate and fuse to replace damaged muscle by the same set of transcription factors involved

in development of the myogenic lineage. Muscle differentiation via satellite cells can occur in *MyoD*^{-/-} muscle, however, cell fusion is less complete and it occurs at a reduced rate through an alternate pathway that is not yet fully characterized (Sabourin, et al., 1999, Cornelison, et al., 2000). Consequently, the *mdx/MyoD* double mutant mice would not be able to undergo extensive muscle regeneration in the absence of *mdx*, and thus would show a Duchenne-like phenotype.

Figure 1. The role of MyoD in muscle regeneration

The muscle-specific transcription factor MyoD plays a critical role in the progression of differentiation of multipotent satellite cells in muscle. Another, as yet unidentified, factor allows a slow, inefficient differentiation process to occur in the absence of MyoD.



Generation of *DMPK*^{-/-}:*MyoD*^{-/-} mice

The phenotype of the *mdx/MyoD* mouse suggests that a significant difference in muscle regeneration rate or capacity exists between mice and humans. This difference in physiology could be the reason behind the relatively mild muscle pathology of the *DMPK*^{-/-} mice when compared to human DM1 patients. To test this hypothesis we generated mice that are deficient in both *DMPK* and *MyoD* genes by crossing the individual knockout strains. The double mutant mice were analyzed to determine if they constituted a more accurate model for Myotonic Dystrophy. Such a model would allow us to investigate more fully the effect that loss of DMPK has on mouse skeletal muscle and heart.

DMPK^{-/-} 129Sv mice from the Housman laboratory and *MyoD*^{-/-} 129Rj mice from the Rudolph Jaenisch laboratory were crossed to obtain *DMPK*^{+/-}:*MyoD*^{+/-} mice. These F1 mice were then bred to each other in the attempt to produce litters that contain wild-type, *DMPK*^{-/-}, *MyoD*^{-/-}, and *MyoD*^{-/-} *DMPK*^{-/-} mice. The expected frequencies of these genotypes are 1/16 for the wild-type and double mutant mice and 1/8 for the single mutant mice.

Initially, we did not observe double mutant mice in any of the litters. The probability of a double mutant mouse being born from an F1 cross of two genes is one in 16, so at first we assumed that the lack of these mice was simply chance. However, after six months without generating any double mutant we decided to perform χ^2 analysis on the sample of mice we had obtained up to this

point. The χ^2 analysis revealed that we did indeed have a distorted proportion of genotypes of the progeny and that the absence of the double mutant mice was significant.

***DMPK* *-/-*:*MyoD* *-/-* neonates are weak and do not thrive in litters with stronger siblings**

To ascertain whether neonatal lethality was responsible for the disproportionate genotypes we analyzed the genotypes of unborn litters at embryonic day 19-20 of development (e19-20). The proportions of these genotypes were normal for independently segregating genes. We concluded that the abnormal proportions of genotypes in the progeny of the F1 crosses was not due to embryonic lethality.

After eight months of breeding, we finally obtained the first few *DMPK/MyoD* mice. These mice seemed weak and small at first compared to their siblings. We hypothesize that the reason we were not obtaining the expected proportions of *DMPK* *-/-*:*MyoD* *-/-* pups was that they were not thriving when in competition with their stronger littermates. To analyze more carefully the neonatal death of the *DMPK* *-/-*:*MyoD* *-/-* pups, we set up breeding pairs that involved crosses of *DMPK* heterozygotes with *MyoD* *-/-* homozygous mutants. As expected, a large portion of the pups that were found dead turned out to be

DMPK -/-:MyoD -/-. Interestingly, the same proportion of *DMPK +/-:MyoD -/-* mice died after birth as well (Table 1).

Table 1: Genotype proportion in neonatal death in <i>MyoD -/-</i> background			
genotype:	<u>DMPK +/+</u>	<u>DMPK +/-</u>	<i>DMPK -/-</i>
number:	<u>4</u>	<u>19</u>	19

When sufficient numbers of *DMPK -/-:MyoD -/-* mice were generated, we intercrossed them and analyzed their progeny. Surprisingly, we observed no widespread postnatal death in the progeny of the double mutant mice. We concluded that the double mutant mice are viable but extremely sensitive to competition by stronger littermates, thus accounting for the neonatal death observed in the F1 crosses. Litter size was reduced in litters from *DMPK -/-* breeding pairs (average n = 6.2) and *DMPK -/-:MyoD -/-* breeding pairs (average n = 5.5) when compared to wild-type and *MyoD -/-* litters (average n = 7.5 and 7.2, respectively). This reduction in litter size could be due to the fact that *DMPK -/-* mice show a slight reduced fertility (Reddy, et al., 1996) as opposed to postnatal death.

Generation of wild-type, *DMPK -/-*, *MyoD -/-*, and *DMPK -/-:MyoD -/-* mice for comparison

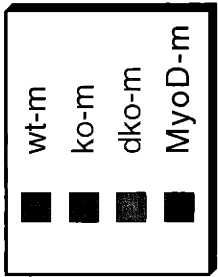
Since it was impractical to intercross *DMPK +/-:MyoD +/-* mice to generate litters of siblings for analysis, we decided to compare age-matched litters of wild-

type, *DMPK*^{-/-}, *MyoD*^{-/-}, and *MyoD*^{-/-}:*DMPK*^{-/-} mice that we obtained from independent crosses.

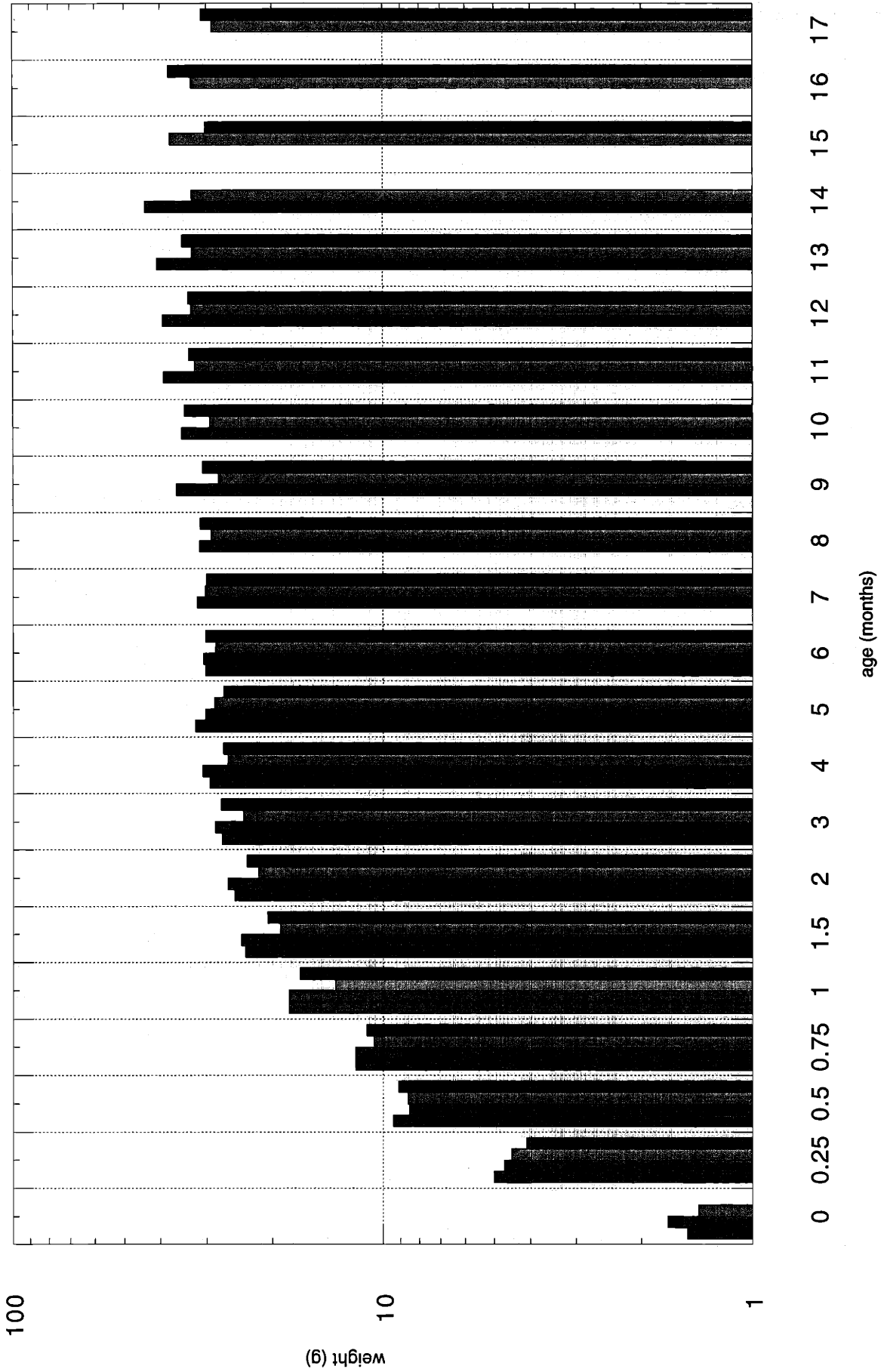
As the *DMPK*^{-/-}:*MyoD*^{-/-} neonates were weaker than their siblings were, we sought to determine if they were smaller and weaker throughout their lifespan to any significant degree. To address this question, weight measurements were taken over time of the mice of each of the four genotypes (wild-type, *DMPK*^{-/-}, *MyoD*^{-/-}, and *MyoD*^{-/-}:*DMPK*^{-/-}) and the results were then compared. These measurements were simple total body weight measurements and did not take into account muscle mass discrepancies or differences in body fat percentage. Observations of these mice during handling and dissection showed that the *MyoD*^{-/-}:*DMPK*^{-/-} mice were smaller, and had less muscle mass and a thicker fatty layer than the other genotypes, however, this was never measured quantitatively. The weight measurements showed that the body weight of all four genotypes is similar up through the age of about five months, at which point we began to see a divergence of total body weight that continued throughout the span of the study, about one year. As Figures 2 and 3 show, wild-type animals were largest, then *DMPK*^{-/-}, then *MyoD*^{-/-}, and the smallest were *MyoD*^{-/-}:*DMPK*^{-/-}. These results could indicate that the loss of both *DMPK* and *MyoD* leads to a coordinate reduction in muscle mass.

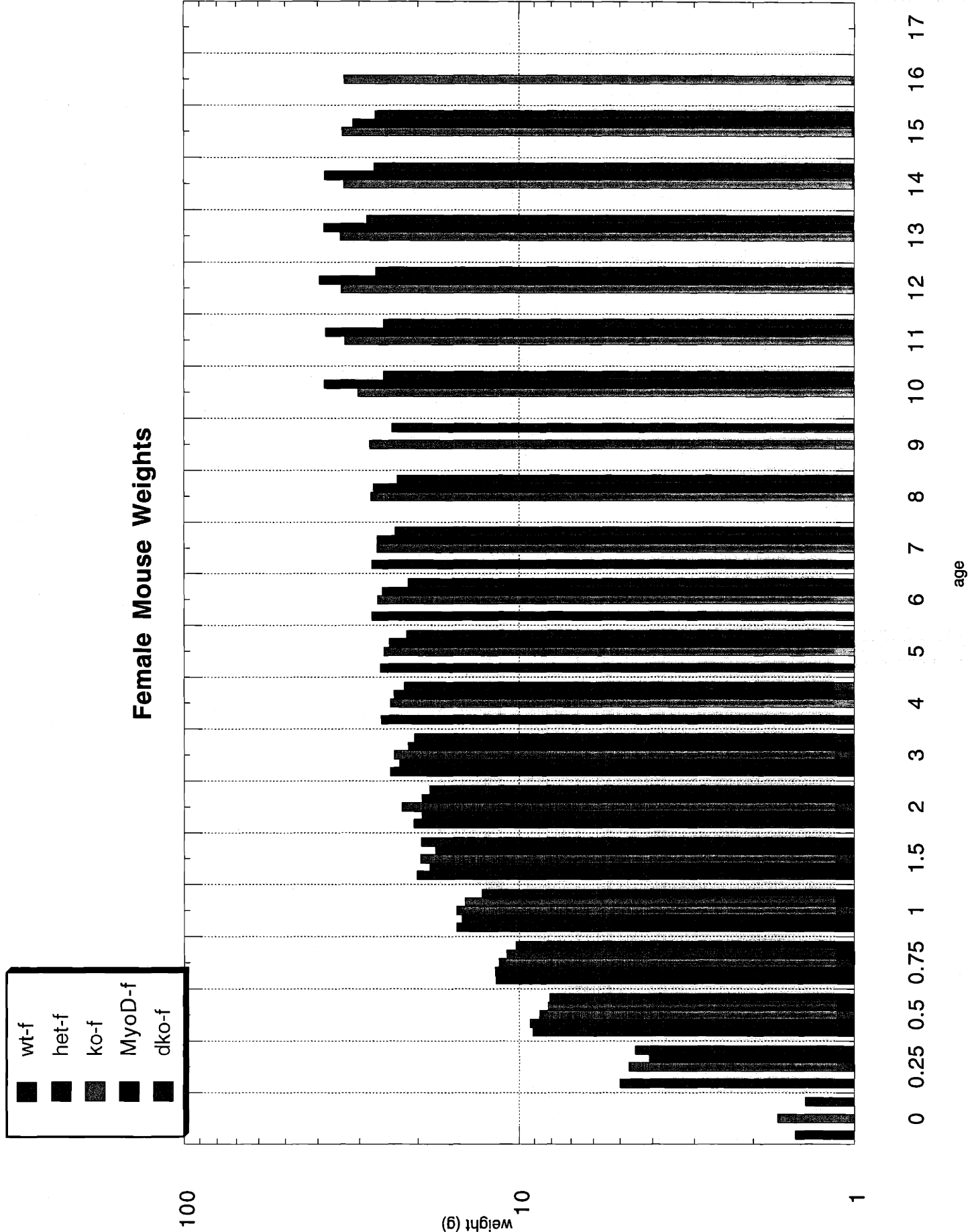
Figures 2 and 3: Weight as a function of age, male and female

Mice were weighed at 3 weeks, 4 weeks, 6 weeks, 8 weeks, 3 months, and monthly after that. Totals were averaged for each genotype and gender over time. Over fifty mice were weighed for each time point up through 6 months. Although we do see age related differences, these differences were not great enough to suggest widespread loss of muscle mass in the double mutant mice.



Male Mouse Weights





Histological analysis of skeletal muscle

To determine whether the *MyoD*^{-/-}:*DMPK*^{-/-} mice showed an earlier-onset of muscle pathology than did *DMPK*^{-/-} mice alone, we, along with collaborators in Nadia Rosenthal's laboratory, examined the skeletal muscle of 5-month-old sibling *DMPK*^{-/-} and *MyoD*^{-/-} mice. The muscles present in the calf, the gastrocnemius and soleus, were chosen because they are easily dissected, are relatively large, and give a good representation of both type I (slow twitch, oxidative) and type II (fast twitch, glycolytic) muscle. Histological analysis of these mice showed that *MyoD*^{-/-}:*DMPK*^{-/-} muscle contained a much higher incidence of type I muscle fibers than *DMPK*^{-/-} muscle (Figure 4). This result suggested that perhaps the *MyoD*^{-/-} *DMPK*^{-/-} mice had early skeletal muscle changes relative to the *DMPK*^{-/-} mice, indicative of an earlier-onset skeletal muscle pathology. Also, as DMPK is expressed more highly in type I fibers than type II, and as these fibers preferentially degrade in muscle of myotonic dystrophy patients, we hoped these mice would provide clues to the biochemistry of the muscle deterioration.

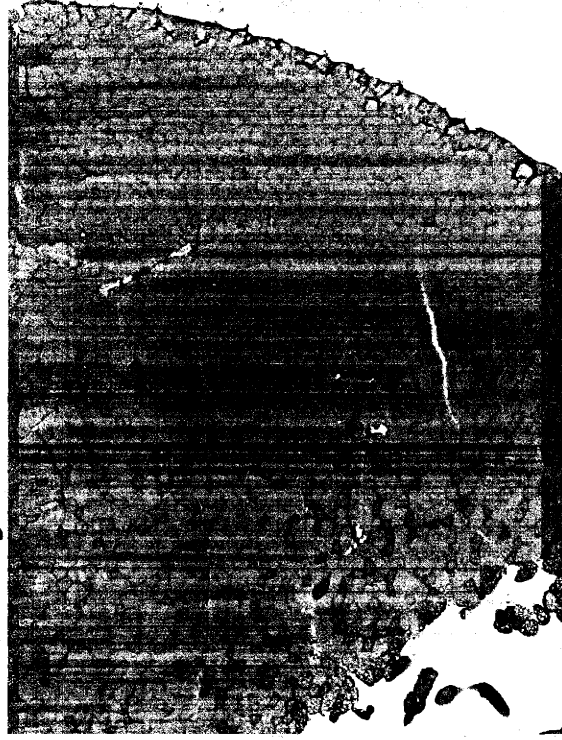
Figure 4. Histological analysis of *DMPK*^{-/-} and *DMPK*^{-/-}:*MyoD*^{-/-} mice

Frozen, unfixed sections of gastrocnemius and soleus muscle from four-month-old mice were stained with hematoxylin. Hematoxylin stains type I (slow, glycolytic) fibers more darkly than it stains type II (fast, oxidative). The double mutant mouse section appears to contain a much larger proportion of type I fibers than the *DMPK*^{-/-} section.

Lateral Cross-Section of Gastrocnemius (calf) muscle

Hematoxylin & eosin stain

MyoD +/- DMPK +/-



MyoD -/- DMPK -/-



Type I (slow) fibers = dark blue
Type II (fast) fibers = lightly stained

The observed muscle pathology was not reproducible

The observed muscle pathology represented preliminary data from only two mice. In order to confirm these data with larger numbers, and in an attempt to track the changes in muscle fiber type over time, we repeated this histological analysis on mice from all four genotypes at various ages. Mice were analyzed at 5 weeks, 10 weeks, 3 months, 6 months, and one year. Fiber type analysis of these mice showed no significant differences between the various genotypes at any age group. At the same time, muscle sections were examined for fiber integrity and no significant signs of fiber deterioration were detected except that which has already been described for the *DMPK* *-/-* mice. This pattern of mild deterioration was seen in the *DMPK* *-/-* mice and the double mutant mice to a similar degree. The nature of the discrepancy between these data and the pilot experiment is not clear.

Smaller muscle mass is not due to classical apoptosis

We had observed that the double mutant mice were smaller than mice of the other genotypes, and during dissection we observed less muscle mass and more fatty deposits in these mice. To determine whether the loss of muscle mass in the *DMPK* *-/-*:*MyoD* *-/-* mice was due to programmed cell death (apoptosis) we performed TUNEL assays on muscle sections from mice of these

same age groups. We detected no evidence of apoptosis in these sections. There is evidence that cell death proceeds through a different mechanism in myotonic dystrophy (Migheli, et al., 1997). We concluded that the difference in muscle cell death in these mice is not due to programmed cell death.

Conclusions: *DMPK* *-/-*:*MyoD* *-/-* mice do not have pronounced skeletal muscle myopathy similar to that of DM1 patients

We generated *DMPK* *-/-*:*MyoD* *-/-* mice in an attempt to recreate the DM1 phenotype in a mouse model. Although these mice appear to have reduced muscle mass, histological analysis of muscle sections representing both type I and type II fibers revealed no pronounced muscle pathology in comparison with controls. The reduced muscle mass is also not due to apoptosis of muscle cells. We concluded that *DMPK* *-/-*:*MyoD* *-/-* do not have pronounced skeletal muscle pathology similar to that of DM1 patients.

Materials and Methods

Mouse Tail Lysis for Genotyping

Mice are anesthetized with avertin and a 1cm section from the end of the tail is cut. The tails are processed according to the following protocol.

Basic Procedure:

The lysis buffer has been adjusted to allow restriction digestion of the DNA without prior organic solvent extractions. Therefore, the procedure just involves three manipulations:

1. Addition of lysis buffer to the tissue or cells
2. Addition of isopropanol.
3. Transfer of precipitate to TE.

1. Lysis: The lysis buffer (usually 0.5 ml) is added to the tissue or cells. Digestion is complete within several hours at 37°C (cells) or 55°C (tissues) with agitation.

2. Isopropanol Precipitation: One volume of isopropanol is added to the lysate and the samples are mixed or swirled until precipitation is complete (viscosity completely gone).

3. The DNA is recovered by lifting the aggregated precipitate from the solution using a disposable p200 tip. The DNA is dispersed in a prelabeled Eppendorf tube containing sterile TE.

Tail Lysis Buffer

100 mM Tris-Cl pH 8.5

5 mM EDTA

0.2% SDS

200 mM NaCl

100 µg/ml proteinase K

(so for each tail, use 500 µl buffer plus 5 µl 20 mg/ml proteinase K)

Avertin Mix

100 % solution:

10 g tribromoethylalcohol

10 ml *tert*-amyl alcohol

Use @ 2.5 %

Aldrich Catalog #:

T4,840-2

24,048-6

DMPK PCR Protocol
designed by Brenda Luciano

Primers:

DMKOF (*DMPK* -/- forward primer): 5' GCT GAC TCT AGA GGA TCC 3'
DMWTF (wild-type forward primer): 5' GCC AAG ATT GTG CAC TAC AG 3'
DMREV (reverse primer): 5' GCG TCA GCG ACA AGT GTT CC 3'

WT band is 340 bp, KO band is 185 bp; All 3 Primers are used in one PCR assay.

One PCR Reaction:

14.94 μ l H₂O
2 μ l 10X amplitaq PCR Buffer
0.6 μ l DMKOF
0.6 μ l DMWTF
0.6 μ l DMREV
0.16 μ l 25 mM dNTPs
0.10 μ l amplitaq
(1 μ l DNA)
20 μ l

Mix x 100

1494 μ l H₂O
200 μ l 10X buffer
60 μ l DMKOF
60 μ l DMWTF
60 μ l DMREV
16 μ l dNTPs
10 μ l amplitaq
(100 μ l DNA)
2000 μ l

PCR Program (Perkin Elmer 9600):

94 @ :30
56 @ :45
72 @ 1:00
x35

For homemade taq, reduce the amount of polymerase by half.

MyoD PCR Protocol
courtesy of Michael Rudnicki laboratory

Primers:

MD-1: 5' GCG AAT AGC AAG GAT AAC AGA 3'
MD-2: 5' CTT GGG TAT CTG CAA CAG GTT 3'
PGK-1: 5' GCG CCA AGT GCC AGC GGG GCT 3'

MD-1 and MD-2 amplify MyoD wild-type allele, about 400 bp

MD-1 and PGK-1 amplify MyoD $-/-$ allele, about 320 bp

<u>Each PCR:</u>	<u>Mix x 100</u>
15.54 μ l H ₂ O	1554 μ l H ₂ O
2 μ l 10X amplitaq buffer	200 μ l
0.6 μ l each primer	60 μ l
0.16 μ l 25 mM dNTPs	16 μ l dNTPs
0.10 μ l amplitaq	10 μ l amplitaq
<u>(1 μl DNA)</u>	<u>(100 μl DNA)</u>
20 μ l	2000 μ l

Dr. Wang uses the following conditions for all the PCR genotyping, and puts only one set of primers into each reaction tube.

PCR program (Perkin Elmer 9600):

94 @ :45
55 @ 1:15
72 @ 2:30
30 cycles

All three primers can be used in one tube if the PCR is working well. PCR of heterozygous mice will look like a ladder instead of two discrete bands.

For using homemade taq, reduce the amount of polymerase by half.

References

1. Reddy, S., D. B. Smith, M. M. Rich, J. M. Leferovich, P. Reilly, B. M. Davis, K. Tran, H. Rayburn, R. Bronson, D. Cros, R. J. Balice-Gordon and D. Housman, 1996. Mice lacking the myotonic dystrophy protein kinase develop a late onset progressive myopathy [see comments] *Biochem Biophys Res Commun* **225**(1): p. 281-288
2. Harper, P. S., *Myotonic Dystrophy*. 1989, W. B. Saunders Company: London.
3. Megeney, L. A., B. Kablar, K. Garrett, J. E. Anderson and M. A. Rudnicki, 1996. MyoD is required for myogenic stem cell function in adult skeletal muscle *Genes Dev* **10**(10): p. 1173-1183.
4. Megeney, L. A., B. Kablar, R. L. Perry, C. Ying, L. May and M. A. Rudnicki, 1999. Severe cardiomyopathy in mice lacking dystrophin and MyoD *Proc Natl Acad Sci U S A* **96**(1): p. 220-225.
5. Sabourin, L. A., A. Girgis-Gabardo, P. Seale, A. Asakura and M. A. Rudnicki, 1999. Reduced differentiation potential of primary MyoD^{-/-} myogenic cells derived from adult skeletal muscle *J Cell Biol* **144**(4): p. 631-643.
6. Cornelison, D. D., B. B. Olwin, M. A. Rudnicki and B. J. Wold, 2000. MyoD^{-/-} satellite cells in single-fiber culture are differentiation defective and MRF4 deficient *Dev Biol* **224**(2): p. 122-137.
7. Migheli, A., T. Mongini, C. Doriguzzi, L. Chiado-Piat, R. Piva, I. Ugo and L. Palmucci, 1997. Muscle apoptosis in humans occurs in normal and denervated muscle, but not in myotonic dystrophy, dystrophinopathies or inflammatory disease *Neurogenetics* **1**(2): p. 81-87.

Appendix B: Selected Protocols

Appendix B: Selected Protocols

Appendix B: Selected Protocols

Sample Preparation for 2-D Electrophoresis, whole cell lysate (Based on protocol from Kendrick Labs, Inc. Madison, WI)

For preparing sample from tissues:

- Weigh the tissue, freeze to -80°C, crush with mortar and pestle, and place in a dounce homogenizer on ice.
 - Add about 0.25 ml of Osmotic Lysis Buffer + 2.5 µl each PI stock I and II per 100 mg of tissue and homogenize.
 - Freeze-thaw once or twice, and then add 1/10 volume of 10X nuclease stock solution.
 - Allow the nucleases to react for 10-15 min on ice.
 - Take a 5 µl aliquot for protein determination.
 - Add an equal volume of CHAPS/Urea buffer.
 - Vortex 5 min.
- Centrifuge out anything not dissolved, do a protein determination, and store at -70 °C until use.

1. Urea Sample Buffer (O'Farrell Lysis Buffer)

- 9.5 M ultrapure urea
- 2% w/v NP-40,
- 5% βME (if using IPG strips, use 100 mM DTT)
- 2% LKB ampholynes
 - 1.6% pH 5-7
 - 0.4% pH 3.5-10

3. Osmotic Lysis Buffer

- 10 mM Tris pH 7.4
- 0.3% SDS

Proteins in solution at a final concentration of 2.0 mg/ml or less may be heated to boiling in this buffer. (There are no sulfhydryl reducing agents in this buffer, so protein assays such as the BCA assay and the Lowry assay may be used).

4. 10X Nuclease Stock solution

- 50 mM MgCl₂
- 100 mM Tris pH 7.0
- 500 µg/ml RNase
- 1000 µg/ml DNase

5. Protease Inhibitor stock solutions I and II (100X)

Stock I

- 20 mM AEBSF from Calbiochem
- 0.34 mg/ml pepstatin
- in absolute ethanol

Stock II

- 1 mg/ml leupeptin

0.36 mg/ml E-64 (Sigma)
5.6 mg/ml benzamidine HCl
Fractionation Protocol 1: 3-Stage Fractionation of Cellular Protein for 2D Gels
Adapted from Molloy, et. al., *Electrophoresis* 1998, 19, 837-844

Following is for 10 mg of lyophilized bacteria. Steps up to step 8 should be done at 4°C:

1. Place tissue in 15 ml snap cap tube with 5 ml of ice cold 40 mM Tris pH 9.5 (include protease inhibitors and phosphatase inhibitors).
2. Use polytron at medium-high setting to break up tissue. Use 3 x 5 second bursts.
3. Add 150U endonuclease/5ml homogenate.
4. Let sit on ice 10 min.
5. Clarify by centrifugation at 12000g for 10 min at 10°C. (17.2K in SS34 rotor)
6. Lyophilize supernatant and reserve for **GEL1**. (Lyophilization will take about ~5 hours.) Pellet is resuspended in Chaps Buffer 1 for loading.
7. Wash pellet 2x with 40 mM Tris (resuspend pellet, then spin again)
8. Dry pellet by centrifugal lyophilization.
9. Reconstitute pellet in 5 ml of Chaps Buffer 2.
10. Polytron 10 sec.
11. Let sit on ice 5 min.
12. Clarify by centrifugation at 12000g for 10 min at 10°C.
13. Reserve supernatant for **GEL2**.
14. Wash pellet 2x with CHAPS II buffer (or 40 mM Tris).
15. Dry pellet by centrifugal lyophilization.
16. Solubilize pellet in 1 ml of enhanced extraction solution, Chaps Buffer 3.
17. Vortex 30 sec.
18. Let sit on ice 5 min.
19. Clarify by centrifugation at 12000g for 10 min at 10°C.
20. Recover supernatant and reserve for **GEL 3**.
21. Wash remaining residue 2X with 40 mM Tris.

22. Resuspend in 100 μ l SDS sample solution. Boil 5 min and use for **GEL 4**.

Solutions:

<u>Chaps Buffer 1:</u>	<u>5 ml</u>	<u>25 ml</u>
8M Urea	2.4g-----	12g
4% CHAPS	0.2g-----	1g
2mM TBP	2.25 μ l of 90% TBP (at 4°C)---	11.25 μ l
40 mM Tris Base (pH 9.5)	200 μ l x 1M-----	1ml
0.5% carrier ampholytes	25 μ l x 100% CA-----	125 μ l
50 μ M Na ₃ VO ₄	1 μ l x 1:4 dilution-----	1.25 μ l
5 mM NaF	25 μ l x 1M-----	125 μ l
5 mM β -glycerophosphate	25 μ l x 1M-----	125 μ l
Complete TM protease inhibitor	200 μ l x 25x-----	1/2 tablet

<u>Chaps Buffer 2:</u>	<u>5 ml</u>	<u>25 ml</u>
8M Urea	2.4g-----	12g
4% CHAPS	0.2g-----	1g
100 mM DTT	500 μ l x 1M-----	386 mg
40 mM Tris Base (pH 9.5)	200 μ l x 1M-----	1m
0.5% carrier ampholytes	25 μ l x 100% CA-----	125 μ l
DNase/RNase	6 μ l/5 μ l-----	30 μ l/20 μ l
50 μ M Na ₃ VO ₄	1 μ l x 1:4 dilution-----	1.25 μ l
5 mM NaF	25 μ l x 1M-----	125 μ l
5 mM β -glycerophosphate	25 μ l x 1M-----	125 μ l
Complete TM protease inhibitor	200 μ l x 25x-----	1/2 tablet

<u>Chaps Buffer 3:</u>	<u>1ml</u>	<u>5 ml</u>
5M Urea	0.3g-----	1.5g
2% Thiourea	0.15g-----	750 mg
2% CHAPS	0.02g-----	0.1g
2% Caprylyl Sulfobetaine	0.02g-----	0.1g
2 mM TBP	0.5 μ l of 90% TBP (at 4°C)---	2.5 μ l
40 mM Tris Base (pH 9.5)	40 μ l x 1M-----	200 μ l
0.5% carrier ampholytes	5 μ l x 100% CA-----	25 μ l
DNase/RNase	1.25 μ l/1 μ l-----	6 μ l/5 μ l
50 μ M Na ₃ VO ₄	1 μ l x 1:20 dilution-----	1 x 1:4 dilution
5 mM NaF	5 μ l x 1M-----	25 μ l
5 mM β -glycerophosphate	5 μ l x 1M-----	25 μ l
Complete TM protease inhibitor	40 μ l x 25x-----	200 μ l x 25x

Fractionation protocol 2: Use of Percoll Gradients to Isolate Intact Mitochondria

References: F. Gasnier, R. Rousson, F. Lerme, E. Vaganay, P. Louisot, and O. Gateau-Roesch
Analytical Biochemistry 1993 **212**, 173-178

Sucrose gradients can cause osmotic damage to mitochondria and sucrose doesn't efficiently resolve mitochondria and lysosomes. This technique was developed to isolate intact mitochondria suitable for investigating outer membrane proteins. Carry out all operations at 4°C.

1. Dice tissue and homogenize in buffer A. Blend at high speed for 5 x 5 seconds.
2. Centrifuge at 960g for 15 min to separate unbroken cells, nuclei, and connective tissue fibers.
3. Poured supernatant through cheesecloth and centrifuge at 8600g for 15 minutes to sediment the mitochondrial fraction.
4. Suspend each mitochondrial pellet in 30 ml of buffer B. Sediment at 8600g. Wash 3 more times in this buffer (3 x 30ml).
5. Resuspend the final pellet in buffer B at a final concentration of 12 mg protein/ml.
6. Layer 1ml portions of this suspension on top of Percoll gradients (see buffers, below).
7. Centrifuge at 60,000g for 45 minutes.
8. Two bands of membranes should be recovered from the gradient: a dense band from approximately two-thirds down the tube corresponds to purified mitochondria while most contaminants (microsomes and lysosomes) are isolated from a band above the mitochondria.
9. Remove the mitochondria with a Pasteur pipette, dilute with 30 ml buffer B, and wash by centrifugation at 10,000g for 15 minutes to remove the Percoll.
10. Analyze prep by marker enzyme activities:
kyneurenine hydroxylase, an outer membrane protein
adenylate cyclase, an inter-membrane space marker
cytochrome oxidase, a matrix marker
11. Analyze purity of prep by non-mitochondrial markers:
NADPH-Cytochrome c reductase, for microsomes
Sphingomyelinase, for lysosomes
12. Store purified mitochondria in liquid nitrogen for future use. Theoretical yield: 6-8 mg of purified mitochondria.

Solutions:

Buffer A:

250 mM sucrose

1 mM EDTA

50 mM Tris-Cl, pH 7.4

Buffer B:

250 mM sucrose

1mM EDTA

10mM Tris-Cl, pH 7.4

Percoll Gradient (each):

2.2 ml of 2.5 M sucrose

6.65 ml of Percoll

12.25 ml of 10 mM Tris-Cl, pH 7.4

1 mM EDTA

Fractionation Protocol 3: Intercalated Disk Preparation

References: C.R. Green and N. J. Severs, Tissue & Cell 1983 **15** (1) 17-26.
C.A. L. S. Colaco and W. Howard Evans, J. Cell Sci. 1981 **52**, 313-325

- 1) Anesthetize mice with 0.3 ml of 2X avertin
- 2) Tack mice down & spray, then cut all open
- 3) Quickly cut out each heart and plunge into ice cold media (BIC)
- 4) Take all to cold room
- 5) With small syringe, perfuse blood from heart
- 6) Chop finely with razor
- 7) Homogenize in 10 ml BIC (speed 4?) 3 x 5 sec between each burst
- 8) Dounce with loose pestle in 2 lots of 5 ml, 3 hand strokes with twisting
- 9) Add 12 more ml (rinse Dounce)
- 10) Let stand 10 minutes with occasional stirring to precipitate nuclear material
- 11) Filter through nylon stocking or 2 layers of muslin or 4 layers of cheesecloth
- 12) Centrifuge in disposable centrifuge tube 5 min, 1900 rpm (gmax 750) in tabletop centrifuge
- 13) Decant supernatant and aspirate any clumps
- 14) Resuspend in 5 ml BIC with strokes of Dounce
- 15) Dilute suspension with 10 ml BIC each
- 16) Centrifuge in tabletop at 1900 rpm for 5 minutes
- 17) Aspirate and resuspend with 5 ml and then 10 ml
- 18) Centrifuge 1900rpm, 5 minutes
- 19) Resuspend in 5 ml BIC/KCl/sucrose
- 20) Add 10 ml to each and put all in 50 ml tall beaker
- 21) Stir 4 hours in the cold room, very low speed
- 22) Aspirate flocculent material with Pasteur pipette
- 23) Centrifuge for 5 min at 2200 rpm (gmax 1000) in table top centrifuge

- 24) Discard clear glassy pellet
- 25) Centrifuge the supernatant at 10,000 rpm (12,000 gmax) in SS34 rotor in RC5 centrifuge
- 26) Discard supernatant
- 27) Small brown pellet contains discs: resuspend in small amount of solubilization buffer
+++++++
- 28) Determine protein concentration and then freeze aliquots at -80°C
- 29) Run on 2D gels

Solutions:

BIC

- 1mM sodium bicarbonate
- 1 Complete™ protease inhibitor tablet per 50 ml medium (add fresh!)
- 20 mM NaF
- 5 mM β-glycerophosphate
- 50 μM sodium orthovanadate

BIC/Sucrose

- BIC plus 8% w/v sucrose

IPG Protocol: Sample Preparation Guidelines

- Always wear gloves when handling IPG strips, SDS polyacrylamide gels, ExcelGel Buffer Strips, and any equipment that these items will contact. The use of gloves will reduce protein contamination that can produce spurious spots or bands in 2D patterns.
- Clean all assemblies that will contact the gels or sample with a detergent designed for glassware and rinse well with distilled water.
- Always use the highest-quality reagents and the purest water available.
- Keep the sample preparation strategy as simple as possible to avoid protein losses. Additional sample preparation steps may improve the quality of the final 2D result, but at the possible expense of selective protein loss.
- The cells or tissue should be disrupted in such a way as to minimize proteolysis and other modes of protein degradation. Cell disruption should be done at as low a temperature as possible and with a minimum of heat generation. Cell disruption should ideally be carried out directly into a strongly denaturing solution containing protease inhibitors.
- Sample preparation solutions should be freshly prepared or stored as frozen aliquots.
- Use high-purity or de-ionized urea.
- Preserve sample quality by preparing the sample just prior to IEF or storing samples in aliquots at -80°C. Do not expose samples to repeated thawing.
- Remove all particulate material by ultracentrifugation. Solid particles and lipids must be removed because they will block the gel pores.
- To avoid modification of proteins, never heat a sample after adding urea. When the sample contains urea, it must not be heated over 37°C. Elevated temperatures cause urea to hydrolyze to isocyanate, which modifies proteins by carbamylation.
- Contaminants that affect 2D results: salts, residual buffers and other charged small molecules that carry over from sample preparation, endogenous small ionic molecules (nucleotides, metabolites, phospholipids, etc.), ionic detergent, nucleic acids, polysaccharides, lipids, phenolic compounds, insoluble material.

Suggested buffer:

8M ultrapure/deionized urea

4% CHAPS

2mM TBP or 100mM DTT

40 mM Tris base pH 9.5

0.5% ampholytes

150U endonuclease

IEF with Multiphor II/IPG strips

1. Select an IPG Buffer with the same pH interval as the Immobiline DryStrip being rehydrated. Add the IPG buffer to an appropriate rehydration or lysis/sample solution.
2. Rehydration stock solution with IPG Buffer. Store this solution in 2.5 ml aliquots at -20°C.

<u>Component</u>	<u>Final Conc.</u>	<u>Amount</u>
Urea	8M	12g
CHAPS	2%	0.5g
IPG Buffer	2%	500 µl
Bromophenol blue	trace	trace
Double-distilled water		16 ml
DTT (add before use)		7mg/2.5 ml

3. The volume of rehydration solution needed depends on the length of the strips and the type of equipment used for rehydration. Up to 12 strips are rehydrated simultaneously in the Immobiline DryStrip Reswelling tray.

<u>Strip Length</u>	<u>Vol of reswelling solution/strip</u>	<u>µl IPG Buffer/rehydration solution</u>
7cm	125 µl	40 µl/2 ml
11 cm	200 µl	60 µl/3 ml
13 cm	250 µl	70 µl/3.5 ml
18 cm	340 µl	100 µl/5 ml (enough for 12 strips)

4. Preparative sample loads (100 µg up to 3 mg) run on Immobiline DryStrip in neutral and acid pH ranges are preferably loaded in the rehydration step (rehydration loading). With basic Immobiline DryStrip (pH intervals 6-9 and 6-11), large amounts of sample (up to 200 µl) are applied at the anode using electrode strips up to 4 cm long soaked in sample solution.

When using large volumes of sample, the concentrations of salt, buffering substances and other impurities that can interfere with the separation should be kept to a minimum. Such substances may prolong the required focusing time and may even disturb the pH gradient.

- The protocol for each type of strip is listed on the back of each package of Immobiline DryStrips. Use an EPS 3501 XL power supply, gradient setting, with the low current cutoff disabled.
- After the run, place strips in a capped glass culture tube (or sterile glass graduated cylinder with parafilm on the top) and add SDS Equilibration Buffer I. Rock the tube

gently on its side for 15 min. Transfer strips to clean tube and add SDS Equilibration Buffer II. Rock gently for 15 min.

Equilibration Solution:

	<u>Final Conc.</u>	<u>Amount</u>
1.5 M Tris-Cl, pH 8.8	50 mM	6.7 ml
Urea	6M	72.07g
Glycerol (87% v/v)	30% v/v	69 ml
SDS	2%	4.0g
Bromophenol blue	trace	a few grains
Double distilled water		to 200 ml

*Store in 40 ml aliquots at -20°C.

For Buffer I: add 100 mg DTT/10 ml solution just prior to use

For Buffer II: add 250 mg (some recipes say 450) iodoacetamide/10 ml solution.

*Recommended volumes are 10 ml for 18 cm, 5-10 ml for 11 and 13 cm, and 2.5-5 ml for 7cm IPG strips.

- Lay the strips on their sides on slightly damp filter paper. Dip the IPG strip in electrophoresis buffer to lubricate it. Position the IPG strip between the plates on the surface of the SDS-PAGE gel with the plastic backing against one of the glass plates. With a thin plastic ruler, gently push the IPG strip down so the entire lower edge of the IPG strip is in contact with the top surface of the slab gel. Ensure that no air bubbles are trapped between the IPG strip and the slab gel surface or between the gel backing and the glass plate.
- Optional: Apply molecular weight marker proteins. The markers are applied to a paper application piece in a volume of 15-20 μ l. For less volume, cut the sample application piece proportionally. Place the IEF application piece on a glass plate and pipette the marker solution onto it, then pick up the application piece with forceps and apply to the top surface of the gel next to one end of the IPG strip. The markers should contain 200 to 1,000 ng of each component for Coomassie staining and about 10 to 50 ng of each component for silver staining.
- Seal the IPG strip in place. Imbedding the IPG strip in agarose prevents it from moving or floating in the electrophoresis buffer. Prepare the agarose sealing solution:

	<u>Final Conc.</u>	<u>Amount</u>
SDS electrophoresis buffer		100 ml
Low-melt agarose	0.5%	0.5g
Bromophenol blue	trace	a few grains

Dispense 2 ml aliquots into screw-cap tubes and store at room temperature.

Melt each aliquot as needed in a heat block at 50°C (can be done while strips are equilibrating). Pipette the amount required to seal the IPG strip in place. Pipetting slowly avoids introducing bubbles. Allow a minimum of 1 minute for the agarose to cool and solidify.

- Run SDS PAGE gel as normal.

Silver Staining of Polyacrylamide Gels for In-Gel Digestion

Adapted from Jensen, Wilm, Shevchenko, & Mann
2D Proteome Analysis Protocols

Use the purest chemicals available at all stages of sample preparation, including gel casting and staining. Avoid contamination by ionic detergents and polymers (polyethylene glycol) by thoroughly cleaning glass plates used for gel casting in methanol and water. It is advisable to let a freshly prepared gel rest overnight to reduce the amount of remaining unreacted acrylamide, which otherwise may react with thiol groups in proteins. Gloves should be worn to avoid contamination by human epidermal proteins (keratins). It is important to rinse gloves with water to remove talcum powder and traces of dust, and to inspect microcentrifuge tubes for dust particles prior to use. Contamination of gloves and tubes is often owing to electrostatic charging, which attracts dust particles.

1. After the gel has been run, soak it for 20-30 min in fix solution (45% methanol, 5% acetic acid).
2. Rinse the gel in 50% methanol for 10 minutes.
3. Rinse the gel in water (30-60 min). Longer incubation times, e.g., 12h, improve the contrast of the stained gel.
4. Sensitize the gel with 0.02% sodium thiosulfate solution for 1-2 min (**do not use glutaraldehyde**—it is a protein crosslinking agent).
5. Discard solution, and rinse the gel slab with two changes of water (1 min each).
6. Incubate the gel in chilled 0.1% AgNO₃ solution for 20-40 min at 4°C.
7. Discard solution and rinse the gel with two changes of water (1 min each).
8. Develop gel with a fresh* solution of 0.04% formaldehyde/2% Na₂CO₃ solution on a shaking table. (Start with a brief rinse using a small amount of solution. Blackish-brown silver oxide may form. Dump this cloudy solution immediately—important for reducing background in the gel. Fill with enough fresh solution to allow the gel to move freely in the dish.) Important: Replace developing solution when it turns yellow. Do not overexpose the gel.
9. Quench development when sufficient staining is obtained (usually after 0.5-5 min) by discarding developer solution and addition of 1% acetic acid.
10. Store the silver-stained gel in 1% acetic acid.

**The silver stain solutions must be made fresh. Add the catalyst (formalin) just before use.*

Sample Preparation for MALDI Peptide Mass Mapping
Adapted from Jensen, Wilm, Shevchenko, & Mann
2D Proteome Analysis Protocols

Matrix/Nitrocellulose Preparation

1. Prepare a saturated matrix solution:
(saturated solution ~ 40g/L) of α -cyano-4-hydroxycinnamic acid in acetone in a 1.5-ml microcentrifuge tube. Vortex briefly. Centrifuge to precipitate insoluble matrix material. This solution should be freshly prepared.
2. Cut out a piece of nitrocellulose membrane and make a nitrocellulose solution:
Mix 50 ml of acetone with 50 ml of isopropanol. Add 1g of nitrocellulose. This solution can be stored for several months.
3. Prepare a fast evaporation/nitrocellulose (FENC) solution:
Mix 4 vol of matrix solution and 1 vol of nitrocellulose solution. Addition of 1-3% (v/v) water to the FENC solution reduces the evaporation rate and thereby promotes formation of a thicker matrix surface.
4. Deposit 0.2-0.3 μ l FENC solution by rapid transfer from the microcentrifuge to the MALDI MS probe (use a 2- μ l adjustable pipette).

Analysis of Extracted Peptides after In-Gel Digestion.

1. Re-dissolve the dried peptide sample in 10-30 μ l of 5% formic acid. Sonicate and vortex briefly. Deposit 0.5-1 μ l of this peptide solution onto an FENC surface.
2. Rinse the FENC surface by depositing 10 – 20 μ l of 5% formic acid followed by immediate wiping or shaking of the probe to remove the liquid. Repeat the rinsing step with 10-20 μ l of pure water. The rinsing procedure can be repeated several times provided that the matrix film is not damaged.
3. Insert the probe into the MALDI mass spectrometer and acquire a spectrum.

Zip Tip_{C18} Peptide Cleanup
(Millipore, Inc. Bedford MA)

To prepare peptides and small proteins (<40 Kd) for mass spectroscopy, use the ZipTip with samples containing picogram to micrograms of sample. The absorption efficiency of ZipTip is sample and concentration dependent.

Prepare the Sample

- Maximum binding to the ZipTip is achieved in the presence of TFA or other ion-pairing agents. To minimize sample dilution and enhance analyte binding, use 10% TFA to achieve a final concentration of 0.1% TFA.
- In the case of excess detergent, dilute sample with 0.1% TFA to achieve acceptable binding conditions, for example SDS (<0.1%), Triton (<1%), and Tween (<0.5%).

Equilibrate the ZipTip for Sample Binding

- Prewet the tip by depressing plunger to a dead stop using the maximum volume setting of 10 μ l. Aspirate wetting buffer into tip. Dispense to waste. Repeat. Wetting buffer: 50% acetonitrile in water
- Equilibrate tip for binding by washing it twice with the equilibration buffer: 0.1% TFA in water

Bind, Wash and Elute the Peptides or Proteins

- Bind peptides and proteins by fully depressing the pipette plunger to a dead stop. Aspirate and dispense sample 5 to 10 cycles depending on sample concentration. Dilute solutions require increased contact time.
- Wash tip and dispense to waste using two cycles of 0.1% TFA, water, or 50% methanol in 0.1% TFA/water mixture. You may require additional washing for electrospray applications or samples containing high salt or detergent.
- Elute by dispensing 2 to 4 μ l of elution buffer to clean vial using a standard pipette tip. Carefully, aspirate and dispense eluant through ZipTip at least three times without pushing air into the sample. For electrospray MS, elute sample into clean vial and apply directly for analysis. For MALDI MS, elute with or without matrix in 50% acetonitrile/water.
- If contamination of polymer or other signal suppressing substance occurs, results can be improved by stepwise elution of sample in increasing concentration of acetonitrile in water. Follow the binding and washing procedures as normal. Begin the elution procedure starting with 2% acetonitrile in water and spot. Repeat with 5%, 10%, 15%, 25%, 50%, and 80% acetonitrile in water, eluting each onto a separate spot on the MALDI probe. Polymer contamination may elute in the first or second fraction.

CAUTION: Acetonitrile is volatile and evaporation can occur rapidly. If this occurs, add more eluant to recover sample.

- Pipette 1 to 2 μl of desalted-concentrated sample directly onto target by depressing plunger until appropriate volume is dispensed. Save or discard the remaining sample with tip.

NOTE: For samples containing $\geq 1 \mu\text{g}$ of protein or $\geq \mu\text{g}$ of peptide, you can achieve maximum recovery by increasing elution volume to 10 μl or by performing multiple elutions (2 x 5 μl).

Equipment:

2-Dimensional SDS-PAGE:

<u>Item:</u>	<u>Company & Cat #</u>
PROTEAN II xi Cell, 20 cm	Bio-Rad 165-1811
PROTEAN II xi Cell 2-D Conversion Kit Includes Tube Gel Adapter, Glass Tubes, gaskets, grommets, stoppers Capable of running 16 1 st -dimension tube gels or 4 2 nd -dimension slab gels	Bio-Rad 165-1815

Isoelectric Focusing Equipment:

<u>Item:</u>	<u>Company & Cat #</u>
Multiphor II Electrophoresis Unit	AP Biotech 18-1018-06
EPS 3501X Power Supply	AP Biotech 18-1130-05
Multitemp III Thermostatic Circulator 115 Vac	AP Biotech 18-1102-77
Immobiline Drystrip Kit	AP Biotech 18-1004-30
IPG Reswelling Tray	AP Biotech 80-6371-84

Consumables:

Immobiline Drystrips, 18cm	AP Biotech, variable
IPG Buffers	AP Biotech, variable
IEF electrode strips	AP Biotech 18-1004-40
IEF/SDS sample application strips	AP Biotech 18-1002-26

2nd Dimension SDS-PAGE:

<u>Item:</u>	<u>Company & Cat #</u>
Hofer DALT Multiple Electrophoresis Tank With buffer circulation pump Capable of running 10 20 x 23 cm gels simultaneously	AP Biotech 80-6068-79
DALT Gel Cassettes	AP Biotech 80-6067-46
DALT Multiple Gel Caster	AP Biotech 80-6330-61
DALT Gradient Maker with Peristaltic pump	AP Biotech 80-6067-65
Multitemp III Thermostatic Circulator 115 Vac	AP Biotech 18-1102-77
Hofer EPS 2A200 Power Supply	AP Biotech 80-6406-99
*DALT Blotting Kit	AP Biotech 80-6069-17
*DALT Transfer Cassette	AP Biotech 80-6069-55

Consumables:

*DALT Blotting Paper	AP Biotech 80-6069-93
----------------------	-----------------------

MALDI-TOF:

<u>Item:</u>	<u>Company & Cat #</u>
MALDI-TOF Sample Plate	PerSeptive Biosystems 5-2204-00-0002

Consumables:

ZipTip pipette tips	Millipore
---------------------	-----------

(10 microliter pipette tip with approximately a half microliter bed of C18 resin fixed in its end. It is intended for concentrating, desalting, and removing detergents from biological samples. Used for sample binding, washing, and elution of peptides or small proteins (<40 Kd) for MALDI-MS, ESI-MS, or other analytical techniques.)

Trypsin sequencing grade

Roche 1418 475

Chymotrypsin sequencing grade

Roche 1418 467

Sequazyme Mass Standards Kit

PerSeptive Biosystems P2-3143-00

Brenda S. Luciano

MIT Center for Cancer Research

David Housman Laboratory

400 Main Street, E18-505

Cambridge, MA 02142

Tel: (617) 253-3010, Fax (617) 253-5202

bluciano@mit.edu

EDUCATION	Ph.D. Biology Massachusetts Institute of Technology, Cambridge, MA	1994-2001
	B.S. (magna cum laude) Chemistry Western Washington University, Bellingham, WA	1990-1993
	A.A. Whatcom Community College, Bellingham, WA	1989-1990
TECHNICAL EXPERIENCE	Graduate Student MIT, Laboratory of Dr. D. E. Housman	1994-2001

Technical Expertise

- Extensive work with proteomic techniques including 2D-PAGE and MALDI-TOF mass spectrometry.
- Molecular biology techniques including PCR, Southern blot, western blot, cloning and subcloning, RNA purification for CHIP analysis.
- Library screening.
- Tissue culture with a variety of mammalian and insectoid cell types, including both transient and stable transfections.
- Protein-related techniques including kinase assays, fractionation, and expression, purification, and characterization of proteins in bacteria, baculovirus, and mammalian cell systems.
- Mouse colony management, genotyping, dissection and histology.

Current Research

In the course of my research I have integrated proteomics into the Housman genomics laboratory by setting up the laboratory's proteomics facility, including purchasing and maintaining equipment, supervising, training other personnel, and consulting for other laboratories.

My project has been to utilize proteomics to further investigate the etiology of the human disease Myotonic Dystrophy (DM), the most common form of adult-onset muscular dystrophy. Although the gene mutated in DM was cloned in the Housman lab in 1992 and is known to encode a serine/threonine protein kinase, DMPK, no information is yet available about its substrate, pathway, or how it is involved in the disease. I have utilized *DMPK*^{-/-} mice in conjunction with 2D-electrophoresis and MALDI-TOF mass spectrometry to identify proteins that are involved in the DMPK pathway. I have compared fractionated extracts from relevant tissues of wild-type and *DMPK*^{-/-} mice and have thus far identified several proteins which may play a role in DM disease pathology. Currently I am working to identify for each protein the modification which produced the shift on the gels, using proteomics and molecular biology techniques.

Teaching Assistant

MIT

Senior Project Laboratory. 1998

Freshman Introductory Biology. 1996

Responsibilities included preparation of laboratories as well as lecturing.

Technician

1993-1994

Georgia Pacific Corporation, Bellingham, WA.

Responsibilities included HPLC, GC, viscosity analysis of products.

Analysis and maintenance of dissolved oxygen, nitrogen, and micro-organism balance in effluent treatment facility.

Independent Research

1991-1993

WWU

Laboratory of Dr. G. Kriz.

Completed independent research for publication in organic chemistry textbook.

Teaching Assistant

1991-1993

WWU

General Inorganic Chemistry, Organic Chemistry Laboratory Survey, Advanced Organic Chemistry Laboratories I, II, and III. Responsibilities included preparation of labs, solutions, and reagents, as well as supervision of laboratory classes.

Tutor

1989-1990

Whatcom Community College, remedial mathematics and algebra.

HONORS AND AWARDS

President's Scholarship. WWU 1990-1991

Knapman Chemistry Scholarship. WWU 1991-1993

Phi Kappa Phi Honor Society. 1994-

PUBLICATIONS AND PRESENTATIONS

Luciano, B. S. and Housman, D.E. Proteomic Analysis of the role of the Myotonic Dystrophy protein kinase (DMPK) (in preparation).

Saba, S., Vanderbrink, B.A., Luciano, B., Aronovitz, M. J., Berul, C. I., Reddy, S., Housman, D., Mendelsohn, M.E., Estes N. A. 3rd, and Wang, P.J. (1999) Localization of the sites of conduction abnormalities in a mouse model of myotonic dystrophy. *Journal of Cardiovascular Electrophysiology* 10 (9): 1214-20.**The International Myotonic Dystrophy Consortium (IDMC).** 2000New nomenclature for Myotonic Dystrophies and DNA testing Guidelines for Myotonic Dystrophy type 1 (DM1). *Neurology* 54 (6): 1218-21.

Luciano, B. S., Davis, B. M., and Housman, D. E. 1999

Functional Analysis of DMPK. Invited speaker, 2nd International Myotonic Dystrophy Conference.